The Dissertation Committee for Diana M. Cittelly Certifies that this is the approved version of the following dissertation:

ROLE OF BCL-X_L IN CELL DEATH AFTER SPINAL CORD INJURY

Committee:

J. Regino Perez-Polo, Ph.D. Supervisor

Olivera Nesic-Taylor, PhD.

Giulio Taglialatela, PhD.

Golda A. Leonard, PhD.

Jacqueline Bresnahan, PhD.

Dean Signature

ROLE OF BCL-X_L IN CELL DEATH AFTER SPINAL CORD INJURY

by

Diana M. Cittelly, BS. MS.

Dissertation

Presented to the Faculty of the Graduate School of

The University of Texas Medical Branch

in Partial Fulfillment

of the Requirements

for the Degree of

Doctor of Philosophy

The University of Texas Medical Branch

December, 2006

Dedication

"In order to appreciate the beauty of a rose and the fragility of her petals—

you must first grasp her thorns"

Ramon Cuevas, 1989

Acknowledgements

I want to first acknowledge my parents, Enrique and Marina Cittelly, and my sister Erika. Despite of the distance, they have believed in me even in those days I did not believe in myself. Their constant support inspires me to do my best so I can make them proud of me. I want to express my most sincere gratitude to my mentor, Dr. Regino Perez-Polo, for his valuable guidance and patience. I want to acknowledge my committee: Drs. Olivera Nesic-Taylor, Golda A. Leonard, Giulio Taglialatela and Jacqueline Bresnahan. Thank you for your time, challenging questions and willingness to help me with anything I need no matter how big or small. I also want to thank my Graduate Program Directors, Drs. Golda A. Leonard and Bernd U.Budelmann, for their constant support, for being there whenever I needed to talk, about science, about the school, about life. Thanks to the faculty of the Neuroscience and Cell Biology Department for their support, including Drs. Claire Hulsebosch, Karin High, Ping Wu and David McAdoo. I want to acknowledge the members of Perez-Polo group; they have been my second family for the past years. Thank to Diana Ferrari, Charmaine Rea, Marty Gill and Danny Rafati, I would not have completed this dissertation without their constant support and encouragement. Their friendship is one of the life-lasting treasures that I found at this lab. Thanks to Julieanne Lee, Donna Masters and Karin-Werrbachperez for your invaluable help. I want to heartily acknowledge Patricia Gazzoli, for her inestimable help in the preparation of this dissertation. Finally, I want to thank all my friends Becky, Veronica, Zobeida, Edna, Federica, Elena, Corinna, Luis Felipe, Peter, and all of those that have been my constant support.

ROLE OF BCL-X_L IN CELL DEATH AFTER SPINAL CORD INJURY

Publication No._____

Diana M. Cittelly, PhD.

The University of Texas Medical Branch, 2006

Supervisor: J. Regino Perez-Polo

Long term functional impairment after rat spinal cord injury (SCI) results from secondary apoptosis regulated in part, by SCI-induced decreases in protein levels of the anti-apoptotic protein Bcl-x_L. In this dissertation, I assessed the role that Bcl-x_L subcellular re-routing and post-translational phosphorylation play in SCI-induced Bcl-x_L decreases, and evaluated the therapeutic potential of Bcl-x_L-administration after SCI. Immunohistochemical analysis showed non-phosphorylated Bcl-x_L in neurons and oligodendrocytes, but not in astrocytes and microglia. Bcl-x_L levels decreased in mitochondria, endoplasmic reticulum, nuclei and cytosolic extracts during the first 24h after SCI, but with a different time course for each organelle; suggesting an independent regulation of Bcl-x_L shuttling from the cytosol to each compartment in the injured spinal cords. A membrane-bound phosphorylated form of Bcl-x_L (P-ser^{62}-Bcl-x_L) was found in neurons in the uninjured SC. SCI did not affect P-ser^{62}-Bcl-x_L levels in organelles; however, P-ser^{62}-Bcl-x_L appeared in the cytosol early after SCI, suggesting a role for phosphorylation in SCI-induced decreases of Bcl-x_L levels. Vinblastine-induced apoptosis of neuronal PC12 cells, showed that cytosolic phosphorylated Bcl-x_L correlated with apoptotic cell death of neurons, suggestive of Bcl-x_L-phosphorylation as a pro-

apoptotic event. I found that activated microglia/macrophages robustly expressed Bcl-$x_{L,}$ 7 days after SCI, and a fraction of this population undergoing apoptosis, expressed P-ser^{62}-Bcl-x_L. Therefore, phosphorylation of Bcl-x_L may have two opposite effects in injured spinal cords: (a) it may decrease levels of the anti-apoptotic Bcl-x_L in neurons and therefore contribute to their death and, (b) it may regulate apoptosis in activated microglia/macrophages, thus curtailing the inflammatory cascades associated with SCI.

To counteract SCI-induced decreases in Bcl-x_L and resulting apoptosis, I used a fusion protein made up of the TAT protein transduction domain and the Bcl-x_L protein (Tat-Bcl-x_L), or to its anti-apoptotic domain BH4 (Tat-BH4). Intrathecal delivery of Tat-Bcl-x_L, or Tat-BH4 for 24h or 7 days after SCI, resulted in a significant decrease in apoptosis at the site of injury. However, the 7 day delivery of Tat-Bcl-x_L or Tat-BH4 impaired locomotor recovery beyond the drug delivery time. Here I show that the 7 day application of Tat-Bcl-x_L or Tat-BH4 increased microglia/macrophage activation and/or survival associated with an increase in neuronal losses. These results suggest that the anti-apoptotic treatment may shift neuronal apoptosis to necrosis, and initiate an inflammatory response (microglial activation) in SCI rats. As a result, Tat-Bcl-x_L/Tat-BH4-induced increases in proinflammatory reactions may amplify SCI-induced neuronal cell death and additionally impair functional recovery. Given that microglial activation and inflammation are main players in shaping pathological outcomes after SCI, these results suggest that the therapeutic potential of Tat-Bcl-x_L or Tat-BH4 in injured spinal cords may be limited. Moreover, chronic treatment of SCI with Tat-Bcl-x_L or other anti-apoptotic treatments targeting Bcl-x_L could be detrimental.

Table of Contents

List of Tables

List of Figures

CHAPTER ONE: CELL DEATH AND SPINAL CORD INJURY

Spinal cord injury (SCI) is a major societal health concern affecting 2.5 million people worldwide (Thuret et al., 2006). More than 130,000 new injuries are reported each year (Fisher et al., 2006) from which 8,000-10,000 occur in the United States (Dumont et al., 2002). Although the life expectancy following SCI is improving as a result of advances in medical and surgical care (Hulsebosch, 2002), SCI has a significant impact on quality of life and becomes an economic burden, with considerable costs associated with primary care and loss of income (Burnett et al., 2001;Krause, 2003;Krause and Terza, 2006). There are no fully restorative therapies for SCI. The design of rational and effective therapies requires understanding the complex pathophysiological mechanisms that characterize SCI.

Early studies of the pathological events triggered by spinal cord trauma showed that the outcome of SCI depended not only on the tissue disruption at the time of trauma, but also on secondary injury processes that could extend for days (Hulsebosch, 2002). Currently, it is accepted that cell death and secondary degeneration after SCI is the result of multiple cascades and that an effective therapy must be a combination of agents targeting multiple processes (Thuret et al., 2006). It is clear that beyond the "necrotic" cell death produced by the impact to the cord, cells that have received less severe injuries can die by active processes such apoptosis (Beattie et al., 2000a). Thus, preventing this delayed cell death must be part of the "cocktail" of targets to improve the functional outcome after SCI. This dissertation is an attempt to identify the mechanisms that lead to the impairment of the function of Bcl-x_L (a key anti-apoptotic regulator in the CNS), as well as to evaluate potential of exogenous administration of Bcl-x_L as a neuroprotective agent after SCI.

In this chapter I will provide a general overview of the main events responsible for the functional impairment after SCI, in particular cell death. Following, I will describe the general mechanisms that control apoptotic cell death, with emphasis in the anti-apoptotic

role of Bcl-x_L. Finally I will present evidence that supports the potential of Bcl-x_L as an anti-apoptotic agent in the context of CNS trauma.

Spinal Cord Injury

Because of the specific organization of the spinal cord conveying both sensory and motor information, SCI leads to a wide range of functional deficits distal to the levels of injury (Ahn et al., 2006). Human SCI can be divided into four distinct groups: solid cord injury, contusion/cavity-type injury, laceration, and massive compression (Grill, 2005). Most human spinal cord injuries are produced by the fracture and dislocation of the spinal column causing contusion and compression (Norenberg et al., 2004). In order to study the acute and chronic events triggered by trauma, and to test therapeutic agents, several approaches have been applied to model spinal cord contusions in animals (Young, 2002;Stokes and Jakeman, 2002). Most of the models that reproduce a pathology similar to that observed in cases of human contusion/compression injury, employ a user-defined weight, dropped from a defined height or with at defined force above the exposed spinal cord to induce a rapid localized displacement of cord tissue (Young, 2002;Grill, 2005). As in human SCI, animal models display graded histological and behavioral loss correlated with graded severity of the contusion (Basso et al., 1995;Basso et al., 1996;Stokes and Jakeman, 2002;Scheff et al., 2003).

Pathophysiology of Contusive Spinal Cord Injury

The series of events occurring in both humans (Bunge et al., 1993) and animal models due to spinal contusion/compression can be divided in three phases (Hulsebosch, 2002;Ahn et al., 2006) including primary (acute), secondary (semi-acute) and chronic mechanisms (**Fig. 1**). During the acute phase, a transient blow and/or sustained compressive event causes tissue displacement resulting in a localized tissue deformation, tissue shear, severing axons, vascular disruption and loss of blood–spinal cord barrier function (Ahn et al.,

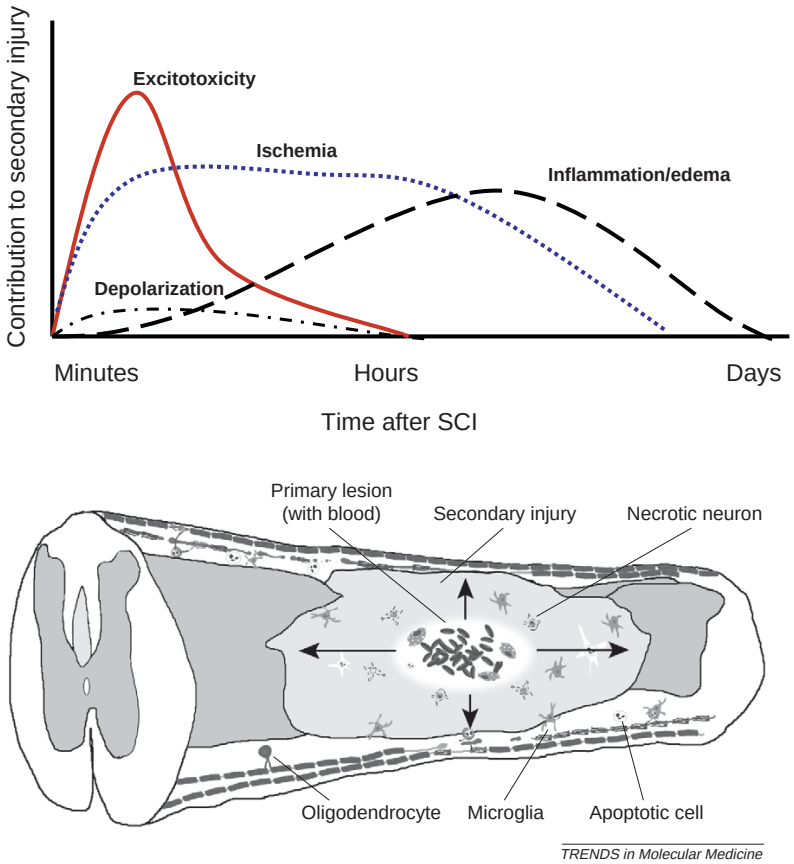

Fig. 1. Pathophysiology of the secondary damage after SCI. A. The initial trauma to the cord starts with loss of membrane integrity (depolarization), glutamate release (excitotoxicity mediated by astrocytes and neurons) and metabolic stress. (Modified from Schwah, JM, et al, 2006). B. A spinal cord injury expands itself during the first weeks post-trauma, due to the delayed cell death of neurons and oligodendrocytes rostral and caudally to the lesion epicenter. Reprinted with permission from Beattie M. TRENDS in Molecular Medicine. 10(12); 580-583. Copyright © 2004 Elsevier Ltd

2006;Baptiste and Fehlings, 2006). This cellular disruption at the center of impact triggers a secondary cascade of rostro-caudal tissue destruction that includes ischemia, metabolic failure due to massive intracellular Ca2+ influx, ionic disregulation, excitotoxicity, free radical formation, membrane damage by lipid peroxidation and necrotic cell death (Hall and Braughler, 1993;Beattie et al., 2000b;Schwab et al., 2006). The disruption of the blood-SC barrier added to necrosis allows for an early infiltration of blood neutrophils (Popovich

et al., 1999) that can increase rapidly levels of cytokines as TNF-a, and macrophages that increase the levels of free-oxygen radicals (Fleming et al., 2006). By 24h post-injury, neuronal death is completed at the lesion epicenter, macrophages have invaded the lesion and a cavity begins to form (Liu et al., 1997;Stokes and Jakeman, 2002). During the chronic phase that occurs from weeks to years, injured axons continue to die away from the site of injury; their distal ends undergo Wallerian degeneration increasing the tissue loss and the disruption of neural circuits (Liu et al., 1997;Zhang and Guth, 1997;Kerschensteiner et al., 2005). The formation of cystic cavities filled with fluid and connective tissue is followed by a proliferation of astrocytes and their processes producing a dense mass of intracellular glial filaments composed of polymerized GFAP (e.g. glial scar formation), which fills in all the spaces left by the degenerating axons and myelin (Silver and Miller, 2004;Rosenberg et al., 2005;Zai and Wrathall, 2005). Reactive astrogliosis occurs along the entire region of axon degeneration including in the region of the axon terminals in the gray matter (Hulsebosch, 2002;Gomes-Leal et al., 2004).

The inflammatory response also plays an important role in the progression of the lesion after SCI. Microglial activation begins 1 day after injury and persist up to 6 weeks (Popovich et al., 1997;Kigerl et al., 2006). Other macrophages enter the cord due to the disruption of the blood-spinal cord barrier or are attracted by inflammatory cytokines, and at chronic stages, they continue infiltrating due to increases in white matter permeability (Zhang et al., 1997;Schnell et al., 1999). By 6 weeks after trauma in rats, there is a two to three fold increase in cell density at the lesion epicenter (Zai and Wrathall, 2005), due mostly to proliferation and infiltration of microglia and macrophages (Popovich et al., 2003;Kigerl et al., 2006). The role of microglia and macrophages in chronic stages after SCI is controversial, since these cells can secrete molecules that may be beneficial or deleterious to regeneration (Jones et al., 2005). However, most evidence suggests that microglial/macrophage response to SCI is responsible for demyelination, oligodendrocyte

death and damage to intact axons (Casha et al., 2001;Popovich et al., 2002;Gomes-Leal et al., 2004;Zai and Wrathall, 2005).

Cell death after SCI: Necrosis vs. Apoptosis

Classically, necrotic cell death is characterized by distortion and degradation of organelles, cellular swelling and loss of the plasma and nuclear membrane integrity (Bredesen et al., 2006). This type of death occurs immediately after SC trauma due to the shearing of membranes that leads to the release of free radicals and excitatory amino acids by dying neurons and other cells (Zhang et al., 1997;Lu et al., 2000;Beattie et al., 2002). In contrast, the secondary apoptotic death of neurons and oligodendrocytes is an active and highly orderly process displaying characteristic morphologic changes that include nuclear pyknosis, chromatin condensation, DNA fragmentation, cytoplasmic condensation, plasma membrane blebbing, and exposure of phosphatidylserine (Lu et al., 2000;Beattie et al., 2000b;Bredesen et al., 2006). The dead cells eventually fragment into membrane bound apoptotic bodies, which are phagocytosed by macrophages and surrounding cells without inducing inflammatory response (Hengartner, 2000).

Although apoptosis and necrosis are mediated through distinct pathways, the same insult can lead to either apoptosis or necrosis depending on its intensity and the neuronal subpopulation involved (Yuan et al., 2003). For instance, the disruption of the cord vasculature creates a hypoxic environment, and it is known that hypoxia can induce cell death by both necrosis and apoptosis (Sastry and Rao, 2000). Also, levels of excitatory amino acids such as glutamate increase dramatically in the spinal cord after injury. High levels of glutamate can activate AMPA and NMDA receptors (Nesic et al., 2002) allowing a Ca^{2+} influx that causes cells to burst in a typical necrotic death. However, cells exposed to lower levels of glutamate can recover, or die not by necrosis but by apoptosis (Yakovlev and Faden, 2004).

There is little that can be done to prevent the necrotic death triggered by the mechanical insult to the cord. However, because is a delayed and programmed process, the secondary apoptotic cell death provides a timeframe for therapeutic interventions that ameliorate the cell loss and subsequent functional deficit after SCI.

Molecular regulation of apoptosis

The previous section has given a brief overview of the main events that lead to the devastating consequences of spinal cord injury. This section explores in more detail the molecular pathways that control apoptotic cell death in the CNS, in particular, the apoptotic death of neuronal and oligodendroglial cells that extends for several days after injury (Beattie et al., 2000a;Beattie et al., 2000b;Grossman et al., 2001).

Cells can initiate the apoptotic process by two known pathways: an intrinsic (mitochondria-dependent) pathway and an extrinsic (receptor-dependent) pathway (**Fig. 2**) (Yuan et al., 2003). In both pathways, the final apoptotic features are the result of the activation of caspases, a family of proteases dependent on a cysteine nucleophile to cleave motifs possessing aspartic acid (caspase)(Chen and Wang, 2002). Caspases are produced as inactive zymogens possessing a large and a small subunit preceded by an N-terminal prodomain. Upstream caspases known as initiators (caspases 8, 9 and 10) are capable of autocatalytic activation and generally have a long prodomain. Downstream "executioners" caspases (i.e. caspase 3, 6 and 7) need initiator caspases for their activation by transprocessing (Earnshaw et al., 1999). The cleavage of many downstream substrates by executioner caspases substrates leads to morphological changes associated with apoptosis, including DNA degradation, chromatin condensation, and membrane blebbing. For example, the cleavage of ICAD (inhibitor of caspase-activated DNAase) by caspase-3 results in the activation of CAD (caspase-activated DNAase), which leads to the formation of DNA ladder (Hengartner, 2000).

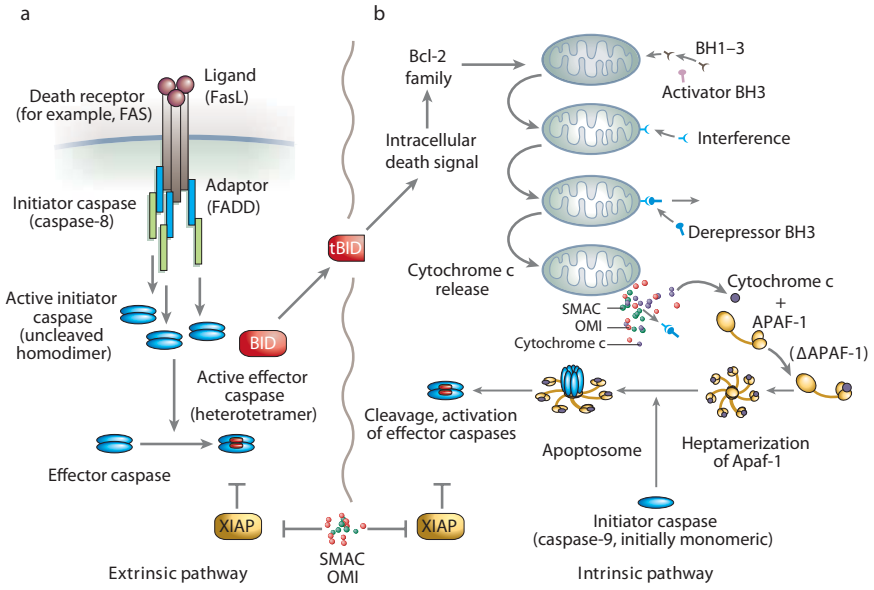

Fig. 2. The intrisinc and extrinsic pathways of apoptotic cell death. In the extrinsic pathway (panel a) Fas is bound by Fas ligand (FasL), recruiting FADD and caspase-8, and subsequent caspase-8 activation. Caspase-8 activates effector caspases (such as caspase-3 and 7) by cleavage. Furthermore, the extrinsic pathway interacts with the intrinsic pathway via caspase-8 cleavage of BID to produce tBID. In the intrinsic pathway (panel b) signals from plasma membrane, endoplasmic reticulum, cytosol or nuclei, lead to the mitochondria-outer membrane permeabilization (MOMP), a process largely regulated by Bcl-2 family members. Cytochrome c is released from mitochodria inducing conformational change and heptamerization of the cytosolic protein APAF-1. The heptamer binds caspase-9, resulting in its activation and cleavage of effector caspases. Reprinted by permission from Macmillan Publishers Ltd. Nature. Bredesen et al. 443(19), 796-802. Copyright 2006.

In the extrinsic pathway to apoptosis, the activation of death receptors (a subset of the TNF receptor-TNFR- family, including TNFR1, CD95, TNF-related apoptosis-inducing ligand-receptor-1 and 2 [TRAI-R1 and R-2]) causes the recruitment and oligomerization of the adaptor molecule FADD (Fas-associated death domain) to form the death-inducing signaling complex (DISC). This complex binds initiator caspases-8 and –10, causing their dimerization and activation (Putcha et al., 2002).

In the intrinsic (mitochondrial) pathway, the executioner caspases are activated by the initiator caspase-9. This caspase can only be activated by dimerization with the adaptor protein Apaf-1, an adapter molecule that exists in the cytosol as a monomer, and depends on the presence of holocytochrome c for its activation. When cytochorme c is available in cytosol, it binds to Apaf-1, dATP gains access to a nucleotide binding site in Apaf-1 inducing a conformational change that leads to its oligomerization. This oligomer known as "apoptosome" recruits and activates initiator caspase-9. The release of holocytochrome c from the mitochondrial intermembrane space is the rate-limiting factor for the generation of the apoptosome, therefore, the mitochondrial-outer-membrane permeabilizacion (MOMP) is the critical event responsible for caspase activation in this pathway (Green and Kroemer, 2004;Spierings et al., 2005).

The MOMP represents the "point of no return" of cell death because it can commit a cell to die even when caspases are not activated (Chipuk et al., 2006). For instance, under ischemic conditions, channels in the inner mitochondrial membrane open to allow movement of solutes and ions, a process know as mitochondrial permeability transition (MPT). This MPT results in a loss of inner membrane function and swelling of the matrix that can lead to rupture of the outer membrane. In this "caspase-independent" cell death, loss of mitochondrial permeability allows the release of other apoptogenic factors such as AIF (apoptosis-inducing factor)(Yakovlev and Faden, 2004). AIF is a mitochondrial flavoprotein with an oxidoreductase domain localized to the mitochondrial intermembrane space in living cells that translocates to the cytoplasm and nucleus under certain apoptotic conditions. AIF can induce nuclear condensation and large-scale DNA fragmentation to 50 kb fragments in a caspase-independent fashion, and it is a downstream mediator of poly(ADP-ribose) polymerase-1 (PARP-1)-induced neuronal cell death (Yu et al., 2002). PARP-1 mediates protein ADP ribosylation in response to DNA damage, and its activation

has been found to play a role in neuronal cell death induced by ischemia-reperfusion injury and in NMDA-induced excitatory neuronal cell death (Yu et al., 2002).

SCI-induced cell death involves caspase-dependent and independent mechanisms

The activation of the cytochrome c-dependent caspase-3 apoptotic cascade in neuronal and oligodendroglial cell death is a common event in human and animals models of traumatic spinal cord injury (Crowe et al., 1997;Springer et al., 1999;Springer et al., 2000;Casha et al., 2001;Knoblach et al., 2005). We have shown increased apoptosis and caspase-3 activity in a rat model of moderate contusion to spinal cord (Nesic et al., 2001). Caspases 3, 8 and 9 are activated from 1 to 72 h after injury in neurons and oligodendrocytes as well as some astrocytes (Citron et al., 2000;McEwen and Springer, 2005). In fact, inhibitors of caspases have been used to prevent SCI-induced apoptosis with different success (Barut et al., 2005;Knoblach et al., 2005;Colak et al., 2005).

Trauma to the CNS also induces the activation of caspase-independent cell death pathways, involving nuclear translocation of AIF and endonuclease G (Zhang et al., 2002). Recently it has been shown that SCI-induced oxidative stress induces AIF and Endonuclease G translocation from the mitochondria to the nuclei in apoptotic motoneurons 1 and 3 days after trauma (Yu et al., 2006). Since the convergence point between caspase-dependent and independent pathways is the regulation of the MOMP, an apoptosis-regulator that works upstream of caspase-activation by regulating the MOMP may be an effective candidate to prevent SCI-induced cell death.

Bcl-2 family of proteins are key regulators of cell death in the CNS

The Bcl-2 family of proteins play a major role in regulating the MOMP (Tsujimoto, 2003;Danial and Korsmeyer, 2004;Sharpe et al., 2004). The Bcl-2 family has been divided into 3 subclasses based on the presence of one or more conserved regions termed Bcl-2 homology (BH) 1-4 domains (Petros et al., 2004), generally corresponding to α helices

which dictate structure and function (**Fig. 3**). The BH3-only proapoptotic members (Bim, Bid, Bad, Bik, Noxa, Puma, Bmf, Hrk) serve as upstream sentinels that selectively respond to a wide variety of damage signals (including DNA damage, growth factor withdrawal), and its activity is controlled by either transcriptional control or posttranslational modification (Tsuruta et al., 2004;Kuwana et al., 2005). The "multidomain" proapoptotic members (BAX, BAK) possess BH1-3 domains and constitute a requisite gateway to the intrinsic pathway (Sharpe et al., 2004;Reed, 2006) . In response to diverse stimuli, transient interactions of BH3-only pro-apoptotic members of the Bcl-2 family, such as tBid and Bim, with the multidomain pro-apoptotic members, such as Bax and Bak, result in the oligomerization of Bax and Bak and the permeabilization of the outer mitochondrial membrane and the efflux of cytochrome c (Kuwana et al., 2005;Chipuk et al., 2006). The antiapoptotic members include Bcl-2, Bcl-x_L (Boise et al., 1993;Gonzalez-Garcia et al., 1994), Mcl-1, A1, and Bcl-w and display conservation in all four BH1-4 domains. These proteins are crucial for preventing cell death since they sequester BH-3-only proteins (Zimmermann et al., 2005) and probably the activated multidomain proteins, preventing the MOMP (Hou et al., 2003;Zhu et al., 2004).

Although Bcl-2 and Bcl-x_L share some structural and functional characteristics, they might play different roles depending on the cell type, their subcellular location, their ability to interact with other Bcl-2 members and their susceptibility to post-transcriptional modifications. In the central nervous system (CNS), both Bcl-2 and Bcl-x_L are present during embryonic development (Fujita et al., 2000;Itoh et al., 2003;Savitt et al., 2005). However, the expression of Bcl-2 is decreased in populations of neurons in the adult CNS remaining mostly in the peripheral nervous system while Bcl-x_L expression is highly expressed during adulthood (Gonzalez-Garcia et al., 1994;Alonso et al., 1997;Parsadanian et al., 1998;Hamner et al., 1999). Immunohistochemical analysis of the central nervous system of rats at various postnatal ages have shown that Bcl-x_L expression is strong in

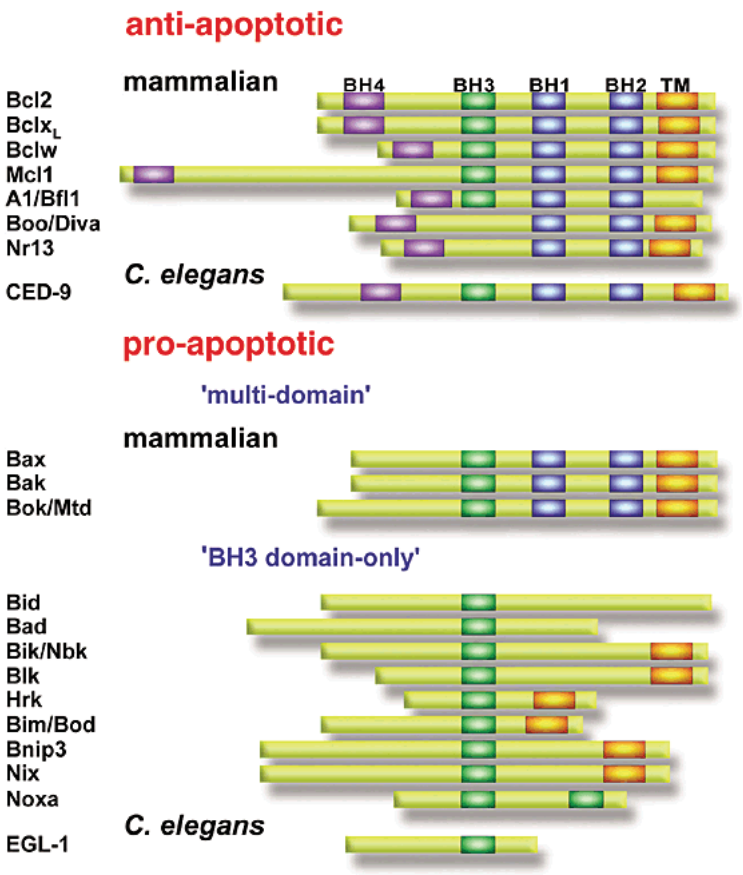

Fig 3. Bcl-2 family of proteins. Bcl-2 family members possess up to four Bcl-2 homology domains (BH1−4) corresponding to α-helical segments (denoted by colored boxes). Some members also possess a carboxy-terminal hydrophobic transmembrane (TM) domain (denoted by a red box). According to their BH domains, they can be subdivided into two categories: anti-apoptotic members and pro-apoptotic members. In general, anti-apoptotic Bcl-2 family members display sequence conservation in all four BH domains. Pro-apoptotic members can be assigned to two subsets based on sequence conservation: the more fully conserved 'multi-domain' members and a divergent subset of 'BH3-domain only' members. The BH3-only proteins cannot induce apoptosis in the absence of Bax and Bak. The BH1, BH2, and BH3 region of the anti-apoptotic and maybe of the BH multi-domain sub-family generate a hydrophobic pocket which can interact with the BH3 domain of the pro-apoptotic proteins. Most of the Bcl-2 family members possess a carboxy-terminal transmembrane domain (TM) implicated in their targeting to intracellular membrane. In Bax and Bcl-w, the C-terminal tail is engaged in the hydrophobic pocket and should fit to allow insertion in the membrane. Reprinted by perimission from Macmillan Publishers Ltd: Nature genetics, 28, 113 – 118, copyright (2001)

neuron-like cell bodies in the brain and the spinal cord, particularly the superficial layers of the dorsal horn (Mizuguchi et al., 1996). Bcl-x_L also colocalizes with immunoreactive astrocytes located throughout the white matter regions of the brain (Alonso et al., 1997). Since little is known about the particular role of Bcl-x_L in the adult CNS and in response to trauma, the next section will describe the current knowledge about Bcl-x_L function and regulation in different cell types, and in some cases, its similarity with the best known role of Bcl-2. Moreover, this section will lead into the next section which describes the potential of Bcl-x_L as an antiapoptotic therapy after SCI and the final goal of this dissertation.

Bcl-x_L structure

The overall structure of Bcl-x_L consists of eight -helices connected by loops of varying length (Aritomi et al., 1997). Two hydrophobic central helices (5 and 6) form the protein core. It contains a C-terminal transmembrane (TM) fragment and a pair of hydrophobic alpha helices (alpha5-alpha6) similar to the membrane insertion fragments of the ion-channel domain of diphtheria toxin (Garcia-Saez et al., 2004). Two basic amino acids flank both ends of the transmembrane domain and constitute the signal targeting Bcl-x_L to the mitochondrial outer membrane (MOM) (Kaufmann et al., 2003).The BH1, BH2, and BH3 regions are proximal to one another and define the top of an elongated hydrophobic groove on the surface of the protein (**Fig. 4**), that is the interaction site with the BH3 domain of proapoptotic members such as Bak and Bad (Petros et al., 2004). The BH4 domain, a conserved sequence located near the N-terminus, forms an helix and is required for the anti-death activity of Bcl-x_L (Shimizu et al., 2000b;Sugioka et al., 2003).

Bcl-x_L function at different subcellular compartments

Although the anti-apoptotic properties of Bcl-x_L have been characterized in various cell-culture systems, the functions of Bcl-x_L at the molecular level are still controversial (**Fig.5**). Current models suggest that both Bcl-2 and Bcl-x_L heterodimerize with and

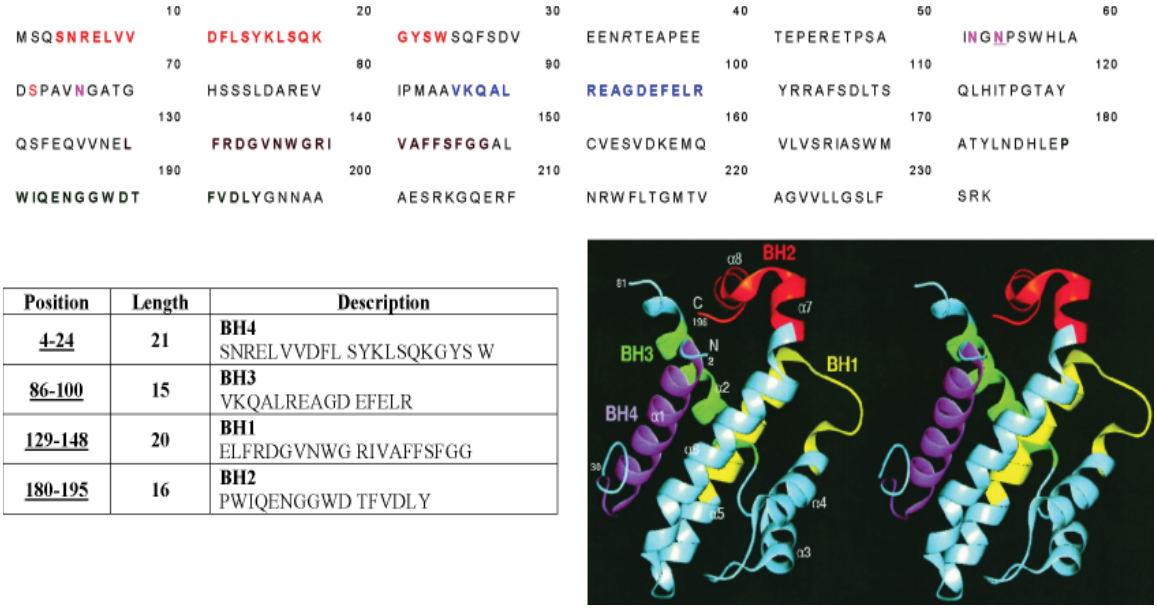

Position	Length	Description
4-24	21	**BH4** SNRELVVDFL SYKLSQKGYS W
86-100	15	**BH3** VKQALREAGD EFELR
129-148	20	**BH1** ELFRDGVNWG RIVAFFSFGG
180-195	16	**BH2** PWIQENGGWD TFVDLY

Fig 4. Rat Bcl-x_L protein sequence and BH domains (A) Swissprot Access Number P53563 . B. Ribbon structure of soluble portion (Met^{1} to Gly^{196}) of rat Bcl-x_L. The Bcl-2 homology regions are indicated by different colors: *yellow* for BH1 (Glu^{129}-Gly^{148}), *red* for BH2 (Pro^{180}-Tyr^{195}), *green* for BH3 (Val^{86}-Leu^{99}), and *purple* for BH4 (Ser^{4}-Trp^{24}). The helices α1, α2, α3, α4, α5, α6, α7, and α8 correspond to Ser^{4}-Lys^{20}, Ala^{84}-Arg^{100}, Ser^{106}-Leu^{112}, Tyr^{120}-Phe^{131}, Trp^{137}-Asp^{156}, Gln^{160}-His^{177}, Glu^{179}-Asn^{185}, and Gly^{187}-Leu^{194}, respectively (Aritomi et al., 1997). Copyright 2006 by The American Society for Biochemistry and Molecular Biology

sequester BH3-only proteins, preventing them from activating pro-apoptotic Bax and Bad (Grad et al., 2000;Jeong et al., 2004). Other evidence suggest that Bcl-2 and Bcl-x_L may modulate the activities of pro-apoptotic Bcl-2 members (Bax) by interfering with essential organelle targeting or membrane-integration processes, (Ganju and Eastman, 2002) or by sequestering Bax in the cytosol in an inactive stage (Reed, 2006). *In vitro* studies of wild type and Bcl-x_L mutants have shown that in contrast to Bcl-2 (always associated with organelles-membrane) the soluble form of Bcl-x_L exists in the cytosol as a homodimer and that this dimeric form is important for Bcl-x_L insertion into the mitochondria and its bioactivity (Jeong et al., 2004). Homodimer formation occurs through the BH-3 binding pocket and the C-terminal hydrophobic anchor of Bcl-x_L (Tsujimoto, 2003). It has been proposed that

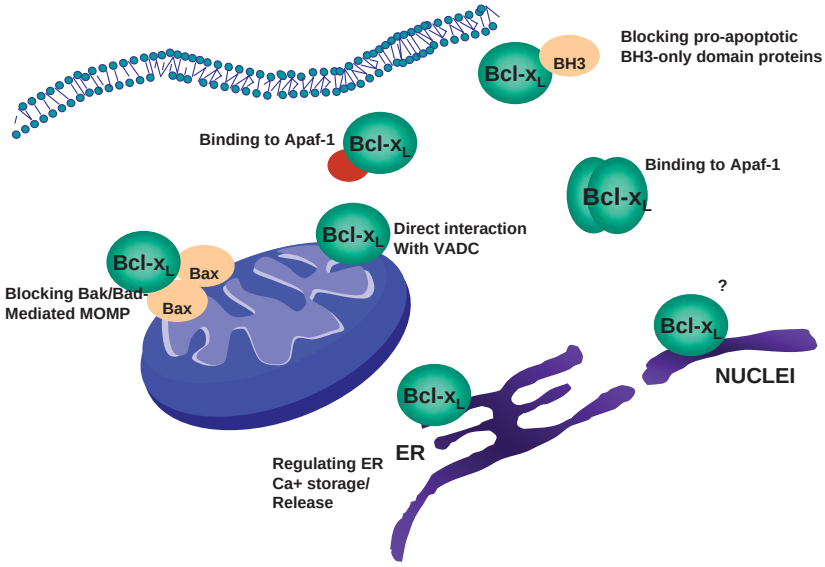

Fig. 5. Functions of Bcl-x$_L$ at different organelles to prevent apoptosis. In the cytosol, Bcl-x$_L$ binds BH-3 only proapoptotic proteins and prevents them to activate Bax/Bak. Bcl-x$_L$ can protect cells by regulation of the mitochondrial voltage-dependent anion channel (VDAC) during the formation of the mitochondrial permeability pore (MPP). Recently, a new role for Bcl-x$_L$ in the modulation of intracellular Ca2+ levels at ER by interaction with ER resident pore-forming molecules has been proposed (Bredesen et al., 2006) .

upon apoptotic stimuli, pro-apoptotic Bad triggers Bcl-x$_L$ to the mitochondrial membrane *in vivo* and *in vitro* by disrupting Bcl-x$_L$ homodimers (Jeong et al., 2004). Additionally, since Bcl-x$_L$ is able to bind Apaf-1, it has been suggested that cytosolic Bcl-x$_L$ could act preventing oligomerization of Apaf-1 and subsequent caspase activation in healthy cells (Yajima and Suzuki, 2003).

Most studies agree that the anti-apoptotic activity of Bcl-x$_L$ occurs at mitochondria, either by blocking pro-apoptotic proteins or by a direct action on the mitochondrial function that can be independent of its interaction with other Bcl-2 members (Cheng et al., 1996;Vander Heiden et al., 1997;Minn et al., 1999;Hammond et al., 2001;WANG et al., 2004). For instance, Bcl-x$_L$ can protect cells by regulation of the mitochondrial voltage-dependent anion channel (VDAC) during the formation of the MPT (Shimizu et al., 2000a;Vander Heiden et al., 2001). Bcl-x$_L$ prevents mitochondrial multiple conductance channel opening,

cytochrome c release and caspase-3 like activity following 6-Hydroxydopamine treatment in the human neuroblastoma cell line SH-SY5Y (Jordan et al., 2004). In non-neuronal cells, Bcl-x_L protects from growth factor deprivation and TNF-α induced apoptosis by increasing ATP levels and sustaining mitochondrial ATP levels (Vander Heiden et al., 1999;Gottlieb et al., 2000).

Although mitochondrial alterations represent a major step in the initiation of apoptosis, increasing evidence implicates the endoplasmic reticulum as an important organelle in the initiation of apoptosis (Reimertz et al., 2003;Faitova et al., 2006;Oakes et al., 2006). The ER-mediated apoptosis occurs either in concert with mitochondria or occurs by a mechanism independent of the mitochondrial pathway (Pinton and Rizzuto, 2006) and seems to be mediated mainly by the modulation of intracellular Ca^{2+} levels (Foyouzi-Youssefi et al., 2000). It has been proposed that Bcl-2 (and probably Bcl-x_L) reduce ER Ca^{2+} levels thus modulating the efficacy of apoptotic mediators that use Ca^{2+} as an activator/potentiator factor (Pinton et al., 2000). The mechanism by which Bcl-2 or Bcl-x_L modulate ER Ca^{2+} permeability are controversial, but several authors suggest that Bcl-x_L or Bcl-2 could facilitate Ca^{2+} leakage from the ER by forming a channel, either by oligomerizing or by interacting with other Bcl-2 family members (Thomenius et al., 2003;Oakes et al., 2005). Alternatively, Bcl-2 and Bcl-x_L could interact with endogenous ER-channels or pore-forming proteins residents in the ER (Ng and Shore, 1998;Tagami et al., 2000). Supporting this model, Foskett's group (2005) demonstrated that Bcl-x_L directly binds to the Inositol 1,4,5-trisphosphate receptor (InsP3R) ER Ca^{2+} release channel and in single channel electrophysiollogy assays with isolated nuclei, addition of Bcl-x_L sensitized the InsP3R to low agonist doses, then reducing ER Ca^{2+} concentration and stimulating mitochondrial bioenergetics (White et al., 2005).

Post-translational modifications of Bcl-x_L that regulate its anti-apoptotic function

Bcl-x_L contains an unstructured loop between the BH3 and BH4 regions that is non-conserved among Bcl-2 family proteins (Aritomi et al., 1997). This loop contains recognition sites for caspase-mediated cleavage and phosphorylation, mechanisms that appear to regulate the function of Bcl-x_L (and Bcl-2) after different insults in multiple cell lines (Ojala et al., 2000;Liang et al., 2003;Muhlethaler-Mottet et al., 2004;Upreti et al., 2006). However, the occurrence of such modifications in the CNS and in the injured spinal cord has not been addressed.

Cleavage

Cheng et al, observed that endogenous and overexpressed Bcl-x_L was cleaved by endogenous caspases during cell death induced by IL-3 withdrawal (Cheng et al., 1997). Bcl-x_L was cleaved between Asp^{61} and Ser^{62} (i.e HLAD61S) and between Asp^{76} and Ala^{77} (i.e SSLD76A) by caspases-3/CPP32 (Cheng et al., 1997;Fujita et al., 1998). Cleavage produced two ~18 KD fragments that can be detected by western blot following apoptotic insult. The smaller cleaved fragment results from the removal of NH-2 terminal 15 amino acid (aa 62 to 76) of the larger cleaved fragment. Interestingly, the proteolytic attack on Bcl-x_L has been found to convert Bcl-x_L into a pro-apoptotic protein (Figueroa, Jr. et al., 2003;Jonas et al., 2004). The cleavage fragments are structurally and functionally similar to the Bax-like death agonist lacking the BH4 domain and promoting apoptotic cell death (Cheng et al., 1997;Fujita et al., 1998). Then, Bcl-x_L protein cleavage by caspases accelerates apoptotic cell death not only by decreasing the expression level of the death-antagonist Bcl-x_L but also by increasing the expression level of the death-agonist 18kDa Bcl-x_L fragments (Clem et al., 1998;Fujita et al., 1998;Kirsch et al., 1999). Several investigators have reported the loss of Bcl-x_L protein expression during apoptosis in cell lines; however, further information on the fate of the Bcl-x_L *in vivo* has not yet been reported.

Phosphorylation

Bcl-x_L contains sequences surrounding Ser^{56}, Ser^{62}, Thr^{47} and Thr^{115} that resemble consensus motif for stress-activated protein kinase/c-Jun N-terminal Kinase (SAPK/JNK) substrate (Kharbanda et al., 2000;Basu and Haldar, 2003). Using isolated and bioenergetically competent rat brain mitochondria, Schroeter et al (2003) demonstrated that JNK catalyzes the phosphorylation of both Bcl-x_L and Bcl-2 (Schroeter et al., 2003), but the mechanism(s) by which phosphorylation impairs the anti-apoptotic role of Bcl-2 or Bcl-x_L are still controversial. Most studies agree that phosphorylation results in a reduction in anti-apoptotic function (Ojala et al., 2000;Simizu et al., 2004;Tamura et al., 2004), possibly by abrogating the ability of Bcl-2 or Bcl-x_L to bind Bax or other Bcl-2 family members (Ishikawa et al., 2003;Schroeter et al., 2003). Moreover, it has been found that Bcl-2 phosphorylation preceded proteasome-dependent degradation of Bcl-2 protein in mitotic arrested cells after microtubule damage (Chadebech et al., 1999). Additionally, Grethe et al found p38 MAPK-dependent ser-thr phosphorylation and proteasome-dependent degradation of Bcl-x_L in response to TNF-induced apoptosis of endothelial cells (Grethe et al., 2004). Studies of Bcl-2 phosphorylation under physiological conditions in human colon, tonsil and other tissues have been reported, and a recent study demonstrated that Bcl-2 phosphorylation in the BH4 domain precedes caspase-3 activation and cell death in a model of neonatal cerebral hypoxia and ischemia (Hallin et al., 2006).

The signals that trigger Bcl-x_L phosphorylation seem to be related to the disruption of microtubule network (Poruchynsky et al., 1998) and DNA damage (Kharbanda et al., 2000). SAPK/JNK phosphorylate Bcl-2 and Bcl-x_L *in vitro* in response to microtubule disarraying agents such as taxol and vinblastine (Fan et al., 2000). While Bcl-2 can be phosphorylated on multiple Ser/Thre residues (Tamura et al., 2004), Bcl-x_L is phosphorylated only on Ser^{62} following taxol exposure of cancer cells. Bcl-x_L can also be phosphorylated

at Thr^{47} and Thr^{115} in response to DNA damage induced by ionizing radiation *in vitro* (Kharbanda et al., 2000). However, microtubule inhibitors characteristically stimulate ser^{62} Bcl-x_L phosphorylation *in vitro*, where as other apoptotic stimuli do not (Du et al., 2005). To date, no studies have addressed the role of Bcl-x_L phosphorylation *in vivo* in the normal or injured CNS.

Bcl-x_L as an neuroprotective target after SCI

The previous section showed that multiple mechanisms could impair Bcl-x_L function and introduced the first objective of this dissertation that is to identify the mechanisms by which the antiapoptotic function of Bcl-x_L could be impaired after SCI and therefore, contribute to the delayed cell death. This section leads to the final goal of this dissertation and it is the potential use of Tat-Bcl-x_L to prevent of cell death after SCI.

We propose that downregulation of Bcl-x_L anti-apoptotic function (i.e by trauma-induced phosphorylation), could be responsible, at least in part, for the delayed cell death occurring after SCI. Several findings support the importance of Bcl-x_L in preventing cell death in the injured CNS. For instance, sections of rhizotomized spinal cord showed a dramatic decrease in the number of intensely Bcl-x_L immunostained axon-like fibers innervating the superficial layers of the dorsal horn ipsilateral to the lesion (Alonso et al., 1997). Also, conditional Bcl-x_L overexpression protected postnatal and adult neurons from traumatic hypoxia (Matsuoka et al., 2002;Wen et al., 2002), and metabolic injury (Xu et al., 1999;Shinoura et al., 2000;Matsuoka et al., 2002;Panickar et al., 2005). Furthermore, exogenous Bcl-x_L has been shown to be highly effective in protecting against cell injury in a variety of injuries such as ischemia (Asoh et al., 2002;Cao et al., 2002b), oxidative stress (Cherbonnel-Lasserre and Dosanjh, 1997) hypoglycemia (Panickar et al., 2005), neurotrophin deprivation (Vander Heiden et al., 1999) and excitotoxicity (Matsuoka et al., 2002).). Since most of these stresses take place in the injured spinal cord, is expected that

restoring Bcl-x_L function could be a key factor in preventing SCI-induced cell death. In support of this hypothesis, short-term administration of Bcl-x_L-fusion protein to the injured spinal cord significantly increases neuronal survival within 24h after spinal injury (Nesic-Taylor et al., 2005).

Exogenous administration of Bcl-x_L in the injured CNS

To overcome the problems related to delivery of the protein into the CNS, several proteins including Bcl-$x_{L,}$ have been linked to "protein transduction domains (PTD)"(Soane and Fiskum, 2005a). These are sequences of about 11 amino acids which are able to pass the blood-brain barrier and into cell membranes (Schwarze et al., 1999;Wadia and Dowdy, 2005). Among several PTDs, the sequence derived from HIV trans-activator of transcription (TAT) can transduce peptides and larger proteins into the brain after systemic administration (Nagahara et al., 1998;Murriel and Dowdy, 2006).

The mechanism of TAT-mediated protein internalization is not completely understood, but it is known that cell heparin sulfate proteoglycans are mediators of TAT-fusion proteins attachment to cell membranes *in vivo* (Wadia and Dowdy, 2005) . Since heparin sulfates are present on the surface of several cell types, Tat-peptides and conjugated proteins are able to penetrate a wide variety of cells including neurons, glial and endothelial cells (Schwarze et al., 1999). Upon attachment, Tat-fusion proteins seem to be internalized through caveolar endocythosis (Potocky et al., 2003) or macropynocytosis (Wadia et al., 2004;Kaplan et al., 2005) in non-neuronal cells. In neurons, Soane et al (2005) demonstrated that TAT-mediated protein internalization occurs though a lipid raft-dependent endocytic process (Soane and Fiskum, 2005b).

The process of fusion-protein intracellular activity is unknown, but several studies have demonstrated their biological activity *in vivo* (Diem et al., 2005) and *in vitro* (Soane and Fiskum, 2005b). In particular, it has been shown that intravenous delivery of TAT-Bcl-

x_L fusion protein efficaciously reduces brain injury in adult models of cerebral ischemia (Asoh et al., 2000;Kilic et al., 2002;Cao et al., 2002a); and is protective against neonatal hypoxic-ischemic brain injury in rats (Dietz et al., 2002;Yin et al., 2006). Furthermore, the BH4-Bcl-x_L domain fused to Tat (TAT-BH4) can prevent apoptotic changes of isolated mitochondria (Shimizu et al., 2000b) and is able to reduce spontaneous caspase activation and cytotoxicity caused by IL-1 in several cell types (Klein et al., 2004), and inhibits apoptosis induced by several mechanisms in vitro and in vivo (Klein et al., 2004;Hotchkiss et al., 2006).

Experimental Rationale and Hypothesis

It has been shown that Bcl-x_L mRNA and protein levels decrease after SCI (Nesic-Taylor et al., 2005) and Bcl-x_L may be inactivated by phosphorylation or cleavage that yields pro-apoptotic fragments. Thus, transcriptional downregulation and post-transcriptional inactivation of Bcl-x_L are two main mechanisms leading to apoptosis of neurons and oligodendrocytes after SCI. Therefore, interventions leading to increased local levels of active Bcl-x_L should decrease apoptotic cell death and improve functional recovery after SCI.

Given this hypothesis, the goal of my dissertation is to further elucidate a role for Bcl-x_L in SCI-induced cell death by identifying the mechanisms that underlie the impairment of its antiapoptotic funtion during the acute phase of trauma, and by evaluating its effect as a potential neuroprotective therapy. I demonstrate that phosphorylated and unphosphoryalted forms of Bcl-x_L are present in different subcellular compartments in the uninjured spinal cord, and that Bcl-x_L subcellular localization of both forms is modulated early after trauma (Chapter 3). Furthermore, I found evidence that relate phosphorylation of Bcl-x_L as a pro-apoptotic event in the injured spinal cord and in an in vitro model (Chapter 3). Finally, I have found evidence that administration of exogenous Bcl-x_L (Tat-Bcl-x_L) and

its anti-apoptotic domain BH4 (Tat-BH4-Bcl-x_L) into the injured spinal cord decrease the apoptotic cell death following SCI, but do not improve the long term locomotor recovery after SC trauma (Chapter 4). These data suggest that phosphorylation can impair the anti-apoptotic function of Bcl-x_L and that administrating exogenous Bcl-x_L in the injured spinal cord could lead to a delayed cell death rather than preventing cell death in the long term.

CHAPTER TWO: MATERIALS AND METHODS

Expresion and purification of tat-bcl-x_L fusion protein and Tat-BH4 peptide

The P-Tat-HA-Bcl-x_L expression vector (a generous gift from Dr. R.Pastori, Miami, FL, with permission of Dr. S.F. Dowdy, St Louis, MO) was generated by cloning the coding region of human Bcl-x_L in frame with the TAT peptide into the pTAT-HA bacterial expression vector (Klein et al., 2004). The vector pTAT-HA has an N-terminal 6-histidine leader followed by the 11-amino-acid TAT-protein transduction domain, a hemaglutinin (HA) tag and a polylinker (Nagahara et al., 1998). To produce the fusion protein, the plasmid was transformed into *E. coli* BL21 competent cells and incubated overnight on Carbenicillin (100ug/ml)-selective LB plates. A single colony was inoculated in LB selective medium and protein expression was induced by incubation with IPTG (1mM final concentration) for 1h. Bacteria were lysed by sonication and denatured in 8M urea. The supernatant was subjected to metal affinity chromatography using a Ni-NTA column. Salt was removed by gel filtration and protein identity was confirmed by western blotting using antibodies against Bcl-x_L and the HA-tag as described below. This procedure was performed by the protein expression and purification core facility at UTMB.

The Tat-BH4 peptide HIV-TAT_{48-57}-β-Ala-Bcl-x_L $BH4_{4-23}$ (Calbiochem, La Jolla, CA) containing the conserved N-terminal homology domain (BH4) of Bcl-x_L (amino acids 4 - 23) is linked to a 10-amino acid HIV-TAT_{48-57} sequence with a β-alanine residue as a spacer.

Cell Culture

PC12 rat pheochromocytoma cells were maintained in RPMI 1640 medium (Sigma-Aldrich, St Louis, MO) supplemented with 5% FBS (Fetal bovine serum, JHR

Biosciences, Lenexa, KS), 5% DHS (Donor horse serum, JRH Biosciences, Lenexa, KS), 100U/ml penicillin, 100mg/ml streptomycin (GIbco, Invitrogen, US), in a 5% CO_2/ 95% air environment.

For differentiation, exponentially growing PC12 cells were seeded at 10^4cells/ml and allowed to adhere overnight. Cells were then treated with NGF (50ng/ml) for 7 days, changing the medium every 2 days.

Cell Immunochemistry and tunel staining

For immunofluorescence analysis of Bcl-x_L phosphorylation in apoptotic cells, PC12 cells were plated on glass coverslips (Warner Instruments, Inc) pre-coated with 0.5mg/ml water solution of poly-D-lysine (Sigma, St. Louis, MO) and differentiated as described previously. After 7days of differentiation, medium containing 200nM vinblastine (Sigma) was added and cells were incubated for 24h. At indicated times, cells were fixed on freshly prepared 3.7% paraformaldehyde for 10 min at 4˚C, and then incubated with 10% normal goat serum (NGS, Gibco, BRL, Life technologies), 0.3% Bovine serum albumin (BSA, Sigma, St. Louis, MO) 0.4% Triton X-100 (St. Louis, MO) to block nonspecific binding. Rabbit polyclonal Anti-Bcl-x_L (1:500, CS-7195, Cell signaling, Danvers, MA); rabitt polyclonal anti-P-ser^{62}Bcl-x_L (1:500, Biosource, Camarillo, CA); were incubated alone or in combination with mouse monoclonal anti-Cytochrome C Oxidase IV (COX-IV, 1:2000, Abcam, Cambridge, MA) overnight at 4˚C. After rinsing in PBS, the slides were incubated with secondary anti-rabbit IgG AlexaFluor 568 and anti-mouse IgG AlexaFluor 488 (1:1000, Molecular Probes, Eugene, OR) diluted in TBST for 1h. Slides were mounted in medium with DAPI (Vector Laboratories, Burlingame, CA). Total number of cells (blue nuclei staining with DAPI), and P-ser^{62}Bcl-x_L expressing cells (red) were counted in three 20X fields from 3 different coverslips from control and vinblastine treated-cells.

To assess cell death, cells were double immunostained with P-ser^{62}-Bcl-2 anitbody (1:200) and counterstained with TdT fluorescenin (Tunel assay TACS In situ Kit, R&D systems, Minneapolis, MN) as follows. After fixation, cells were permeabilized with Cytonin (R&D Kit) for 1h at room temperature, washed in 1X PBS and incubated overnight at 4˚C with primary antibody (P-ser^{62}Bcl-x$_L$, 1:200) diluted in 1% NGS, 0.3% BSA, 0.4% Triton X-100. After washing, cells were incubated with secondary anti-rabbit IgG AlexaFluor 568 (1:1000) for 1h at room temperature, and then washed 3 times with PBST. Cells were incubated for 1min in 1X TdT labeling buffer and then incubated with 50ul of Labeling reaction mix (containing TdT dNTP mix, TdT enzyme, Mg++, TdT Buffer) for 1h at 37˚C. After washing, cells were incubated with Strept-Fluor solution for 20 min at room temperature, then washed in 1X PBS and mounted in medium with DAPI. With this method, apoptotic cells appear green under the fluorescein filter (495nm) and all the cells nuclei appear blue with DAPI staining.

Rat Spinal Cord Contusion Model

Weight-matched Sprague-Dawley male rats (175-200g, 200-225g) were obtained from Harlan Laboratories (Indianapolis, IN) and housed at UTMB Animal Care facilities until surgery-weight was reached (225-240g). All rats were anesthetized with 35 mg/kg pentobarbital (Nembutal Sodium, Abbott Laboratories, Chicago, IL) intraperitoneally, and subjected to laminectomy over spinal segments T10. A moderate spinal contusion injury over the spinal segment T10 was performed with the Infinite Horizon spinal cord impactor (single time, 150 Kdynes producing a 0.8mm displacement) as described previously (Nesic-Taylor et al., 2005). The wound was closed by suturing the muscle and fascia and the skin closed with surgical staples. Following injury, animals were injected subcutaneously with 5mL of 0.9% sterile saline and placed on a heating pad to maintain body temperature. Animals were kept under anesthesia and sacrificed if sampling occurred during the next

hours. Animals received prophylactic antibiotic (Baytril, 2.7mg/Kg twice a day for 5 days), analgesic (Buprenorphin, 0.1mg/Kg twice a day for 3 days) and saline (5ml, daily for 5 days) to prevent dehydration. Bladders were voided manually twice a day until normal function returned. Sham-treated animals were exposed to the same procedure without the contusion injury. All procedures complied with the recommendations in the NIH Guide for the Care and Use of Laboratory Animals and were approved by the UTMB Animal Care and Use Committee.

Intrathecal delivery of drugs in the rat spinal cord

Animals that were used in experiments involving intrathecal catheters also received a partial laminectomy of the thirteenth thoracic vertebrae before being impacted by the IH device. Avoiding damage to the spinal cord, the dura was raised with an extrafine forceps and cut with fine scissors. Sterilized polyethylene tubing (32G/PE-60; Rethaco, LLC, Allison Park, PA) was inserted into the intrathecal space through the punctured dura at T13-L1 and extended so that the tip of the catheter was directly beneath the T11 vertebrae. The catheter was connected to a primed miniosmotic pump that was placed in a subcutaneous pocket made over the sacral vertebrae caudal to the incision. The catheter was secured by suture and superglue to both the L1-L2 vertebral junction and the fascia over the paravertebral muscles at the incision margin, the wound was closed by suturing muscle and fascia and the skin closed with surgical staples.

Tat-Bcl-x_L and Tat-BH4 were dissolved in saline (vehicle) and filtrated throughout a 0.2um sterile filter. The specific doses and delivery rate of either drug or vehicle into the spinal cord were achieved by using mini-osmotic pumps (Alzet, Durect Co. Palo Alto, CA) 1003D (24h) or 1007D (7days) as detailed in chapter 4. To prime the pumps, the interior container was filled with either Tat-Bcl-x_L, Tat-BH4 or saline and incubated overnight at 37˚C. Animals surviving for 60 days were anesthetized and the catheter was retrieved from

the spinal cord by day 7. Post-surgical antibiotic and pain relievers were administered as previously described.

Protein extraction and subcellular fractionation from rat spinal cord segments

For protein extractions, rats were perfused with PBS and spinal cord-segments were immediately frozen in liquid nitrogen. The tissue was homogenized in ice-cold Buffer M (250 mM sucrose, 20 mM Hepes, 1 mM EDTA, 1 mM EGTA, 1 mM dithiotheitol, 1 mM PMSF, pH 7.4, protease inhibitor cocktail and phosphatase inhibitor cocktail 2 (Sigma, Saint Louis, MO) using a Dounce homogenizer. To obtain different subcellular fractions the homogenate was centrifuged three times at 800*x g* for 20 min (Eppendorf 5810R centrifuge) to collect nuclei and cell debris (pellet). The supernatant was set aside and the pellets collected at each step were pooled and washed two times with 500 µl of Buffer M to separate the nuclei from complete cells and cytosolic proteins. Nuclear pellets were mixed in a vortex plate at 1,400 rpm, 4°C for 20 min in 70 µl of nuclear extraction buffer (10 mM Hepes, 10 mM KCl, 0.1 mM EDTA, 0.1 mM EGTA, 1 mM DTT, 0.5 mM PMSF, 2 µg/mL antipain, 2 µg/mL chymostatin, 2 µg/mL pepstatin, 2 µg/mL leupeptin). After centrifuging at 10,000 *x g* for 10 minutes, the nuclear proteins contained in the supernatant were aliquoted and the pellet discarded. The supernatant-containing cytosolic proteins, mitochondria and endoplasmic reticulum (ER) was centrifuged at 8,000 *x g* for 20 min (Eppendorf 5810R centrifuge). The resultant pellet, containing intact mitochondria, was washed two times by titration with Buffer M and suspended into 40 µl of mitochondrial extraction Buffer (Active Motif CN40015, Carlsbad CA). The cytosolic fraction was finally separated from ER by centrifuging at 100,000 *x g* for 1 h. The last pellet containing ER was resuspended in the same lysis buffer used to disrupt mitochondria (Active Motif CN40015, Carlsbad CA). All procedures were performed at 4°C. Protein concentrations were determined by using

the BioRad Protein Assay, according to the manufacture's instructions (BioRad, Hercules, CA).

Measurement of apoptotic cell death in Spinal cord tissues by elisa

Levels of apoptotic cell death 24h and 7 days after spinal cord injury were examined by commercially available sandwich technique ELISA kit (Roche Applied Science, Germany). The assay measures the amount of oligonuclesomes released to the cytosol, an event that occurs during apoptotic cell death, but not during necrotic processes. Briefly, 80 μg of cytosolic extract from spinal cords were added to ELISA microplates covered with an anti-histone antibody. Complexes formed by the antibody and histones present in cytosolic oligonucleosomes were detected by a second peroxidase-conjugated antibody against DNA. Oxidized peroxidase enzymatic products in the microplate wells were read at 405 nm absorbance in a MRX Miroplate Reader (Dynex Technologies, INC).

Western Blotting

Protein extracts were boiled for 5 min in Laemmli buffer (100 mM Tris, pH 6.8, 250 mM 2-mercaptoethanol, 4% SDS, 0.01% bromophenol blue, 20% glycerol). Equal amounts of protein (40 μg) were separated by using 10%–15% SDS-polyacrylamide gel electrophoresis and electrotransferred overnight (4ºC, 25volts) onto a Immobilon-P® membrane (Millipore, Billerica, MA). Membranes were then blocked in 5% nonfat milk in PBS and then probed with different antibodies (3% BSA replaced nonfat milk when antibodies against phosphorylated proteins were used). The primary antibodies were diluted in 1% Blocking buffer as follows: rabbit polyclonal Anti-Bcl-x_L (1:1000, SC-7195, Santa Cruz Biotechnology, Santa Cruz, CA); rabbit polyclonal Anti-Bcl-x_L (1:2000, CS-7195, Cell signaling, Danvers, MA); rabitt polyclonal anti-P-ser^{62}Bcl-x_L (1:1000, Biosource, Camarillo, CA); rabbit polyclonal anti- HA-tag (1:4000, Abcam Cambridge, MA) mouse monoclonal anti-Cytochrome C Oxidase IV (COX-IV, 1:2000, Abcam, Cambridge, MA)

and mouse monoclonal anti-calnexin (1:2000, Abcam, Cambridge, MA). Secondary antibodies anti Mouse-IgG or rabbit IgG conjugated with HRP (Bio Rad, Hercules, CA) were used accordingly. Visualization of the proteins was accomplished using an enhanced chemiluminescence detection kit (ECL, Amershan Biosciences, UK). The relative amount of immunoreactive protein in each band was determined by scanning densitometric analysis of the X-ray films. Autoradiographs were scanned (canonScan 4200F) and densitometry was performed with AlphaEasy v5.5 Software. Density readings were normalized against control samples on the same-blot. When membranes were reprobed, the bound antibodies were incubated in stripping buffer (Pearce, Rockford, IL) for 15 min, followed by two washes in TBS for 20 minutes.

Control peptide experiments were performed by incubating samples according to the western protocol described, with the exception that the primary antibody is preabsorbed with 5 µg of control peptide at room temperature for two hours before use.

To test the specificity of the P-ser^{62}-Bcl-x_L antibody used in western blot assays, identical cytosolic samples were transferred to two membranes and incubated overnight at 30^{o}C with either 500 units of calf intestine phosphatase (Roche Applied Science, Germany) in the manufacturer-supplied reaction buffer or reaction buffer alone. The membranes were washed 5 times with TBS-T and immunoblots using P-ser^{62}-Bcl-x_L antibody were performed as described above.

Spinal cord processing for histological analysis

Rats were intracardially perfused with 300ml of 0.1M PBS, followed by 500 mL of 4% paraformaldehyde in 0.1 M phosphate buffer. The spinal cords were removed and post fixed in 4% paraformaldehyde for 2 h at 4°C, then rinsed and cryoprotected in 30% sucrose in phosphate buffer for 48 h at 4°C. Spinal cords were cut in 1.5cm segments centered at the lesion site and equivalent segments of different experimental groups were embedded in a

single block in OCT (Optima Cutting Temperature) medium (Fisher Scientific, Suwannee, GA). Transverse serial sections (10μm) through the complete segment were mounted on glass-slides and frozen at –20°C.

Double-Immunofluorescent Labeling of Spinal cord sections

Slides were rinsed three times in Tris-phosphate-buffer 0.3 % Triton-X (TBST), pH 7.4, for 10 min and then blocked with 5% normal goat serum, 1% BSA (Sigma, St. Louis, MO) TBS for 30 min at room temperature (RT). The samples were incubated overnight with IgG primary antibodies diluted in TBST 1% BSA, 1% NGS as indicated. Rabbit polyclonal anti-Bcl-x_L SC-7195 (1:100, Santa Cruz Biotechnology, Santa Cruz, CA), rabbit monoclonal anti-Bcl-x_L E-1018 (1:200 Epitomics, Burlingame, CA), rabbit polyclonal anti-Bcl-x_L CS-2762 (1:200, Cell Signalling), rabbit polyclonal anti P-ser^{62}-Bcl-x_L (1:200, Biosource, Camarillo, CA), rabbit polyclonal anti HA-tag against exogenous Tat-Bcl-x_L (1:1000, Abcam, CA) were used alone or in combination with mouse monoclonal antibody recognizing neurons (NeuN, 1:5000, Chemicon, Temecula, CA); oligodendrocytes (Ab-7-CC1, 1:100 Oncogene, Boston, MA); microglia (OX-42 Anti-rat CD11b, 1:200, Serotec, Raleigh, NC); astrocytes (GFAP, 1:500, Serotec, Raleigh, NC); neuron-specific ß-III tubulin Tuj-1 (Covance Research products, Berkeley, CA); phosphorylated nurofilaments M and H (1:1000, Chemicon, Temecula, CA) and mitochondria (COX-IV 1:1000, Abcam, Cambridge, MA). When using more than one antibody, these were premixed at final concentrations prior to use. After rinsing three times in TBS for 10 min, the slides were incubated with secondary anti-rabbit IgG AlexaFluor 568 and anti-mouse IgG AlexaFluor 488 (1:1000, Molecular Probes, Eugene, OR) diluted in TBST for 1h. Sections were coverslipped using mounting medium with DAPI (Vector Laboratories, Burlingame, CA). Negative controls omitting the primary antibodies were performed each time. Imaging was performed using laser scanning confocal microscopy (Nikon Eclipse 800 with Roper

CoolSnap FQ monochrome digital camera, Nikon DXM1200 color digital camera and Laser sharp 2000 software). For confocal analysis, up to 10 sequential optical sections were collected over an optical scanning plane of 10 μm and then stacked to create the final image.

Competition assays on Spinal cord sections

Competition assays to test the specificity of the anti-P-ser^{62} Bcl-x_L antibody were performed by incubating the sections according to the described protocol, with the exception that the primary antibody was preabsorbed either with 500 μg of non-phosphorylated Bcl-x_L control peptide or 500ug of phosphorylated Bcl-x_L control peptide, at room temperature for two hours before use. Aditionally, to discard a possible cross-reaction with phosphorylated neurofilaments, some slides were incubated overnight with a 10 fold excess of anti-neurofilament M and neurofilament H phosphorylated forms antibody (Chemicon, Temecula, CA) either prior to or concomitant with the anti-P-ser^{62}-Bcl-x_L antibody.

Microglia and macrophages immunohistochemistry

Frozen sections were dried for 2h at room temperature followed by 2h at 37C. After rinsing with 0.2M PB for 1 min, sections were blocked with 4% horse serum (HS) in 0.1M PBS for 1h at room temperature. Mouse monoclonal antibody against OX-42 or ED-1 (1:400; Serotec) diluted in 0.1M PBS 1% HS was incubated overnight at 4C in humidified chambers. After rinsing, sections were incubated overnight with biotinylated secondary antibody (rat-preabsorbed, 1:400 in 0.1M PBS; Vector Laboratories, Burlingame, CA). After rinsing, endogenous peroxidase acitivity was quenched by incubating with 6% H_20_2/methanol for 15 min. The reaction was visualized with Elite ABC-reagent for 1h (Vector Laboratories, Burlingame, CA) followed by DAB substrate (Vector Laboratories, Burlingame, CA). Sections were dehydrated in ascending alcohols, cleared in xylene and mounted in synthetic resine (permount).

Quantitative analysis of immunohistochemistry

Neuronal survival was evaluated by counting Neu N staining cells at the dorsal and ventral horn 4mm rostral and 4mm caudal to the lesion epicenter. Total number of NeuN/DAPI staining cells present in a 20X objective at both dorsal and ventral horn of two sections spaced by 200μm were counted and averaged per animal.

Microglia/macrophage density analysis was performed by measuring the proportional area (PA) of immunoreactive cells relative to the total sample area as reported by Popovich et al (2006). The immunoreactivity expressed as proportional area (PA) has been shown to be an accurate measurement for changes in number and size of labeled microglia in the rat spinal cord. Briefly, images of three consecutive sections containing the lesion epicenter or 4mm rostral to the epicenter, stained with OX-42, were analyzed by using the Image Pro-Express analysis system. At the lesion epicenter, the intensity of OX-42 staining over a $3mm^2$ area (containing all the cross section of the cord) was measured for three consecutive sections per animal. At the rostral sections, intensity of OX-42 staining of a $0.25mm^2$ area was measured at the dorsal funiculus, ventral horn and lateral funiculs in 3 consecutive sections per animal. The final PA value for animal, represent the average of values obtained for the 3 consecutive sections at a given area.

Behavioral assesment

Open-field locomotor testing using the Basso-Bettie-Bresnahan (BBB) locomotor rating scale was performed daily for the first 14 days after injury and once every two weeks thereafter for 6 weeks. Rats were tested pre-operatively and trained to locomote in an open field. All the animals were coded and behavioral analyses were performed for an investigator blinded with respect to the treatment groups. The BBB scale is a 21 point ordinal scale that assigns scores based in behavioral categories. Recently, a transformation of the BBB scale that pools scores 2/3/4 in the lower part of the scale, was reported to

enhance the metric properties of the scale, allowing the application of parametric statistic techniques (Ferguson et al., 2004). Thus, we report the combined transformed BBB scores for left and right hindlimbs tallied by groups and plotted as a function of time after injury.

Statistical analysis

Group-mean of western blot densitometric values, immunohistochemical and morphometric measures were compared by using one-way ANOVA and Tukey's honestly significant difference test for post-hoc analysis. Changes in transformed BBB scores over time were analyzed using repeated-measures two-way analysis of variance (ANOVA) with treatments and time as factors, followed by Bonferoni Pots-hoc analysis. Results were considered statistically significant at $P<0.05$. All data points represent group mean ± SD.

CHAPTER THREE: PHOSPHORYLATION OF BCL-XL AFTER SPINAL CORD INJURY

Introduction

Traumatic spinal cord injury induces delayed cell death of neurons and oligodendroglia at and around the site of injury with accompanying loss of motor and sensory functions. Delayed cell death beyond the impacted site displays apoptotic features (Beattie et al., 2000a); regulated in part by antiapoptotic Bcl-2 and Bcl-x_L proteins (Parsadanian et al., 1998;Sastry and Rao, 2000;Zaidi et al., 2001). Although the precise function of Bcl-2 and Bcl-x_L has not been fully defined for the central nervous system (CNS), we and others have shown that Bcl-x_L is the most robustly expressed pro-survival Bcl-2 molecule in adult spinal neurons and glia (Alonso et al., 1997;Qiu et al., 2001;Nesic-Taylor et al., 2005) and that Bcl-x_L mRNA and protein levels decrease promptly after spinal cord injury (SCI) (Qiu et al., 2001;Nesic-Taylor et al., 2005). We have shown that administration of Bcl-x_L-fusion protein to the injured spinal cord significantly increases neuronal survival (Nesic-Taylor et al., 2005). Thus, interventions that reverse SCI-induced decreases in Bcl-x_L activity could also reduce delayed cell death and alleviate functional impairment. A definitive knowledge of the mechanism(s) that regulate Bcl-x_L levels in injured spinal cord is essential to the development and implementation of such therapeutic approaches.

Unlike the constituvely membrane-bound Bcl-2, Bcl-x_L is present in the cytoplasm, from where it transfers to mitochondria as part of an anti-apoptotic process (Gross et al., 2000;Jeong et al., 2004). A major function of Bcl-x_L is to modulate mitochondrial membrane permeability and prevent release of apoptotic mediators from the intermembrane mitochondrial space into the cytoplasm (Gross et al., 2000;Nomura et al., 2003;Tsujimoto, 2003;Sharpe et al., 2004). Bcl-x_L anti-apoptotic activity depends in part on its association with pro-apoptotic proteins, including Bax and Bad (Grad et al., 2000;Jeong et al.,

2004;Kuwana et al., 2005;Uo et al., 2005). Bcl-x_L can also preserve mitochondrial membrane permeability and prevent apoptosis by inactivating mitochondrial voltage dependent anion selective channel (VDAC) (Shimizu et al., 2000;Jonas et al., 2003;Jonas et al., 2004).

Bcl-x_L contains sequences that are likely candidates for phosphorylation by stress-activated protein kinases (Basu and Haldar, 2003). Phosphorylation of these Bcl-x_L sites precedes cell death induced by microtubule disruption in cancer cell lines (Du et al., 2005), and in isolated rat brain mitochondria, it has been shown that JNK-depedent phosphorylation of Bcl-2 and Bcl-x_L induce release of cytochrome C from mitochondria (Schroeter et al., 2003). Also, p38 mitogen activated protein kinase (MAPK)-dependent phosphorylation and proteasome-dependent degradation of Bcl-x_L is part of TNF-induced apoptosis in endothelial cells (Grethe et al., 2004). SCI induces the upregulation and activation of kinases, including p38 MAPK (Crown et al., 2006), and p38 MAPK activation leads to neuronal death after SCI (Wang et al., 2005). However, the role of phosphorylation in the regulation of Bcl-x_L anti-apoptotic activity after SCI, or any other CNS injury, has not been characterized.

Here we report Bcl-x_L and P-ser^{62}-Bcl-x_L levels in different subcellular compartments in sham-treated and injured spinal cords. The results suggest that Bcl-x_L phosphorylation and decreases in Bcl-x_L in different subcellular compartments may contribute to the failure of Bcl-x_L in preventing apoptosis after trauma. Our results suggest that phosphorylation of Bcl-x_L is a pro-apoptotic event in neurons *in vitro* and also after SCI, in association with its presence near disrupted neurofilaments. We also found that SCI triggered expression of Bcl-x_L in activated glial cells, and induced phosphorylation of Bcl-x_L in a subpopulation of activated microglia/macrophages undergoing apoptosis

Experimental Design

To study the levels of Bcl-x_L and P-ser^{62}Bcl-x_L in the injured spinal cord, a total of 66 rats were distributed as detailed in Table 1. Sham and injured animals were subjected to laminectomy at spinal segment T10 and injured animals were exposed to the moderate contusion injury as described in chapter 2. As indicated, animals were perfused with PBS and three spinal cord segments 5mm length containing the site of injury (T10), or immediately rostral (T9) or caudal (T11) were used for protein extractions and western blot analyses. For immunohistochemical analysis, SC segments 1 cm long containing the lesion epicenter were serially cut in 10 μm frozen sections as detailed in the methods section.

Table. 1. Description of experimental groups

	Sham SC		Injured SC		
Time after injury	n (WB)	n (IHQ)	n (WB)	n (IHQ)	Total
15 min	4		4		8
1h	4		4		8
2h	3		3		6
4h	4		4		8
24h	4	3	5	3	15
3 days	4		4		8
7 days	4	3	4	3	14
Total	27	6	27	6	66

n(ELISA, WB), number of animals for which Bcl-x_L levels were quantified by western blot. n(IHC), number of animals used for immunohistochemistry analysis.

Time course analysis of Bcl-x_L and P-ser^{62}Bcl-$x_{L,}$ protein levels were assayed by immunoblot and densitometric analysis of bands was performed. To calculate the changes in expression levels over time compared to sham values after injury, individual optical

density (OD) measurements were normalized to the average optical density of the sham-treated group at each time point. Normalized data were assessed by a one-way analysis of variance (ANOVA) to compare changes of protein levels over time in different subcellular compartments of injured animals using GraphPad software. $P<0.05$ was considered significant. Correlation analyses were used to evaluate the trend of changes in Bcl-x_L and P-ser^{62}-Bcl-x_L in the different cellular compartments over time after SCI.

In vitro analysis of Bcl-x_L phosphorylation was performed in NGF-differentitaed PC12 cells as described in Chapter 2.

Results

Characterization of antibodies used to detect unphosphorylated (Bcl-x_L) and phosphorylated Bcl-x_L.

The reactivity of antibodies to Bcl-x_L in the rat spinal cord was assessed by western blot assays and immunohistochemistry (**Table 2**). Rat spinal cord homogenates were used as antigen bearing samples to test commercially available antibodies against different Bcl-x_L epitopes. As shown in **Fig. 6A**, rabbit polyclonal antibodies against the C-terminus of Bcl-x_L (sc-7195, E-1018) showed a single 29 Kd protein band, while a polyclonal antibody against a short sequence surrounding Asp^{61} of human Bcl-x_L (CS-2762) showed a 29 and 31 Kd MW doublet thought to reflect the different isoforms or post-transcriptional modifications of Bcl-x_L (Basu and Haldar, 2003). An antibody against a phosphorylated form of Bcl-x_L (P-ser^{62}-Bcl-x_L, Biosource), known to occur in cell lines undergoing apoptosis, detected a single band at 31 Kd. This 31 Kd species was no longer detected when membranes were pre-incubated with calf alkaline phosphatase (not shown).

The reactivity of anti-Bcl-x_L antibodies was further evaluated by immunohistochemistry using naive rat spinal cord sections. Since antibody SC-7195 showed a very weak reactivity in immunofluorescence, a rabbit monoclonal antibody against a similar epitope of human

Table 2. Bcl-x_L antibodies used in this study

Antibody	Source	Epitope recognized	Western Blot	Immunolabeling
Anti Bcl-x_L SC-7195	Rabbit polyclonal	Residues 126-188 human Bcl-x_L	29 Kd *	Low reactivity
Anti Bcl-x_L CS-2762	Rabbit polyclonal	Bcl-x_L loop region (Asp^{61}-Ser^{62}) of human Bcl-x_L	29 and 31 Kd	In cell bodies, neurites, axons
Anti Bcl-x_L (E-1018)	Rabbit	Peptide in loop region between BH3-BH4 of human Bcl-x_L	29 Kd	Strong punctuated in cell bodies, weak in axons
Anti P-ser^{62}-Bcl-x_L	Rabbit polyclonal	Peptide surrounding phosphorylated Ser^{62} of human Bcl-x_L	31 Kd*	Strong in axons, weak punctuated pattern in cell bodies

* Since antibody SC-7195 and P-ser^{62}-Bcl-x_L detected different single forms of Bcl-x_L in the spinal cord, these were chosen to measure levels of unphosphorylated and phosphorylated Bcl-x_L by western blot.

Bcl-x_L (E1018) was assayed. This antibody strongly stained cell bodies, but not axons, in gray and white matter (**Fig 6B**), while antibody CS-2762 stained cell bodies and axons in gray and white matter. Staining of P-ser^{62}-Bcl-x_L was strong in axons and neurites but weak in cell bodies in gray and white matter.

To evaluate if phosphorylated Bcl-x_L was associated with microtubular structures present in neurons, we used sections double-labeled with neuron-specific ß-III tubulin (Tuj-1), an antibody that does not identify ß-tubulin found in glial cells. As shown in **Fig 6C**, Bcl-x_L (CS-2762) and P-ser^{62}-Bcl-x_L showed a robust co-localization in axons labeled with Tuj-1 in both gray and white matter. To test the specificity of the P-ser^{62}-Bcl-x_L staining, we performed competition assays with an antibody against phosphorylated neurofilaments (NeuF/H), known to be abundant in axons. When spinal cord sections were pre-incubated with an excess of antibody against phosphorylated Neurofilament H and L (neuF/H), neither the intensity nor the distribution of P-ser^{62}-Bcl-x_L labeling was modified, suggesting that the

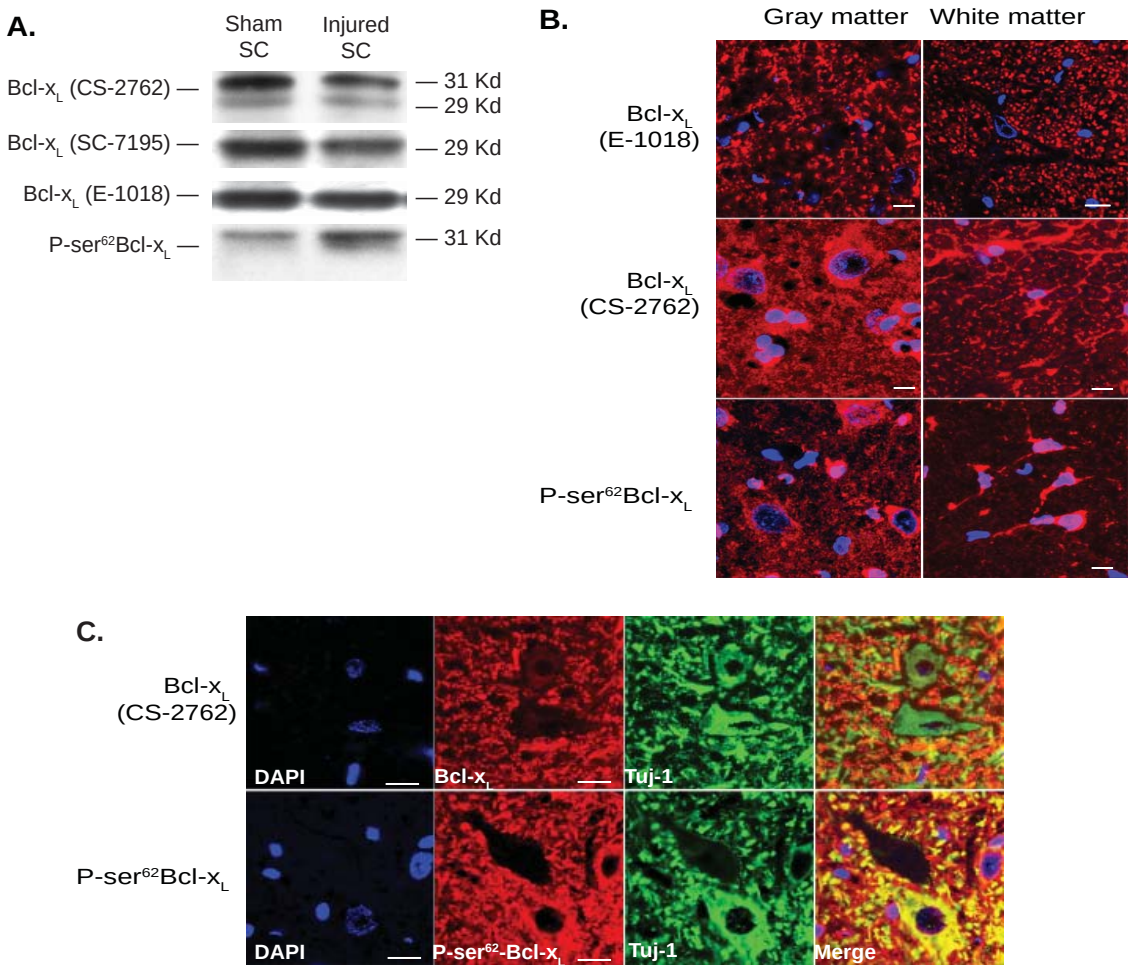

Fig.6. Reactivity of antibodies to Bcl-x_L and P-ser^{62}Bcl-x_L in rat spinal cord. A. Antibodies against unphosphorylated (sc-7195, E-1018, CS-2762) and phosphorylated Bcl-x_L (P-ser^{62}-Bcl-x_L) were assayed by western blotting on spinal cord homogenates. Antibody CS-2762 detected two bands of 29 and 31 Kd approximately, while antibody SC-7195 and E-1018 detected only the 29 Kd form. **B.** Immunofluorescence staining of naive rat spinal cord with antibody CS-2762 showed Bcl-x_L distributed throughout cell bodies and axons in gray and white matter; E-1018 stained mainly cell bodies and P-ser^{62}-Bcl-x_L strongly stained axons. **C.** Double immunofluorescence staining shows strong co-localization of P-ser^{62}Bcl-x_L and Bcl-x_L (CS-2762) with neuron-specific ß-III tubulin (Tuj-1) occuring through neurite-like structures in both white matter and gray matter. Colozalization is observed as a yellow/orange staining in the merge panel. Confocal images are a projection of 10 slices 1µm apart over a 10µm section. Scale bars: 10 µm.

observed staining did not result from a cross-reaction with phosphorylated neurofilaments. Furthermore, pre-absorption of spinal cord sections with P-ser^{62}-Bcl-x$_L$ antigenic peptide (a phosphorylated sequence containing 12 residues surrounding Ser^{62} of the rat Bcl-x$_L$) completely abolished P-ser^{62}Bcl-x$_L$ immunostaining, while the unphosphorylated version of this peptide did not (not shown).

Subcellular distribution of Bcl-x$_L$ and P-ser^{62} Bcl-x$_L$ in neurons *in vitro*

To further corroborate the existence of phosphorylated Bcl-x$_L$ in neurons, we performed immunocytochemical labeling of NGF-differentiated PC12 pheochromocytoma cells with antibodies against Bcl-x$_L$ (CS-2762, recognizing both Bcl-x$_L$ isoforms) and P-ser^{62}Bcl-x$_L$. When cultured on low serum supplemented with NGF, PC12 cells acquire a neuronal phenotype characterized by extended, long cellular processes (Gollapudi and Oblinger, 1999;Vyas et al., 2004). As shown in **Fig. 7** both Bcl-x$_L$ and phosphorylated Bcl-x$_L$ (in red) stained NGF-differentiated PC12 cells in a punctuated pattern suggestive of mitochondrial localization. Double immunolabeling with the mitochondrial marker COX-IV showed Bcl-x$_L$ and phosphoBcl-xl staining mitochondria in cell bodies and developing neurites (**Fig 7A**). Furthermore, double staining of P-ser^{62}Bcl-x$_L$ with an antibody against phosphorylated neurofilaments (NeuF/H) show phosphorylated Bcl-x$_L$ along neurites, but did not strongly colocalize with phosphorylated neurofilament abundant in the growth cones or the forming neurites (green)(Riederer et al., 1997), supporting our previous observation that the staining did not result from a cross-reaction with phosphorylated neurofilaments (**Fig. 7B**).

Cellular and subcellular distribution of Bcl-x$_L$ and P-ser^{62}-Bcl-x$_L$ in the uninjured rat spinal cord.

In order to ascertain the role of Bcl-x$_L$ phosphorylation in the uninjured spinal cord, we assessed the presence of Bcl-x$_L$ and P-ser^{62}-Bcl-x$_L$ in different cell phenotypes by

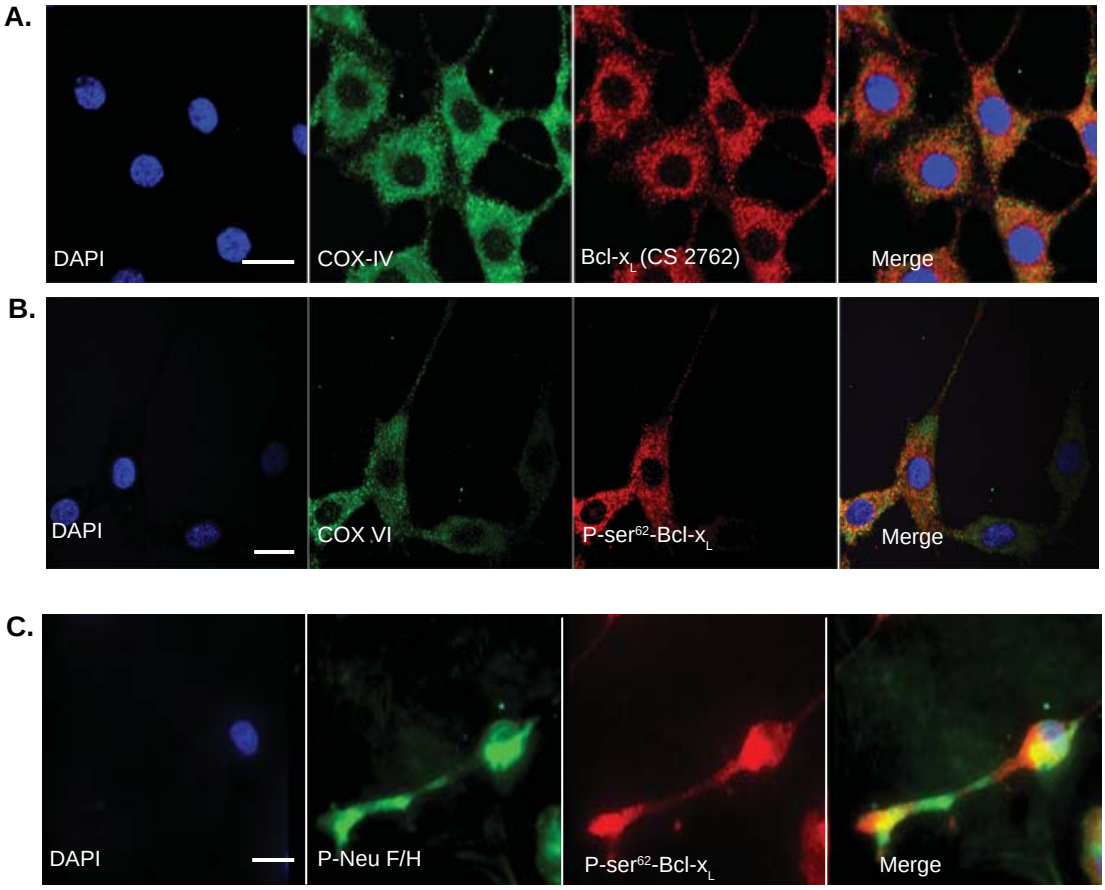

Fig.7. Bcl-x_L and P-ser^{62}Bcl-x_L staining in neurons in vitro. Rat pheocytochrome PC-12 cells differentiated with 100µM NGF for 5 days showed a neuronal-like phenotype forming long neurites. A. Double immunofluorescence staining with antibody CS-2762 showed Bcl-x_L (red) distributed throughout cell bodies in a punctuated patterns, and colocalizing with mitochondria (COX-IV, green). B. P-ser^{62}Bcl-x_L (red) localized in mitochondria (COX-IV, green). C. P-ser^{62}Bcl-x_L (red) staining occurrs through forming neurites, but did not colocalized with phosphorylated neurofilaments (NeuF/H), occurring at the growth cones in developing neurites. Nuclei are stained with DAPI (blue). Colozalization is observed as a yellow/orange staining in the merge panel. Scale bars: 10 µm.

immunohistochemistry. Consistent with our published results (Qiu et al., 2001;Nesic-Taylor et al., 2005), double labeling of spinal cord sections showed Bcl-x_L present throughout spinal cord neurons (NeuN, **Fig 8A,B**) and oligodendrocytes (CC-1, **Fig. 8A,C**), but not astrocytes (GFAP, **Fig, 8A**) or microglia (OX-42; **Fig. 8A**). P-ser^{62}-Bcl-x_L was present in a punctuated pattern in neuronal cell soma (**Fig. 8D,E**) but absent from the cell bodies of oligodendrocytes, astrocytes or microglia (**Fig. 8D**).

In agreement with the subcellular localization of Bcl-x_L in differentiated PC12 cells, double immunolabeling of spinal cord sections with mitochondrial marker COX-IV showed Bcl-x_L and P-ser^{62}Bcl-x_L colocalizing with mitochondria in neurons in the ventral horn. Bcl-x_L staining was stronger in cytosolic mitochodria while P-ser^{62}Bcl-x_L mostly colocalized with axonal mitochondria (**Fig.9**). Bcl-x_L staining was also strong surrounding neuronal nuclei.

To further characterize the subcellular distribution of both the unphosphorylated and the phosphorylated forms of Bcl-x_L in the uninjured spinal cord, we used western blot analyses of cytosolic, heavy mitochondrial (M), endoplasmic reticulum (ER) and nuclei (N) enriched subcellular fractions obtained from uninjured rat T10 spinal segments. To check for cross-contamination, fractions were probed with antibodies against established subcellular markers including lamin B1 (nuclei) and cytochrome C oxidase IV (COX-IV, mitochondria). While Bcl-x_L was present in all subcellular fractions, P-ser^{62}-Bcl-x_L was only present in mitochondrial, ER and nuclear, but not cytosolic fractions (**Fig.10**). Taken together, our results suggest that, opposite to unphosphorylated Bcl-x_L, phosphorylated Bcl-x_L is restricted to membrane-bound organelles.

Subcellular distribution of Bcl-xL after spinal cord injury

To evaluate the effect of spinal cord injury on Bcl-x_L shifts to the different organelles, we measured Bcl-x_L protein levels in cytoplasmic, mitochondrial, ER and nuclear fractions

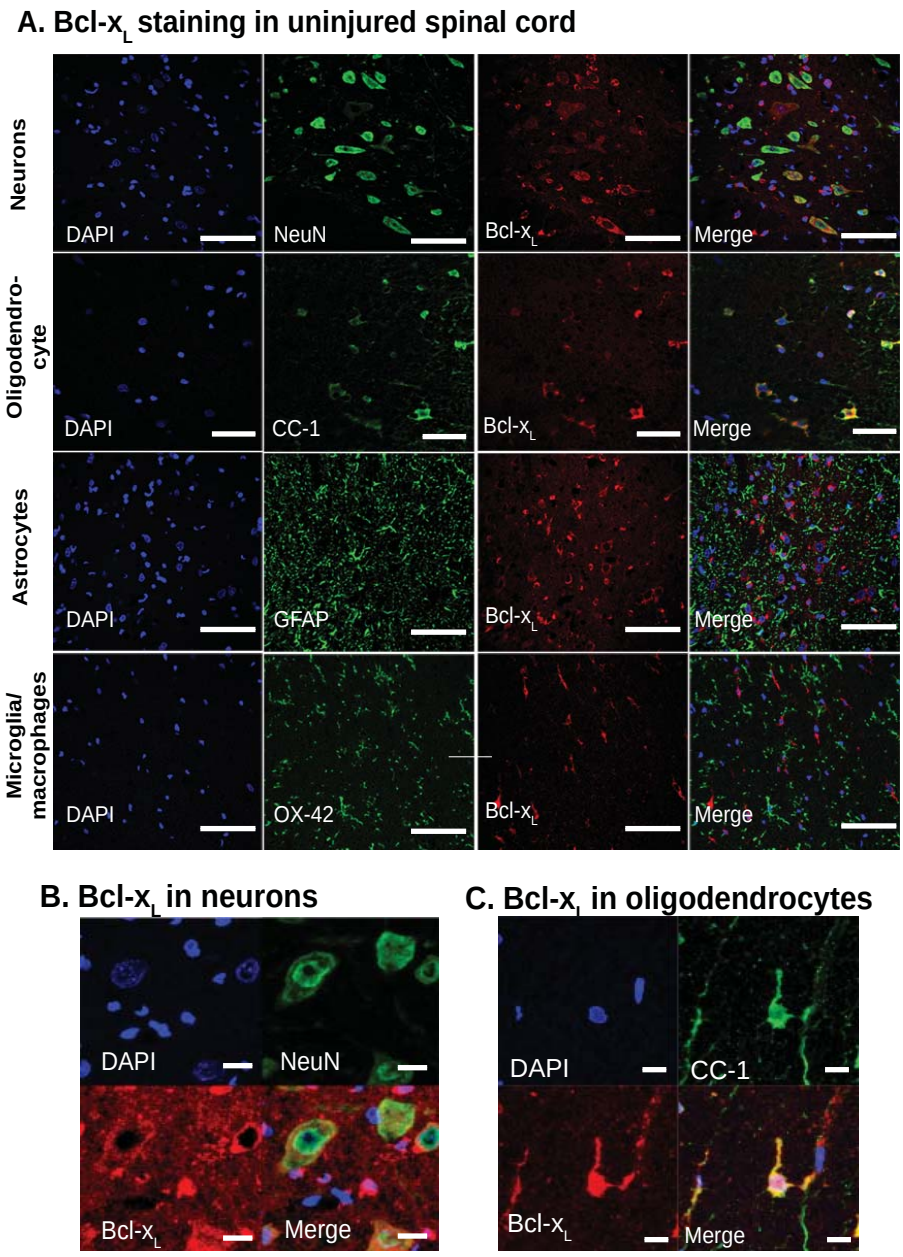

Fig. 8 Cell type distribution of Bcl-x_L and P-ser^{62}Bcl-x_L in uninjured rat spinal cord. A. Double immunolabeling of uninjured spinal segment T10 with Bcl-x_L (red) and neuronal and glial markers (green) showed Bcl-x_L co-localizing with neurons (NeuN) and oligodendrocytes (CC-1) but not with reactive astrocytes (GFAP) or microglia (OX-42). Scale bars: 50 µm. B. High resolution imaging showed Bcl-x_L in neurons (NeuN) in the ventral horn. Scale bars: 10 µm. C. High resolution imaging showing Bcl-x_L in an oligodendrocyte in white matter. Scale bars: 10 µm

D. P-ser^{62}Bcl-x$_L$ staining in uninjured spinal cord

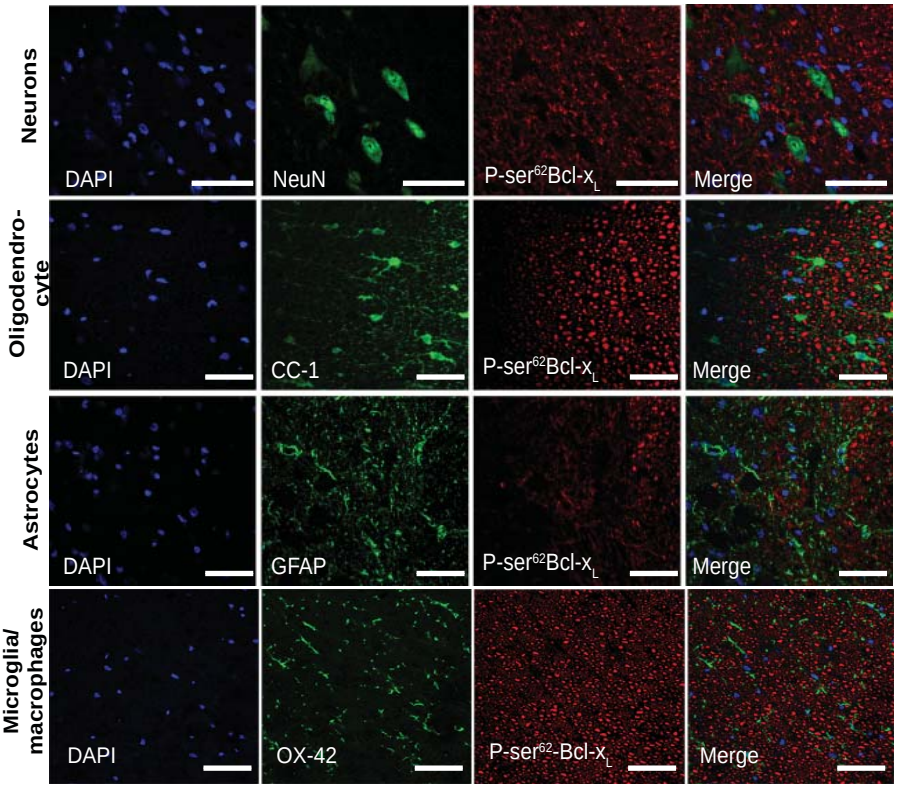

E. P-ser^{62} Bcl-x$_L$ in neurons

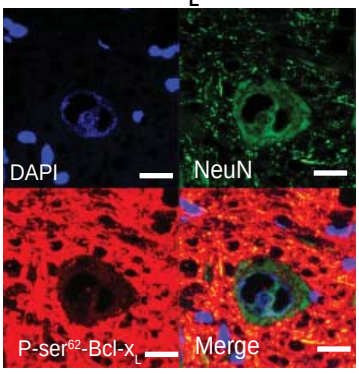

Fig. 8. (Continued) D. Double immunolabeling of uninjured spinal cord with an antibody against human P-ser^{62}- Bcl-x$_L$ (red) in axons of neurons (NeuN) but not in glial cells (CC1, GFAP, OX-42). Scale bars: 50 µm. E. High resolution imaging showed P-ser^{62}- Bcl-x$_L$ in a neuron (NeuN) in the ventral horn. Scale bars: 10 µm. Confocal high resolution images were generated by the projection of 10 images spanning 10µm in the Z-direction. Nuclei are stained blue (DAPI). Colocalization is observed as a yellow/orange staining in the merge panel.

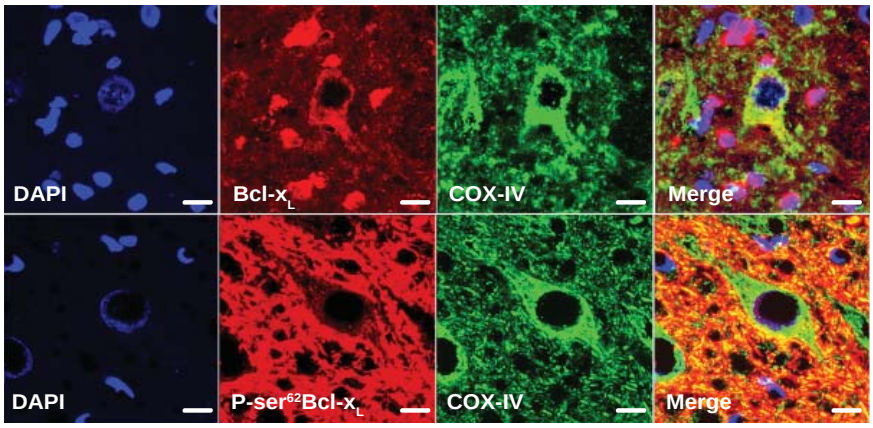

Fig. 9 Subcellular localization of Bcl-x_L and P-ser^{62}- Bcl-x_L in uninjured spinal cord. Double immunofluorescence staining and confocal imaging of uninjured spinal cord showed Bcl-x_L and P-ser^{62}Bcl-x_L colocalizing with cytosolic and axonal mitochondria (COX-IV) in neurons in the ventral horn. Colocalization is observed as a yellow/orange staining in the merge panel. Bcl-x_L also colocalizes with nuclei (stained blue, DAPI). Confocal high resolution images were generated by the projection of 10 images spanning 10µm in the Z-direction. Scale bars: 10 µm

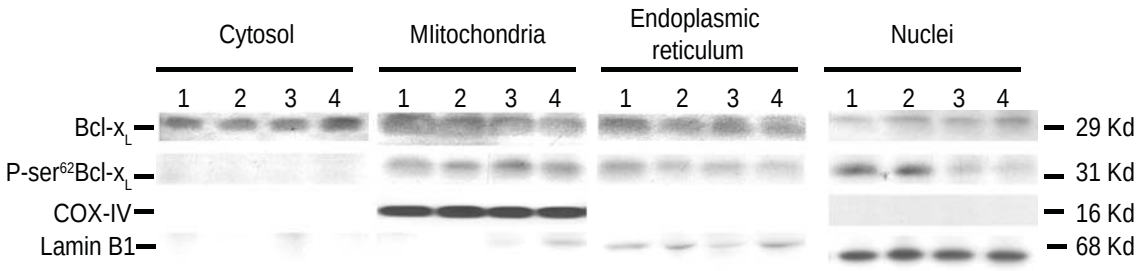

Fig. 10. Subcellular localization of Bcl-x_L and P-ser^{62}- Bcl-x_L in uninjured spinal cord protein extracts. Representative western blot of subcellular fractions extracted from four sham-treated spinal cords (1, 2, 3, 4). Protein extracts were probed with antibodies against P-ser^{62}-Bcl-x_L and Bcl-x_L (SC-7196) respectively. Unphosphorylated Bcl-x_L (29Kd) was found in all subcellular fractions; while P-ser^{62}- Bcl-x_L band (31Kd) was present in mitochondrial, nuclear and endoplasmic reticulum (ER) enriched extracts but not in the cytosolic fraction. The purity of the fractions was assessed with antibodies against subcellular markers including Lamin B1 (nuclei) and cytochrome oxidase IV (COX-IV, mitochondria).

from sham-treated and contused rat spinal cords at the injured spinal segment (T10), at 15 min, 1, 2, 4, 12, 24 h, 3 and 7 days after SCI (**Fig. 11**). Bcl-x_L levels in the sham-treated animals at each time point for each subcellular fraction were not statistically different (P=0.7), but SCI did decrease cytosolic Bcl-x_L levels as early as 2 h and for up to 3 days after injury (**Fig. 11A, B**). However, the time course of SCI-induced Bcl-x_L changes in the other subcellular compartments did not reflect the expected Bcl-x_L shift from the cytosol to the mitochondria. Mitochondrial Bcl-x_L levels decreased at 12 and 24 h post-injury; ER Bcl-x_L was downregulated at 24 h and 3 days and nuclear Bcl-x_L decreased within 2 h after trauma (**Fig. 11C**) These results suggest that decreases in Bcl-x_L at each compartment occur at different rates after SCI.

Analysis of SCI-induced changes in Bcl-x_L levels around the site of injury during the first 24 h, showed that, compared with T10, there was a delay in the onset of decreases in cytosolic Bcl-x_L levels rostrally and caudally to the site of injury (**Fig. 11D**). These results are consistent with secondary apoptotic "waves" radiating away from the site of injury.

To evaluate if the decreases in Bcl-x_L protein levels seen in western blot assays were concomitant with a decreased expression of Bcl-x_L in neurons and oligodendrocytes (the main populations expressing Bcl-x_L in the uninjured spinal cord), we performed double immunohistochemical analysis of Bcl-x_L and NeuN or CC-1, in spinal cord sections from sham-treated or injured animals, 24 h after injury. In comparison with sham-treated spinal cord, there was a significant decrease in the intensity of Bcl-x_L staining in surviving neurons located 2mm rostral to the lesion epicenter; but there were no significant changes were observed in the Bcl-x_L expression in oligodendrocytes at this time point (**Fig.12**). Thus, the overall decreases in Bcl-x_L protein levels occurring during the first 24h post-trauma correlate with decreased Bcl-x_L in neurons and support the hypothesis that neuronal Bcl-x_L depletion is a pro-apoptotic event.

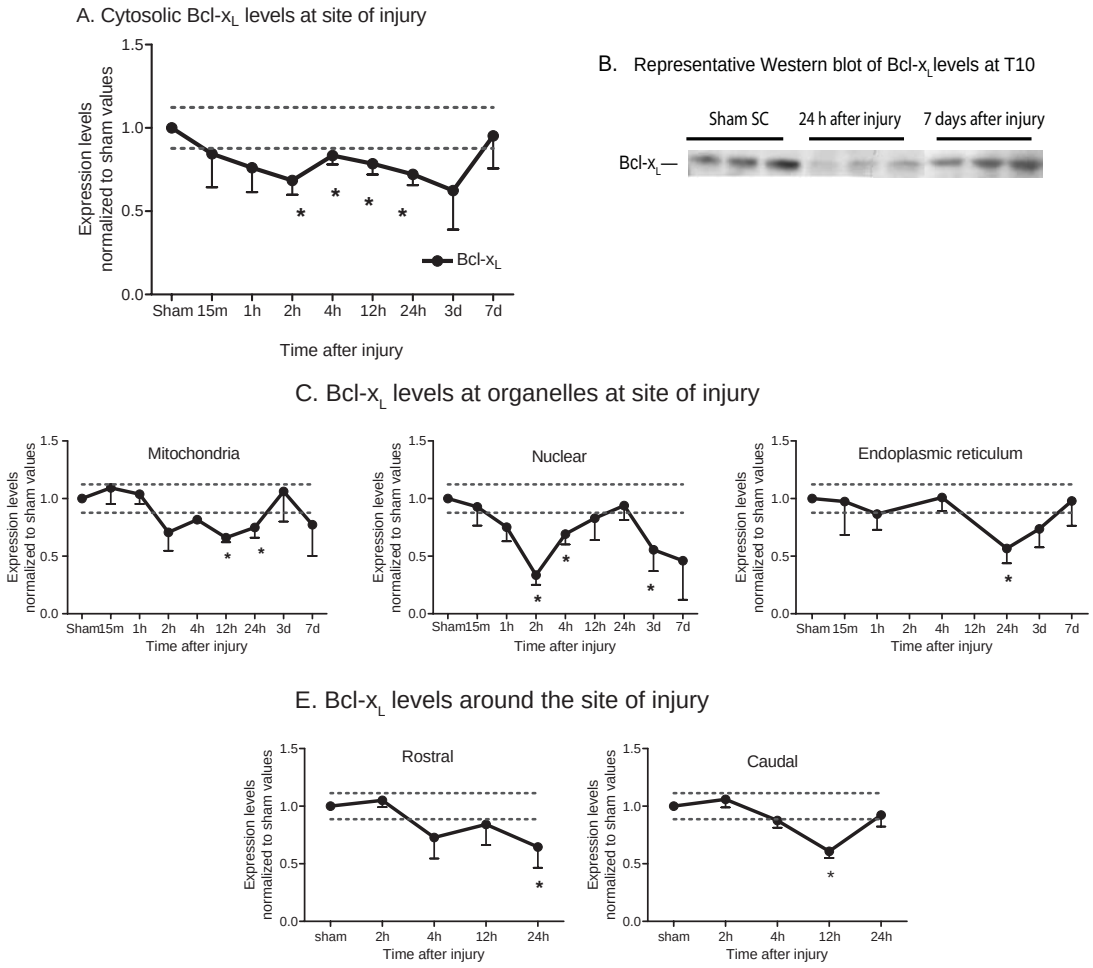

Fig. 11. Time course of SCI-induced changes in Bcl-x_L levels based on western blot analyses. At the indicated time points, cytosolic, mitochondrial, endoplasmic reticulum (ER) and nuclear enriched fractions from sham-treated and contused-rat spinal cords segments (5 mm long) were assessed for Bcl-x_L expression. A. SCI-induced significant decreases in Bcl-x_L levels in cytosolic fraction from 1 to 24h after injury. By day 7, Bcl-x_L levels are comparable to that of sham-treated spinal cords. B. Representative Western blot showing cytosolic Bcl-x_L levels at the site of injury, in 3 sham and 3 injured spinal segments T10 (site of injury), 24h and 7 days after trauma. C. SCI-induced Bcl-x_L changes in subcellular fractions at site of injury during first week after trauma. SCI-induced decreases in Bcl-x_L levels peaked at 12 and 24h in mitochondrial fraction (blue); at 24h in endoplasmic reticulum and at 2 and 4h in nuclear fractions. D. Cytoplasmic levels of Bcl-x_L in rostral (T9) and caudal (T11) segments to the lesion epicenter during the first 24h after trauma. Values are Mean OD ± SD normalized to the sham treated group (see methods). For clarity purposes, X-axis is categorical and it does not represent a time-scale. Dotted lines represent the average standard deviation of Bcl-x_L levels at all subcellular fractions of sham-treated SC. *$p<0.05$ compared to sham treated group (repeated measures Anova with post-hoc corrections).

Subcellular distribution of P-ser^{62}-Bcl-x$_L$ after spinal cord injury

To assess if phosphorylation is involved in the downregulation of Bcl-x$_L$ after injury, we performed western blot analyses of P-ser^{62}-Bcl-x$_L$ expression levels in all subcellular compartments. As shown in **Fig. 13** (**A,B**), SCI caused a dramatic increase in cytosolic

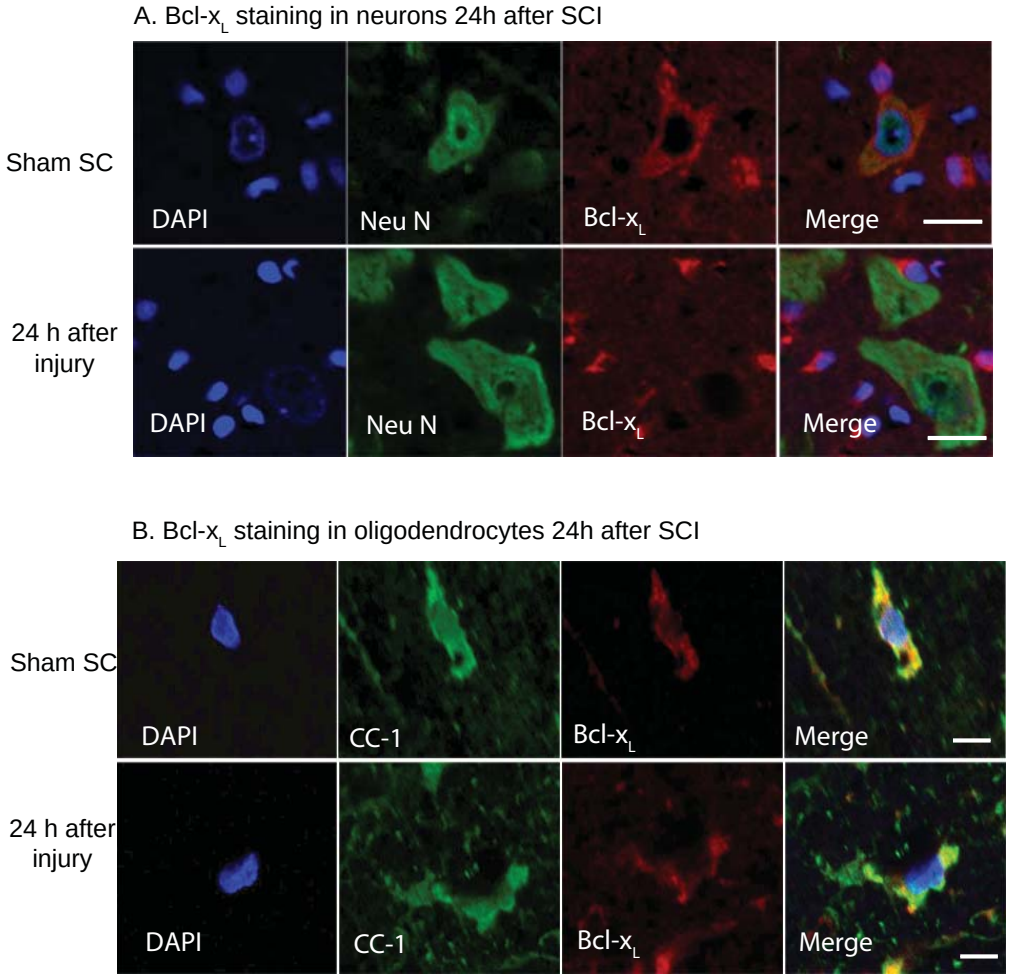

Fig. 12. Bcl-x$_L$ expression in neurons and oligodendrocytes 24h after SCI. A. Double immunolabeling of a section 3mm rostral to the lesion epicenter segment showed the decreased expression of Bcl-x$_L$ (red) in surviving neurons (NeuN) in the ventral horn 24h after injury, in comparison to sham-operated spinal cords. B. Double immunolabeling of an equivalent section showed a similar expression of Bcl-x$_L$ (red) in oligodendrocytes in white matter (CC-1) 24h after injury, in comparison to sham-operated spinal cords. Scale bars: 10 μm.

P-ser^{62}-Bcl-x_L without significantly affecting its expression levels in mitochondria, ER or nucleus during the first 24 h after trauma. In agreement with these results, double immunostaining of spinal cord sections 2mm rostral to the lesion epicenter, showed P-ser-^{62}-Bcl-x_L in the cytoplasm of neurons, 24 h after trauma (**Fig. 13C**) . Therefore, the presence of phosphorylated Bcl-x_L in cytosol at early time points after injury could explain the decreases in cytosolic Bcl-x_L in neurons and contribute to the impairment of its anti-apoptotic function (**Fig 14A**). Furthermore, during the first 24h, the levels of P-ser^{62}-Bcl-x_L and Bcl-x_L in organelles (shown only for mitochondria, **Fig. 14B**) appeared to be inversely proportional to each other, consistent with cycles of phosphorylation and dephosphorylation taking place at organelles after SCI.

Phosphorylation of Bcl-x_L in apoptotic neurons *in vitro*

To further test the hypothesis that Bcl-x_L phosphorylation correlates with apoptosis in neurons, we determined weather Bcl-x_L phosphorylation occurs in neurons undergoing apoptosis *in vitro*. It has been shown that drugs that alter microtubule kinetics (i.e vinblastine) induce apoptosis in differentiated cells of neuronal origin(Kim et al., 2002). In PC12 cells, microtubule disassembly has been reported to be an early step during the execution phase of apoptosis(Nuydens et al., 2000). Thus, we exposed NGF-differentiated-PC12 cells to 200nM vinblastine for 24h, and measured its effect in the expression levels of P-ser^{62}Bcl-x_L. Vinblastine treatment decreased the number of cells about 27% (235.5 ± 8.9 DAPI stained nuclei per 20X field) in comparison to non-treated control (319.0 ± 13 per 20X field) ($P<0.001$). As shown in **Fig 15(A,B),** vinblastine treatment significantly increased the number of differentiated PC12 cells expressing cytosolic P-ser^{62}Bcl-x_L ($P<0.001$). Furthermore, some cells over-expressing P-ser^{62}Bcl-x_L also had condensed nuclei (**Fig. 15C**) suggestive of apoptosis. However, double immunofluorescence analyses using TUNEL staining showed that only a fraction of the P-ser^{62}Bcl-x_L expressing cells

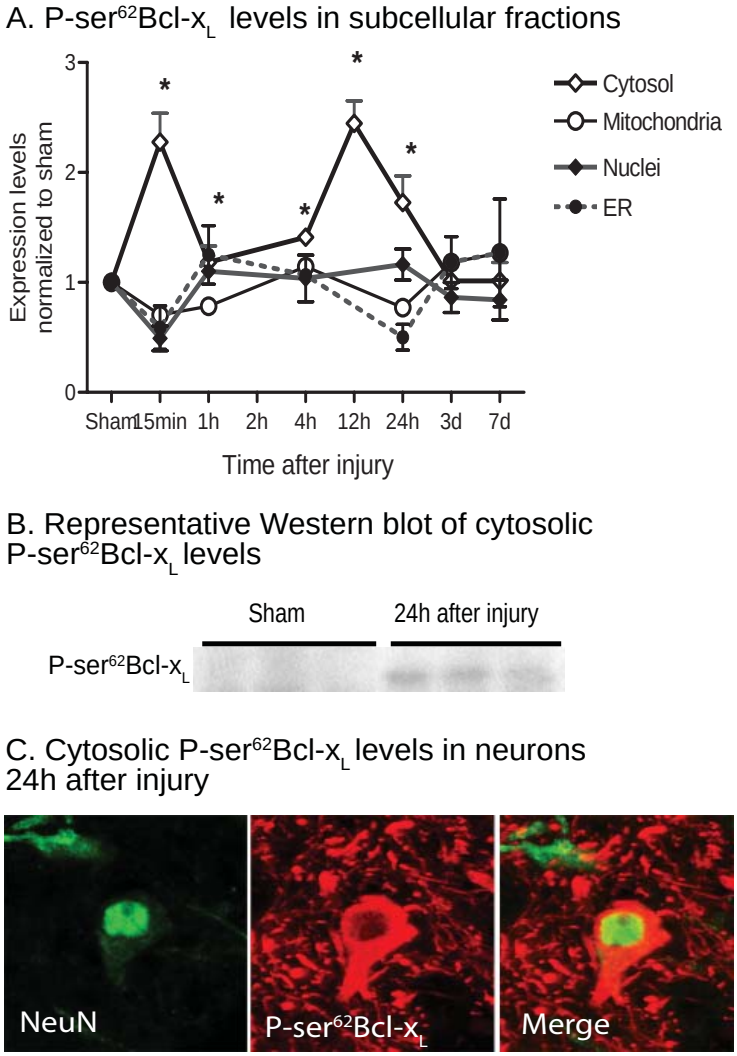

Fig. 13. Time course of SCI- changes in phosphorylated Bcl-x_L at different subcellular compartments. A. Quantitation of P-ser^{62}-Bcl-x_L levels based on western blot analyses showed Bcl-x_L in the cytosolic fraction as early as 15m after trauma. No significant changes were found in P-ser^{62}Bcl-x_L levels at mitochondria, ER or Nuclei. Values are Means ± SD normalized to sham group. Dotted lines represent the average standard deviation of P-ser^{62}-Bcl-x_L levels at all subcellular fractions of sham group. *$p<0.05$ compared to sham treated group (repeated measures Anova with post-hoc corrections). B. Representative Western blot showing P-ser^{62}-Bcl-x_L levels in 3 sham-treated and 3-contused spinal cords at T10, 24h after trauma. C. Double immunolabeling of a section 3mm rostral to the lesion epicenter segment showed P-ser^{62}-Bcl-x_L (red) in the cytoplasm of a neuron (NeuN) in the ventral horn 24h after injury. High resolution confocal image was generated by the projection of 10 images spanning 10μm in the Z-direction. Scale bar: 10 μm

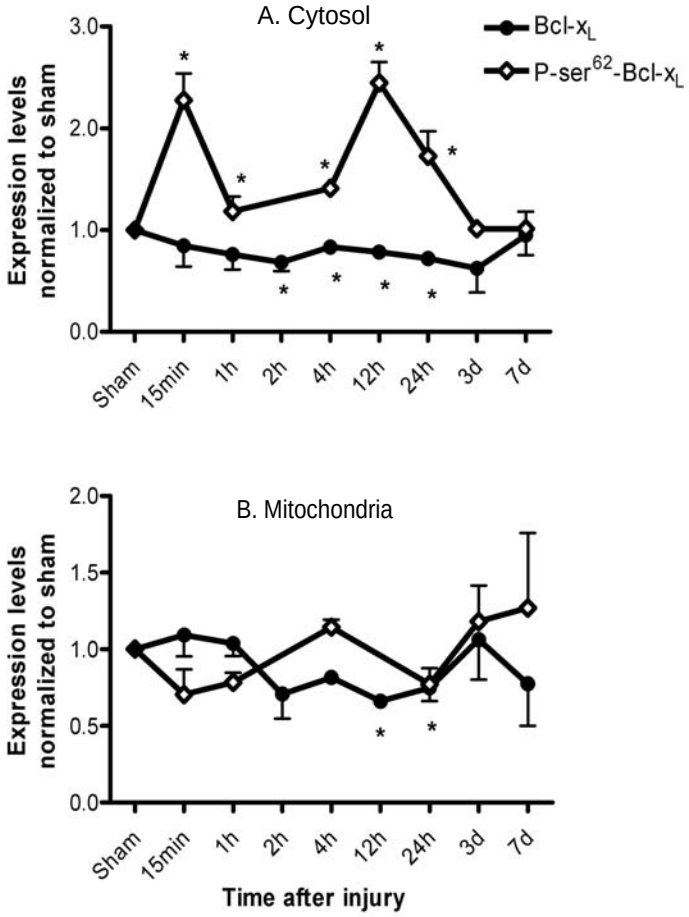

Fig 14. Time course of SCI-induced Bcl-x_L and P-ser^{62}-Bcl-x_L levels in subcellular fractions. Time course of SCI-induced Bcl-x_L and P-ser^{62}-Bcl-x_L changes in A. Cytosol and B. Mitochondria were plotted for comparison. Values are Mean OD ± SD normalized to the sham treated group (see methods). Dotted lines represent the average standard deviation of P-ser^{62}-Bcl-x_L levels at all subcellular fractions of sham-treated SC. *$p<0.05$, compared to sham treated group (Repeated measures Anova with post-hoc corrections).

colocalized with fragmented DNA, suggesting that phosphorylation of Bcl-x_L occurs early in the apoptotic process, probably before the final step of DNA fragmentation takes place (**Fig 15D**).

Taken together, these results suggest that Bcl-x_L phosphorylation is an early event in neuronal apoptosis, and supports the hypothesis that phosphorylation of Bcl-x_L has apoptotic consequences after SCI

Cell specific expression of Bcl-x_L and P-ser^{62}-Bcl-x_L one week after SCI

The bulk of neurons and oligodendrocytes (the cell populations normally expressing Bcl-x_L) are lost by day 7 at the lesion epicenter (Zai and Wrathall, 2005), and Bcl-x_L levels were expected to remain at the SCI-induced low levels. However, by day 7 after injury Bcl-x_L levels in all compartments returned to control levels comparable to sham levels (**Fig 11**). This observation is consistent with there being new cell populations that were responsible for the increases in Bcl-x_L; or that spared cells were stimulated to increase Bcl-x_L levels. Double immunolabeling of spinal cord sections at the T10 epicenter (site of injury) with Bcl-x_L and cell type markers showed that OX-42 positive cells (macrophages and microglia), GFAP (astrocytes) and CC1 (oligodendrocytes) were the predominant cell populations that expressed Bcl-x_L seven days after injury (**Fig. 16A**).

One week after injury, P-ser-^{62}-Bcl-x_L levels in the cytosolic fraction decreased, which agrees with the neuronal loss that had occurred at the site of impact. Immunohistochemical analysis of phoshphorylated Bcl-x_L with cell type markers showed P-ser^{62}-Bcl-x_L to be absent in GFAP and CC-1 staining cells (not shown), however, there was a subpopulation of microglia (OX-42) with condensed nuclei that expressed high levels of P-ser^{62}-Bcl-x_L (**Fig. 16B**).

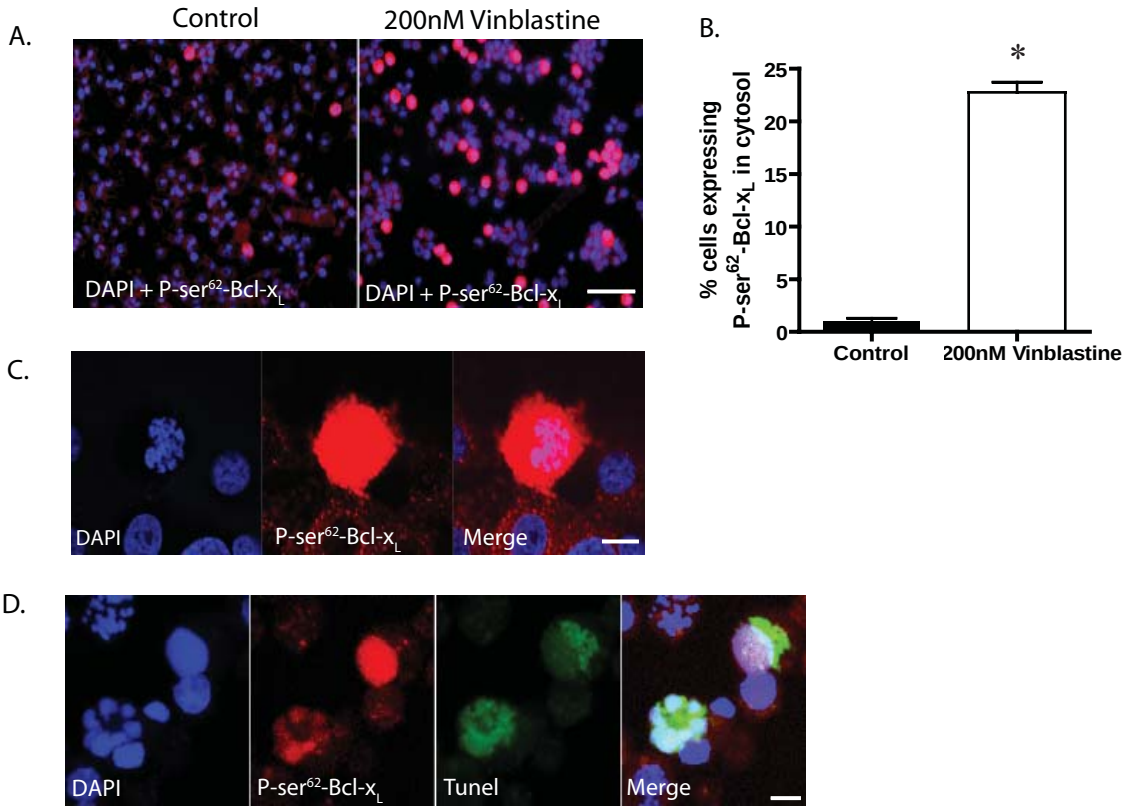

Fig. 15. Bcl-x_L phosphorylation in apoptotic neurons *in vitro*. PC12 cells were NGF-differentiated for 5 days and then exposed to 200nM of Vinblastine for 24h. A. Representative image showing the expression of P-ser^{62}Bcl-x_L (red) in control and vinblastine-treated PC12 cells. Nuclei are stained with DAPI. Scale bar: 100 µm. B. Vinblastine-treatment significantly increased the number of cells expressing cytosolic P-ser-Bcl-x_L. Plotted data represent the percentage of cytosolic P-ser^{62}-Bcl-x_L expressing cells respect to the total number of nuclei (stained with DAPI) in a 20X field. (*) $P<0.001$ compared to non-treated control cells. Data were analyzed using unpaired t-student test. C. High magnification imaging of vinblastine treated PC-12 cells, shows cytosolic P-ser^{62}-Bcl-x_L highly expressed in cells with condensed nuclei (DAPI), suggestive of apoptotic cell death. Scale bar: 10 µm. D. Apoptotic-DNA fragmentation was visualized by Tunel immunoflurescence assay, concomitant with P-ser^{62}Bcl-x_L staining. High resolution confocal image shows cells expressing P-ser^{62}-Bcl-x_L in the cytosol (red) with a positive tunel-staining (green nuclei). Scale bar: 10 µm

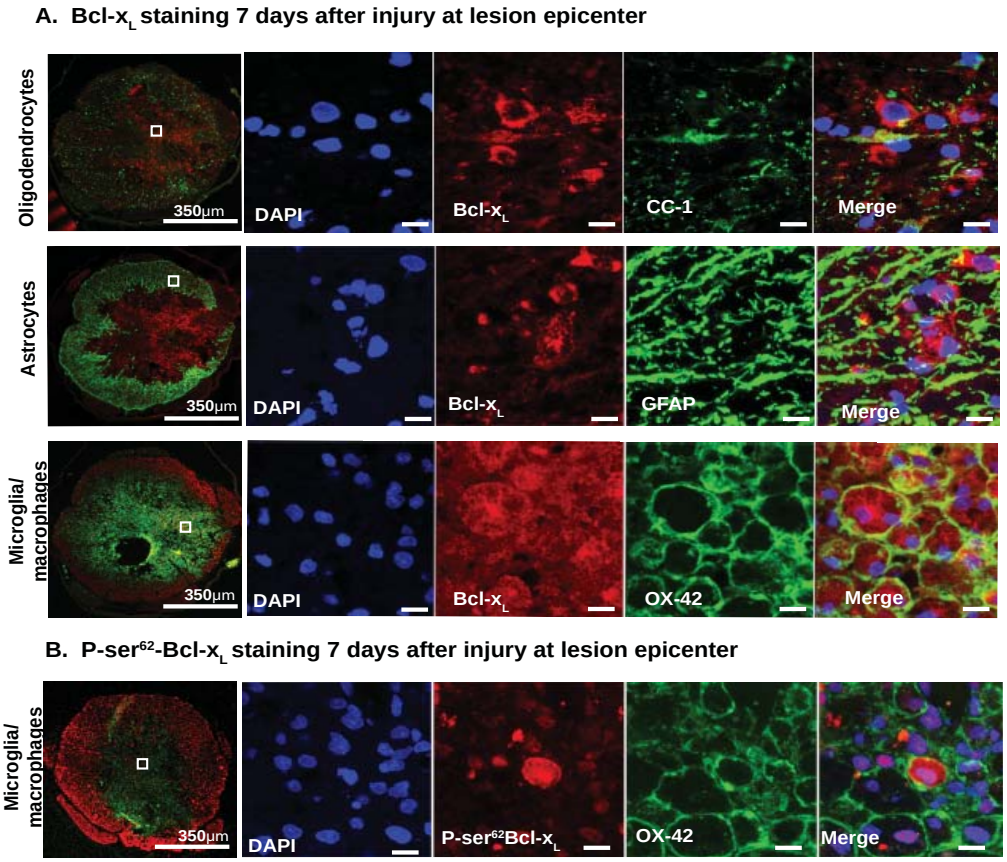

Fig 16. New cell populations express Bcl-x_L 7 days after trauma. A. Double immunolabeling of Bcl-x_L (red) with glial markers showed Bcl-x_L co-localizing with oligodendrocytes (CC-1) and microglia/macrophages (OX-42) but not with astrocytes (GFAP) 7 days after trauma at the lesion epicenter. B. Double immunolabeling of P-ser^{62}-Bcl-x_L expression and OX-42 showed a population of macrophage/microglia with condensed nuclei expressing P-ser^{62}-Bcl-x_L. High resolution confocal images were generated by the projection of 10 images spanning 10µm in the Z-direction. Scale bars: 10 µm, except for low magnification images (scale bar 350 µm). Nuclei are stained blue (DAPI) and colocalization appears purple.

Discussion

Apoptosis is an important mediator of the secondary damage that occurs after SCI (Liu et al., 1997;Beattie et al., 2000b). We and others have shown that Bcl-x_L is highly expressed in neurons and oligodendrocytes in the uninjured spinal cord (Qiu et al., 2001;Nesic-Taylor et al., 2005) and that Bcl-x_L levels decrease significantly as early as 1h after SCI at the lesion epicenter (Nesic-Taylor et al., 2005), thus preceding the neuronal cell death that is fairly complete 24h after SCI (Liu et al., 1997;Grossman et al., 2001;Qiu et al., 2001). SCI-induced Bcl-x_L decreases spread away from the lesion epicenter over time (**Fig. 13D**) consistent with the time course of delayed spreading of neuronal death after SCI in segments surrounding site of injury (Beattie et al., 2000a). In agreement with this hypothesis, we showed a significant decrease in the levels of Bcl-x_L staining 24h after injury (**Fig.12**) in surviving neurons rostral to the injury epicenter, suggesting that Bcl-x_L decreases precede neuronal cell death. Furthermore, decreases in Bcl-x_L during the first 24h (**Fig.11**) reflect changes in neuronal Bcl-x_L levels but not oligodendrocyte Bcl-x_L levels suggesting that SCI-induced changes in oligodendrogial Bcl-x_L occurs after the first 24h after trauma. This is consistent with the reported delayed death of glial cells that extends over weeks after injury (Shuman et al., 1997;Casha et al., 2001;Grossman et al., 2001;Warden et al., 2001;McEwen and Springer, 2005).

We have shown that exogenous application of Bcl-x_L fusion protein spares neurons after SCI (Nesic-Taylor et al., 2005), supporting the hypothesis that decreases in Bcl-x_L levels are likely to contribute to SCI-induced cellular losses. Here, we characterized SCI-induced posttranslational phosphorylation of Bcl-x_L (P-ser^{62}-Bcl-x_L), and the differential distribution/shuttling of Bcl-x_L and P-ser^{62}-Bcl-x_L among the various subcellular compartments. Our results suggest that SCI-induced modifications and redistributions of Bcl-x_L may have an important role in regulating apoptotic cell loss at and around the lesion

site. Furthermore, we present evidence that suggests that Bcl-x_L phosphorylation has pro-apoptotic consequences in neurons *in vitro* and *in vivo*.

Subcellular distribution of Bcl-x_L and P-ser^{62}-Bcl-x_L in the uninjured rat spinal cord.

Shuttling of Bcl-x_L may play different roles in different organelles.

Although recent studies have shown that Bcl-2 proteins are present in the endoplasmic reticulum (ER) and nuclei in cell lines (Ng and Shore, 1998;Tagami et al., 2000), the localization of Bcl-x_L in subcellular compartments other than cytosol and mitochondria in the CNS has not been previously reported. Our results show that in the uninjured spinal cord, Bcl-x_L is present in all compartments: cytoplasm, mitochondria, nuclei and ER, at levels that cannot be explained by simple cross-contamination among fractions. The presence of Bcl-x_L in mitochondria is well known (Zamzami et al., 1998;Jonas et al., 2003;Garcia-Saez et al., 2004;Jonas et al., 2004), but its shuttling to nuclear and/or ER fractions is a novel finding. The Bcl-x_L transmembrane domain contains a localization signal that targets Bcl-x_L to mitochondria, but not to nuclei or ER, as reported for cells *in vitro* (Kaufmann et al., 2003). It is thus possible that ER Bcl-x_L localization occurs through the interaction of Bcl-x_L with ER resident proteins, including other Bcl-2 family members (Morishima et al., 2004). For example, it has been shown that Bcl-x_L interacts with the ER-associated proteins Inositol Phosphate-3 receptor (IP3R), Bap31 and RTN-XL *in vitro* (Ng and Shore, 1998;Tagami et al., 2000;White et al., 2005).

The role of nuclear or ER Bcl-x_L in uninjured spinal cords is also unknown. Recent studies have suggested that nuclear Bcl-2 may control and be controlled by cell cycle kinetic changes associated with cellular proliferation (Lu et al., 1994;Hoetelmans et al., 2000;Hoetelmans et al., 2003;Hoetelmans, 2004). Thus, it is possible that the nuclear Bcl-x_L in spinal cord plays a role in neuronal proliferation during development. In the ER, both Bcl-2 and Bcl-x_L bind to IP3R, modify its sensitivity to IP3, and modulate Ca^{2+} release from

intracellular stores (Foyouzi-Youssefi et al., 2000;Pinton et al., 2000;White et al., 2005). Therefore, it is tempting to speculate that ER Bcl-x_L plays a role in Ca^{2+} homeostasis in the spinal cord, and that disturbance of ER Bcl-x_L impairs Ca^{2+} homeostasis and consequently affects neuronal survival after spinal cord injury (Bassik et al., 2004).

Translocation of P-ser^{62}-Bcl-x_L and its possible roles in different organellae.

Our finding that the uninjured spinal cord contains a phosphorylated form of Bcl-x_L that is abundant, but restricted to certain subcellular organelles agrees with the hypothesis that the organelle-specific actions of Bcl-x_L involve post-translational modifications. Interestingly, it has been shown that Bcl-2 is consitutively phosphorylated at Ser^{87} in human normal blood cells, but it is dephosphorylated by protein phosphatase 2A (PP2A) in human tumor cell lines (Simizu et al., 2004). Furthermore, the localization of Bcl-2 on mitochondria is required for the dephosphorylation by PP2A (Tamura et al., 2004). Our finding that phosphorylated Bcl-x_L is also expressed in mitochondria in differentiated neuronal PC12 cells, further support the hypothesis of a role for Bcl-x_L phosphorylation in the normal functioning of neurons.

It has been shown that phosphorylation of Bcl-2 in the loop region (equivalent to that in Bcl-x_L) inhibits its anti-apoptotic role. Phosphorylated Bcl-2 localizes mainly to the ER and is unable to bind pro-apoptotic proteins (Bassik et al., 2004;Upreti et al., 2006). Since these studies have only been perfomed in transformed cell lines overexpressing Bcl-2, little is known about the phosphorylated Bcl-x_L in the CNS. We found phosphorylated Bcl-x_L to be mainly present in axonal mitochondria suggesting that in the uninjured spinal cords, Bcl-x_L phosphorylation may be involved in the maintenance and stability of the axonal cytoarchitecture. Consistent with this hypothesis, Kretz et al. showed that excess Bcl-x_L dramatically increases axonal elongation of adult retinal ganglion cell cultures (Kretz et

al., 2004). Our finding that P-ser^{62}-Bcl-x_L was expressed in mitochondria along the newly formed neurites in NGF-differentiated PC12 cells *in vitro* further support this hypothesis.

Subcellular distribution of Bcl-x_L after spinal cord injury

The anti-apoptotic role of Bcl-x_L may depend in part on its subcellular location: in the cytosol Bcl-x_L might form homodimers or bind BH-3-only domain pro-apoptotic members of the Bcl-2 family, while in mitochondria it can block Bax activity (Shimizu et al., 2000;Abe et al., 2004;Jeong et al., 2004). Thus, decreases in cytosolic and/or mitochondrial Bcl-x_L and/or misrouting to different cell compartments could be responsible for the impaired anti-apoptotic activity of Bcl-x_L after SCI.

To evaluate the extent to which SCI-induced Bcl-x_L downregulation reflects re-routing among compartments, we analyzed SCI-induced decreases in Bcl-x_L protein levels in different subcellular fractions. Interestingly, SCI-induced Bcl-x_L decreases in the cytosolic fraction during the first 24h after SCI did not reflect Bcl-x_L translocation from cytosol to mitochondria. SCI-induced decreases in Bcl-x_L levels in the cytosol and mitochondria showed different time profiles that were not synchronized, suggesting that downregulation of Bcl-x_L in cytosol and mitochondria are independently regulated processes. In contrast, Bcl-x_L decreases in mitochondria mirrored concomitant increases in nuclear or ER levels and vice versa. These results suggest that SCI induces Bcl-x_L shuttling from mitochondria to nuclei/ER thus preventing Bcl-x_L from exerting its anti-apoptotic function at mitochondria.

Phosphorylation of Bcl-x_L correlates with neuronal apoptosis *in vitro* and after SCI

It has been shown that phosphoryation of Bcl-x_L is associated with apoptotic cell death *in vitro* (Poruchynsky et al., 1998;Basu and Haldar, 2003;Xue et al., 2003). Agents that promote apoptosis by causing microtubule disruption or stabilization, induce Bcl-x_L phosphorylation (Poruchynsky et al., 1998;Fan et al., 2000;Nuydens et al., 2000;Brichese

et al., 2002;Basu and Haldar, 2003;Bassik et al., 2004;Grethe et al., 2004;Upreti et al., 2006); however, the role of Bcl-x_L phosphorylation in post-mitotic neurons has not been investigated.

Bcl-x_L phosphorylation *in vitro* has been associated with the activation of p38 MAPK (Grethe et al., 2004). It is likely that the increased activity of kinases after SCI (Wang et al., 2005;Crown et al., 2006) may stimulate phosphorylation of Bcl-x_L in neurons resulting in overall decreases in anti-apoptotic Bcl-x_L levels. Given that we found significant increases in cytosolic phosphorylated Bcl-x_L after SCI, we believe that phosphorylation of cytosolic Bcl-x_L in neurons may either prevent anti-apoptotic Bcl-x_L activity in both cytosol and mitochondria, or be directly pro-apoptotic. Phosphorylation of Bcl-2 and Bcl-x_L occurs before the appearance of morphological apoptotic features, indicating that elimination of Bcl-2 function may be a pre-requisite for cell death (Ojala et al., 2000). Consistent with this hypothesis, cytosolic P-ser^{62}Bcl-x_L levels increased as early as 15 min after SCI, while DNA fragmentation and caspase activation has been demonstrated by 4h after injury.

To determine whether there is a correlation between phosphorylation of Bcl-x_L and neuronal apoptosis, we used an *in vitro* model of NGF-differentiated neuronal PC12 cells exposed to vinblastine. Similar to the reported Bcl-x_L phosphorylation in response to microtubule inhibitor-induced apoptosis *in vitro* (Du et al., 2005), vinblastine treatment induced cell death in differentiated PC12 cells, and a significant expression of cytosolic P-ser^{62}Bcl-x_L in cells showing condensed nuclei. Interestingly, cells that were in advanced stages of the apoptotic process (TUNEL positive) had a lower intensity of P-ser^{62}Bcl-x_L in cytosol, consistent with the hypothesis that Bcl-x_L phosphorylation occurs early in the apoptotic process. Recently Du et al (2005) demonstrated that cycles of phosphorylation and dephosphorylation of Bcl-x_L and Bcl-2 take place in cancer cell lines exposed to vinblastine, and suggested that reversal of phosphorylation, not phosphorylation per se, acts as a switch for apoptotic induction (Du et al., 2005). In agreement with this hypothesis,

we found that levels of P-ser^{62}-Bcl-x_L and Bcl-x_L during the first 24h after SCI in the cytosol and mitochondria (**Fig. 14**) are inversely proportional to each other, suggesting that cycles of phosphorylation and dephosphorylation may take place in those compartments in the injured SC.

Therefore, we hypothesize that SCI-induced phosphorylation and dephosphorylation of Bcl-x_L occur in response to the neuronal microtubule-disruption following spinal cord trauma and results in neuronal apoptosis. In this scenario, phosphorylated Bcl-x_L found in the axonal mitochondria in the uninjured spinal cord would play a key role in the surveillance of neuronal integrity *in vivo*, while phosphorylation and dephosphorylation cycles after SCI may contribute to the apoptotic death of neurons.

If the phosphorylation affects Bcl-x_L shuttling to other organelles, there would be a negative correlation between increases of phosphorylated Bcl-x_L in one compartment and concomitant decreases in some other organelle. However, SCI-induced fluctuations in P-ser^{62}-Blc-x_L levels showed a similar ("positively correlated") time course for all organelles (**Fig.13**), suggesting that mechanisms other than phosphorylation may regulate re-shuttling of P-ser^{62}-Bcl-x_L among the different compartments in injured spinal cords Consistent with our findings, Du et al (2005) has shown that vinblastine induced- Bcl-x_L phosphorylation does not promote subcellular re-shuttling of Bcl-x_L.

Glial expression of Bcl-x_L and P-ser^{62}-Bcl-x_L after SCI

Our immunofluorescence analyses showed that astrocytes and microglia in uninjured spinal cords do not express Bcl-x_L. In contrast, 7 days after injury, microglia/macrophages at the lesion epicenter in injured spinal cords showed robust presence of Bcl-x_L. Similarly, brain areas affected by neurodegeneration in patients with Alzheimer disease have shown high expression of Bcl-x_L in activated microglia (Drache et al., 1997), suggesting that activated glia in diseased or injured CNS may have increased Bcl-x_L expression, thus

allowing them to resist pro-apoptotic stimuli existing in injured CNS. Given that increased expression of Bcl-x_L in activated glia takes place several days after the initial Bcl-x_L down-regulation, therapeutic approaches to spare neurons/oligodendrocytes that counteract SCI-induced decreases in Bcl-x_L would have to target neurons and oligodendrocytes within that time window (1-7days). If prolonged, therapies that are based on increasing Bcl-x_L levels in injured spinal cords may amplify glial activation, which predictably are not beneficial (Popovich et al., 2002).

We also found phosphorylated Bcl-x_L in a population of OX-42 positive cells, but not in GFAP-positive astrocytes. However, co-expression of OX-42 and P-ser^{62}-Bcl-x_L was found only in microglia/macrophages showing nuclear condensation, suggestive of cells undergoing apoptosis (Fig 8). Thus, phosphorylation of Bcl-x_L may also be involved in apoptotic death of microglia following SCI, which has been reported to occur from 24h to 21 days after injury (Shuman et al., 1997). Therefore, Bcl-x_L may help activated glia to resist the pro-apoptotic environment after SCI, in contrast to P-ser^{62}-Bcl-x_L which may precede their death.

In summary, phosphorylation of Bcl-x_L may have two opposite effects in injured spinal cords: (a) trigger death of neurons and thus contribute to the SCI-functional impairment, or (b) regulate apoptosis of activated microglia/macrophages and thus curtail the inflammatory cascades associated with SCI (Popovich et al., 2002). Taken together, our results show that SCI perturbs Bcl-x_L subcellular localization and post-translational modifications and gives rise to new Bcl-x_L expression patterns in activated glia. These findings should be taken into account when anti-apoptotic therapies are designed to interfere with Bcl-2-like activities, or when results of anti-apoptotic therapies are interpreted.

CHAPTER FOUR: DETRIMENTAL EFFECTS OF ANTI-APOPTOTIC TRETMENTS IN SPINAL CORD INJURY

Introduction

Mechanical trauma to the spinal cord triggers events resulting in death of neurons and glial cells over several weeks after the initial injury (Liu et al., 1997;Ahn et al., 2006). In the early acute phase, there is a cascade of excitatory amino-acid-induced Ca^{2+} entry and energy failure, nitric oxide (NO) production, oxidative stress and membrane breakdown that leads to early necrotic cell death (Park et al., 2004;Bao and Liu, 2004;Bao et al., 2006), that is followed by apoptosis-mediated cell death of neurons and glia (Beattie et al., 2000;Lu et al., 2000;Park et al., 2004). Neuronal apoptosis begins as early as 4h near the site of impact and persists for the first 24h after trauma, while neuronal and oligodendroglial apoptosis lasts for a couple of weeks in areas away from the injury site (Liu et al., 1997;Shuman et al., 1997;Casha et al., 2001). Since the functional outcome after spinal cord injury (SCI) is largely dependent on the extent of secondary cell death, it has been suggested that the prevention of delayed apoptosis after SCI is likely to have a beneficial effect by reducing the extent of tissue damage(Schwab et al., 2006). With the belief that the final steps of apoptotic death are highly conserved and likely to be mediated by a similar set of caspases, inhibitors of caspases have been used to prevent SCI-induced apoptosis with variable success (Barut et al., 2005;Knoblach et al., 2005;Colak et al., 2005). However, apoptotic cell death is known to be triggered through different pathways, caspase-dependent and caspase-independent, that both converge at the mitochondria (Yuan et al., 2003). For example, the release of mitochondrial cytochrome c is indispensable for the activation of caspases (Hengartner, 2000); while the release of mitochondrial apoptosis-inducing factor (AIF) leads to DNA fragmentation in a caspase-independent fashion(Yakovlev and Faden, 2004). Main regulators of apoptotic processes in mitochondria are members of

Bcl-2 family of proteins. The Bcl-2 family of proteins, containing pro-apoptotic (Bax, Bad, Bid) and anti-apoptotic (Bcl-2, Bcl-x_L) members, is central to the regulation of both caspase-dependent and caspase-independent apoptosis, by modulating the mitochondrial outer membrane permeability (Tsujimoto, 2003;Sharpe et al., 2004). Among the Bcl-2 family, Bcl-x_L is the principal anti-apoptotic member in the postnatal and adult central nervous system (Gonzalez-Garcia et al., 1994;Gonzalez-Garcia et al., 1995;Alonso et al., 1997;Parsadanian et al., 1998); and is highly expressed in neurons and oligodendrocytes in the rat spinal cord (Qiu et al., 2001;Nesic-Taylor et al., 2005;Cittelly et al., 2005).

Manipulation of the levels of Bcl-2 proteins could provide new treatment paradigms that prevent apoptosis associated with SCI. Conditional Bcl-x_L overexpression protected postnatal and adult neurons from traumatic hypoxia (Matsuoka et al., 2002;Wen et al., 2002), and metabolic injury (Xu et al., 1999;Shinoura et al., 2000). Furthermore, exogenous Bcl-x_L has been shown to be highly effective in protecting against cell injury in response to several injuries such as ischemia (Cao et al., 2002b), oxidative stress (Cherbonnel-Lasserre and Dosanjh, 1997) hypoglycemia (Panickar et al., 2005), neurotrophin deprivation (Vander Heiden et al., 1999) and excitotoxicity (Matsuoka et al., 2002). We have also found that Bcl-x_L levels are significantly reduced after SCI and that short-term administration of Bcl-x_L-fusion protein to the injured spinal cord significantly increases neuronal survival within 24h after spinal injury (Nesic-Taylor et al., 2005). However, the long-term effects of such anti-apoptotic therapy have not been assessed in rat model of SCI.

In our previous study (Nesic-Taylor et al., 2005), we used a Bcl-x_L fusion protein, a construct in which Bcl-x_L was fused into a 254 amino acid nontoxic derivative (lethal factor, LFn) of anthrax toxin to render the Bcl-x_L cell permeable (Liu et al., 2001). The transduction of LFn-Bcl-x_L requires the binding of the LFn domain to another anthrax toxin component, protective antigen (PA)(Liu et al., 2001), which binds to an unidentified cell surface receptor and mediates the transports of the Bcl-x_L fusion protein into the

cell (Friedlander, 1986). In the present study, we chose TAT-mediated delivery of Bcl-x_L because it offered several important advantages over the anthrax-toxin delivery system (Yin et al., 2006). First, TAT-mediated protein transduction in the CNS does not require co-administration of helper proteins. The TAT sequence is only 11 amino acid residues long, which does not substantially increase the size of the fusion protein and thus, is less likely to interfere with the activity of the transduced protein (Cao et al., 2002a). Tat-Bcl-x_L has been shown to rapidly transduce into mammalian cells (Nagahara et al., 1998)) via an endocytosis-mediated, but receptor-independent mechanism (Potocky et al., 2003;Wadia et al., 2004;Kaplan et al., 2005). In addition, the ability of the Tat peptide to bind to ubiquitous targets such as heparan sulfate, chondroitin sulfate, or even phospholipid heads in the lipid bilayer (Wadia and Dowdy, 2005) allows for consistent transduction into multiple cell types (Schwarze et al., 1999).The anti-apoptotic BH4 domain of Bcl-x_L has also been fused to the Tat–peptide (Sugioka et al., 2003) , providing an additional tool to asses the anti-apoptotic activity of Bcl-x_L. Thus, Tat-Bcl-x_L is a useful tool to evaluate the long-term effects of exogenously administered Bcl-x_L into the injured rat spinal cords. In the present work, we found that administration of exogenous Bcl-x_L (Tat-Bcl-x_L) and its anti-apoptotic domain BH4 (Tat-BH4-Bcl-x_L) into the injured spinal cord decreased apoptotic cell death 24h and 7 days after SCI. However, long-term administration (7 days) of exogenous Bcl-x_L impaired locomotor recovery and increased neuronal loss to a greater extent than SCI alone. Furthermore, long-term administration of TAT-Bcl-x_L significantly increased microglia/macrophage levels in injured spinal cords compared to vehicle treated SCI rats, suggesting an enhanced inflammatory reaction induced by Tat-Bcl-x_L treatment. Taken together, these results would suggest that delayed effects of anti-apoptotic therapy maybe pro-inflammatory and detrimental over time, although the initial effects 24h after SCI could be beneficial.

EXPERIMENTAL DESIGN

To study the effect of Tat-Bcl-x_L and Tat-BH4 in the injured spinal cord, a total of 105 rats were distributed as detailed in **Table 3.** Sham and injured animals were subjected to laminectomy at T10 and T13-L1 and injured animals were exposed to the moderate contusion injury as described in Materials and methods. Sterile 0.9% saline solution was used as vehicle.

Table. 3. Description of experimental groups

Time after injury	Groups	Drug delivery	n (E,WB)	n (H,IHC)	n (BBB)	Total
24h	Sham + Vehicle	1ul/hr for 24h 10ug/day	4	3	NA	7
	Sham + Tat-Bcl-x_L		4	-	NA	4
	Injury + Vehicle		5	3	NA	8
	Injury + Tat-Bcl-x_L		5	3	NA	8
7days	Sham + Vehicle	0.5ul/hr for 7 days 5ug/day.	7	3	NA	10
	Injury + Vehicle		7	3	NA	10
	Injury + Tat-Bcl-x_L		7	3	NA	10
	Injury + Tat-BH4		7	3	NA	10
60 days	Sham + Vehicle	0.5ul/hr for 7 days 5ug/day.	3*	3	10	10
	Injury + Vehicle		3*	3	10	10
	Injury + Tat-Bcl-x_L		3*	3	8#	10
	Injury + Tat-BH4		3*	3	10	10
TOTAL					48	105

* Only WB analysis but no Cell death ELISA was performed in this group. # An additional injury at the site of catheter implantation was observed at the time of perfusion in two Tat-Bcl-x_L treated animals. Data from these animals were omitted from the analysis. n(ELISA, WB), number of animals for which apoptotic cell death was measured by ELISA and analysis of Bcl-x_L levels were quantified by western blot. n(H, IHC), number of animals used for histology and immunohistochemistry analysis. n (BBB), number of animals for which BBB scores were obtained. NA, Not applicable

RESULTS

Intrathecal administration of Tat-Bcl-x_L increases total Bcl-x_L levels in injured spinal cords.

To examine the ability of intrathecally delivered Tat-Bcl-x_L to transduce cells located in deep layers in the spinal cord, we delivered 10ug of Tat-Bcl-x_L (1µl/hr, during 24h) or vehicle into the intrathecal space of contused-spinal cord rats, and measured the levels of exogenous Tat-Bcl-x_L by immunohistochemistry and Western blot assays. Immunofluorescence labeling using an antibody against the hemaglutinin (HA) -tag present in the fusion protein, showed Tat-Bcl-x_L to be throughout white and gray matter (**Fig 17A**) in transverse spinal cord sections located 3mm rostral to the lesion epicenter (T10), 24h after trauma.

We have shown that SCI induces decreases in Bcl-x_L levels in cytosol and mitochondria that correlate with apoptotic cell death of neurons occurring 24 h after trauma (Nesic-Taylor et al., 2005;Cittelly et al., 2005). To determine if the delivery of exogenous Tat-Bcl-x_L counteracts SCI-induced decreases in Bcl-x_L, we performed Western blot analysis of Bcl-x_L levels in cytosolic and microsomal extracts (containing mitochondria and endoplasmic reticulum) of 1 cm long spinal cord segments that contained the site of injury T10 (**Fig. 17B**). We analyzed spinal cords from three groups of rats: sham rats that received vehicle for 24h, SCI rats that received vehicle, and SCI rats treated with Tat-Bcl-x_L. As expected, SCI induced decreases in Bcl-x_L protein levels, while Tat-Bcl-x_L treatment restored Bcl-x_L levels in SCI-treated rats to levels compared to those of sham-treated rats, in both cytosolic and microsomal fractions **(Fig 17B)**.

Anti-apoptotic effects of Tat-Bcl-x_L

24H AFTER SCI. To examine the antiapoptotic activity of Tat-Bcl-x_L we measured the levels of oligonucleosomes in the cytosol of uninjured and injured spinal cords, using

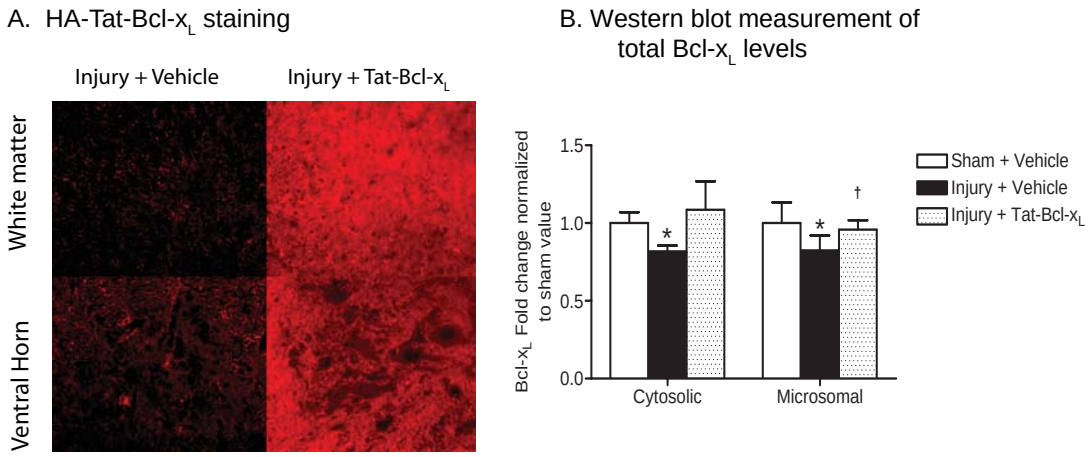

Fig.17. Protein transduction of Tat-Bcl-xL in the injured spinal cord 24h after trauma**. A.** Immunofluorescence staining of a transverse section of spinal cord 3mm rostral to lesion epicenter, 24h after injury using an antibody against HA-tag. The HA immunoreactivity was strong in gray and white matter in Tat-Bcl-x_L-treated, but not vehicle-treated spinal cords. Scale bar: 50 µm.**B.** Quantitation of cytosolic and microsomal Bcl-x_L levels based on western blot analyses. We used an antibody against a sequence surrounding Asp61 in the loop region of Bcl-x_L that recognized both endogenous Bcl-x_L and Tat-Bcl-x_L. Total Bcl-x_L levels at cytosolic and microsomal fractions increased in Tat-Bcl-x_L treated animals to levels comparable to those of sham spinal cords. Bcl-xL expression values were normalized to sham values and presented as mean ± SD. n=4/5 per group as indicated in table 1. **(*)** $p<0.05$ compared to sham-vehicle group**; ‡** $p<0.05$ compared to the injury-vehicle treated group; Two way ANOVA with Tukey's post-hoc correction).

Elisa cell death assay. A total of 10µg of Tat-Bcl-x_L or vehicle was intrathecally delivered over 24h after SCI (1µl/hr, 24µl). The presence of cytosolic oligonucleosomes was tested in protein extracts of thoracic spinal cords segments (1 cm long) containing the site of injury (T10). Vehicle-treated injured spinal cords showed significant increases in cytosolic oligonucleosomes when compared to sham rats treated with vehicle (**Fig. 18**), in agreement with our earlier reports (Nesic et al., 2001;Qiu et al., 2001;Nesic-Taylor et al., 2005) that showed that significant apoptotic cell death occurs during the first 24 h after injury. As expected, Tat-Bcl-x_L treatment significantly decreased levels of cytosolic oligonucleosomes, confirming the anti-apoptotic effectiveness of Tat- Bcl-x_L.

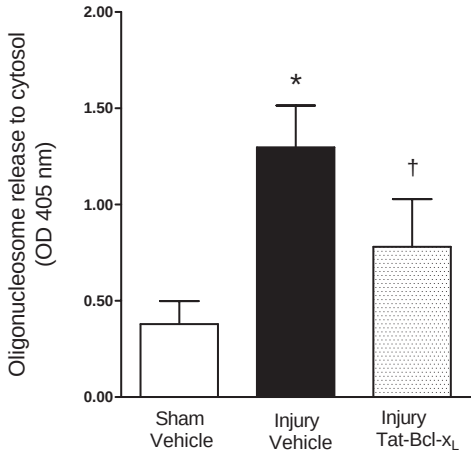

Fig. 18. Tat-Bcl-x_L decreased apoptosis 24h after injury. The release of oligonucleosomes to the cytosol during the first 24h after trauma was evaluated in cytoplasmic extracts from spinal cords of sham-vehicle treated (n=4), injury-vehicle(n=5) or injury-tat-Bcl-x_L (n=5) treated rats. Apoptotic cell death was significantly reduced in Tat-Bcl-x_L treated rats in comparison to vehicle-treated rats. Data represent mean ± SD (*) $p<0.05$ compared to sham-vehicle group. (‡) $P<0.05$ compared to the injury-vehicle treated group (Two way Anova with Tukey's post-hoc correction).

7 days after SCI . To assess effects of longer lasting administration of Tat-Bcl-x_L to counteract late SCI-induced Bcl-x_L decreases we intrathecally delivered 35ug of Tat-Bcl-x_L at a rate of 0.5ul/hr for 7 days (5ug/day). Cytosolic fractions were extracted from the 1 cm-spinal cord segments containing the epicenter of the lesion (T10). In agreement with our previous results (**Fig. 18**), Tat-Bcl-x_L administration significantly increased cytosolic levels of Bcl-x_L at seven days (1.67±0.32 fold increase in comparison with SCI-vehicle treated cords, $p<0.05$; n=7 per group). As shown in **Fig. 19**, cytosolic oligonucleosomal levels were significantly reduced after Tat-Bcl-x_L treatment.

Tat-Bcl-x_L vs. Tat-BH4. We have shown that SCI induces phosphorylation of endogenous Bcl-x_L, and thus possibly inactivates anti-apoptotic effects of Bcl-x_L (Cittelly et al., 2005). Therefore, we hypothesized that some fraction of the exogenous Tat-Bcl-x_L may also undergo phosphorylation and thus prevent its full anti-apoptotic effect. To assess whether phosphorylation diminishes anti-apoptotic effect of Tat-Bcl-x_L we used Tat-BH4 peptide, a construct that contains only the BH4 (Bcl-2 homology 4) antiapoptotic domain of Bcl-$x_{L;}$ and measured its ability to prevent apoptosis in the injured spinal cords. A total of

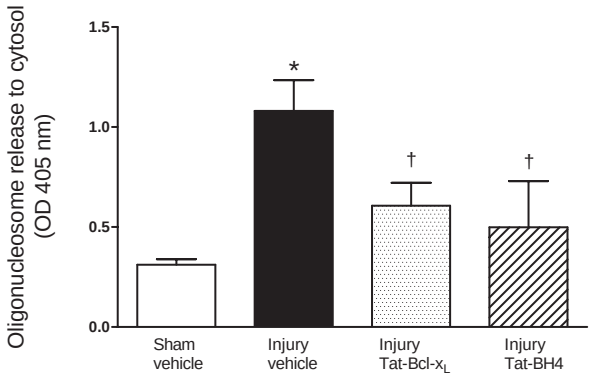

Fig. 19. Tat-Bcl-x_L and Tat-BH4 decreased apoptosis 7 days after injury. Elisa assays were use to measure the levels of oligonucleosomes in the cytosol 7 days after SCI in spinal cords isolated from four groups of rats: (a) sham-and vehicle treated (n=7); (b) SCI+vehicle (n=5); or (c) SCI+Tat-Bcl-xL (n=5); and (d) SCI+Tat-BH4 (n=5). In all measurements we used 1cm-long thoracic segments containing the site of injury, T10. Both Tat-Bcl-xL and Tat-BH4 treatment significantly decreased apoptosis compared to vehicle-treated animals. Data represent mean ± SD. (* $p<0.05$ compared to sham-vehicle group; (‡ $p<0.05$ compared to the injury-vehicle treated group; Two way ANOVA with Tukey's post-hoc correction).

35ug of Tat-BH4 was intrathecally delivered at a rate of 0.5ul/hr (5ug/day) for 7 days and cytosolic fractions were extracted as previously described (see **Fig. 18**). As shown in **Fig 19**, Tat-BH4 induced decreases in cytosolic oligonucleosomes levels to a similar extent of that of Tat-Bcl-x_L treatment. This result would suggest that significant phosphorylation of Tat-Bcl-x_L is unlikely, and that full anti-apoptotic effect of the exogenously applied Bcl-x_L was achieved.

Effect of Tat-Bcl-x_L and Tat-BH4 on locomotor recovery.

It is known that treatments that significantly spare spinal cord tissue after SCI also improve locomotor recovery (Pearse et al., 2004;Colak et al., 2005;Yates et al., 2006). To evaluate whether antiapoptotic activity of Tat-Bcl-x_L and Tat-BH4 had an effect on hindlimb locomotor recovery after SCI, we intrathecally administered Tat-BH4 or Tat-

Bcl-x_L (5ug/day) to injured spinal-cords for 7 days after SCI. Locomotor function was measured daily for 14 days, and then biweekly for 60 days. Vehicle-treated sham rats did not show visible impairments in locomotor function at any time. Consistent with published reports, an injury induced with 150 Kdynes impact force caused complete paralysis of the hind limbs in the first days after SCI that partially improved over time, as reflected in the increased BBB scores over a two month period (**Fig. 20**). However, locomotor recovery of SCI-rats treated with either Tat-Bcl-x_L or Tat-BH4 did not improve, but rather worsened in comparison to vehicle-treated SCI rats. As shown in **Fig. 20,** BBB scores were significantly lower from days 4 to 9 ($P<0.05$) in both Tat-Bcl-x_L and Tat-BH4 treated animals.

Effect of Tat-Bcl-$_{xL}$ on neuronal loss.

To evaluate whether impaired locomotor recovery results from additional loss of neurons in Tat-Bcl-x_L-or Tat-BH4 -treated SCI rats, we counted the number of neurons labeled with the neuronal specific marker, NeuN in sections located 4mm rostral to the lesion epicenter. As shown in **Fig. 21A**, the number of neurons was significantly lower in Tat-Bcl-x_L - and Tat-BH4-treated SCI rats, compared to the vehicle treated-SCI rats. This result suggests that while anti-apoptotic treatment protected neurons from apoptotic cell death, it did not prevent them from dying, likely due to necrosis. Thus, it is possible that the anti-apoptotic activity of Tat-Bcl-x_L and Tat-BH4 shifted neuronal death from apoptosis to necrosis, and thus amplified neuronal death due to necrosis-induced inflammatory reactions.

Effect of Tat-Bcl-x_L and Tat-BH4 on microglia/macrophage activation

To test the hypothesis that both Tat-Bcl-x_L and Tat-BH4 induced increased inflammatory reaction in injured spinal cords, we quantified the density of microglia/ macrophages 4 mm rostral to the lesion epicenter (the same region where we counted the number of neurons), by measuring the proportional area of cells expressing OX-42,

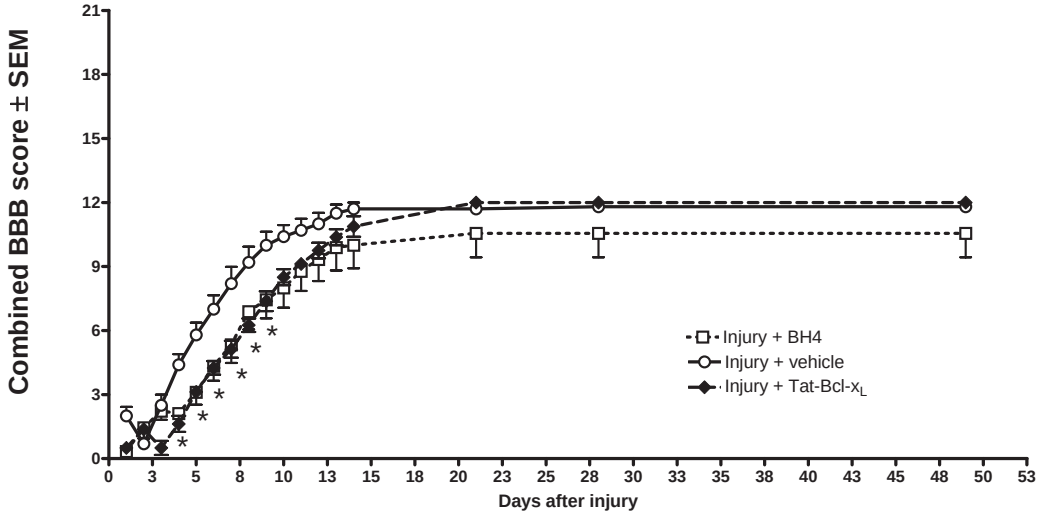

Fig. 20 Impaired locomotor recovery in Tat-Bcl-xL and Tat-BH4-treated rats. Transformed BBB scores for left and right hindlimb per animal were averaged and analyzed as combined score. Plotted data represent the mean ±SEM per time point of combined BBB score of Tat-Bcl-x_L (n=8); Tat-BH4 (n=9) and vehicle treated (n=9) injured rats. Rats treated with either Tat-Bcl-x_L or Tat-BH4 showed a decreased locomotor recovery during the first 10 days after injury in comparison to vehicle treated animals. (*) $p<0.05$ compared to vehicle –treated group. Transformed data were analyzed using Two-ways Repeated measures ANOVA with Bonferoni post-hoc corrections).

corresponding to the area of tissue occupied by immunohistochemically stained cellular profiles within a defined target area (Popovich et al., 1997). As shown in Fig. 5B, C (Left panel), SCI rats treated with either Tat-Bcl-x_L or Tat-BH4 showed a robust and significant increase in the total intensity of OX-42 staining in a 3mm^2 area (containing all the cross section of the cord) in comparison to vehicle-treated injured spinal cords (**Fig 21B**, **C**), indicating an increased inflammatory reaction in Tat-Bcl-x_L and Tat-BH4 treated SCI rats. Furthermore, consistent with the spatial and temporal profile of microglial/ macrophage activation/ infiltration after rat SCI (Popovich et al, 1997), an increased OX-42 immunolabeling in a 0.25mm^2 area at the dorsal horn, ventral horn and lateral funiculus was observed rostral to the lesion epicenter 7 days after injury. However, OX-42 immunolabeling was significantly higher in Tat-Bcl-x_L and Tat-BH4 treated SCI rats. Intense OX-42 labeling in gray matter

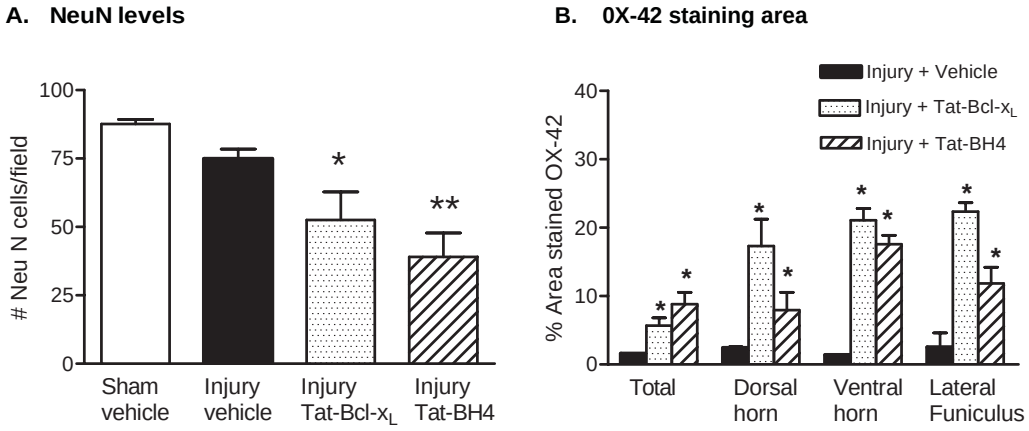

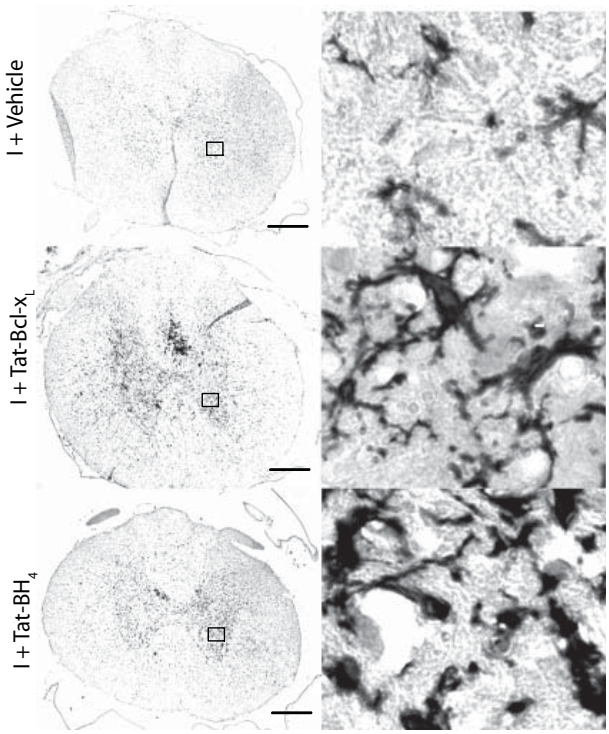

Fig. 21. Neuronal and microglial/ macrophage densities after Tat-Bcl-xL and Tat-BH4 treatment. **A.** Quantitative analysis of NeuN-labeled cells in the dorsal and ventral horn. Neurons were counted 4mm rostral to the lesion epicenter in sections of Tat-Bcl-x_L (n=3); Tat-BH4 (n=3) and vehicle-treated rats (n=3) 7 days after SCI. The number of Neu-N-positive cells was significantly lower in Tat-Bcl-x_L and Tat-BH4 treated injured spinal cords in cord (*$p<0.05$). **B.** Semi-quantitative analysis of OX-42 staining 4mm rostral to lesion epicenter in Tat-Bcl-x_L (n=3); Tat-BH4 (n=3) and vehicle-treated rats (n=3) 7days after SCI. Data represent the proportional area of OX-42 staining in a 3mm^2 region (total OX-42 labeling) or a 0.25mm^2 region at the dorsal horn, ventral horn and lateral funiculus. (See methods for details of quantification methods). Sections are adjacent to those used for Neu N counting. **C.** Representative example of OX-42 staining of microglia and macrophages 4mm rostral to the lesion epicenter, 7 days after injury. Left panel: cross sectional OX-42 staining showing increased microglia/macrophage activation in Tat-Bcl-x_L and Tat-BH4 treated injured spinal cords in comparison to vehicle-treated injured spinal cords. Scale bar: 350 µm. Right panel: high magnification of the area marked in the left panel as squares, shows intense labeling of OX-42 in long processes and round cell bodies surrounding gray matter cells, likely neurons, in Tat-Bcl-x_L and Tat-BH4 treated-injured spinal cords, and a moderate OX-42 labeling in vehicle treated injured spinal cords.

was observed surrounding neurons in the damaged spinal cords. In treated cords, OX-42 labeling stained hypertrophic cell bodies with short pseudopodic processes or round cells presenting morphology of activated microglia/macrophages (**Fig 21 C**)**.**

Discusion

Anti-apoptotic Tat-Bcl-x_L and Tat-BH4 impaired functional recovery after SCI.

Using intrathecal delivery we demonstrated that Tat-Bcl-x_L restored Bcl-x_L levels in both cytosolic and microsomal fractions of SCI rats during the 24h or 7 days delivery period, thus confirming that our chosen concentration and delivery method of Tat-Bcl-x_L were effective. To confirm that anti-apoptotic effect of Tat-Bcl-x_L that we observed was due to its role in protecting mitochondrial permeability, we used Tat-BH4 peptide. Bcl-2 and Bcl-x_L possess four conserved Bcl-2 homology (BH) domains, designated BH1 through BH4(Aritomi et al., 1997;Petros et al., 2004). It has been shown that the BH4 domain of Bcl-x_L is essential for the prevention of apoptotic mitochondrial changes (Shimizu et al., 2000;Sugioka et al., 2003). Our results showed that both Tat-Bcl-x_L and Tat-BH4 treatment significantly decreased levels of cytosolic oligonucleosomes to a similar extent, thus confirming that anti-apoptotic effects of Tat-Bcl-x_L in injured spinal cords was solely due to its well known protective role in mitochondria. We also used the BH4 construct because Tat-BH4 is not susceptible to phosphorylation or cleavage, both processes capable of reducing anti-apoptotic effects of Bcl-x_L (Kharbanda et al., 2000;Brichese et al., 2002;Simizu et al., 2004;Tamura et al., 2004). Bcl-x_L possesses an unstructured loop between BH3 and BH4 that contains recognition sites for phosphorylation and caspase-mediated cleavage, mechanisms that appear to regulate the function of Bcl-x_L after different insults in multiple cell lines (Fujita et al., 1998;Ojala et al., 2000;Figueroa, Jr. et al., 2003). We have also shown that SCI induces phosphorylation of endogenous Bcl-x_L and thus possibly inactivate

its anti-apoptotic effect (Cittelly et al., 2005). Therefore, it was possible that a fraction of the exogenous Tat-Bcl-x_L undergoes phosphorylation in injured spinal cords, and thus prevents its full anti-apoptotic effect. Our results showed that both Tat-Bcl-x_L and Tat-BH4 treatment significantly decreased levels of cytosolic oligonucleosomes to the same extent, suggesting that phosporylation of Tat-Bcl-x_L did not occur and that the Tat-Bcl-x_L treatment increased local levels of functional Bcl-x_L. Thus, the full anti-apoptotic effect of the exogenous Bcl-x_L was achieved.

In agreement with other reports (Kilic et al., 2002;Dietz et al., 2002a;Hotchkiss et al., 2006), Tat-Bcl-x_L significantly reduced total apoptotic death at 24h and 7 days after SCI, thus suggesting that the recovery of functions may be improved in Tat-Bcl-x_L or Tat-BH4-treated SCI rats. This expectation was also based on the reports of other anti-apoptotic treatments targeting Bcl-2 and Bcl-x_L that showed beneficial effects on the functional recovery after CNS trauma (Cao et al., 2002a;Yin et al., 2006). Surprisingly, the recovery of locomotor function of SCI-rats treated with Tat-Bcl-x_L or Tat-BH4 did not improve during the first 14 days, but rather worsen in comparison to vehicle-treated SCI rats. After day 14, SCI rats in all groups reached BBB scores above 14, which can not be analyzed with the transformation applied (Ferguson et al., 2004). To the best of our knowledge, this is the first report showing negative effects of long-term anti-apoptotic treatments after SCI.

Tat-Bcl-x_L and Tat-BH4 increased neuronal loss and microglial activation

In agreement with the negative effect of the long-term delivery of Tat-Bcl-x_L and Tat-BH4 on the recovery after SCI, we also found additional losses of neurons in the Tat-Bcl-x_L or Tat-BH4 treated SCI rats 7 days after injury. Since both treatments decreased SCI-induced apoptotic levels at seven days (**Fig. 19**), neuronal losses likely occurred through necrotic cell death. It has been shown in excitotoxic models of acute SCI that necrotic neuronal death early after trauma is linked to increased microglial activation in

gray matter (Gomes-Leal et al., 2004). Thus, it is possible that the anti-apoptotic activity of Tat-Bcl-x_L and Tat-BH4 shifted neuronal death from apoptosis to necrosis, and possibly amplified neuronal death due necrosis-induced inflammatory reactions. Consistent with this hypothesis we found an increase in neuronal death in Tat-Bcl-x_L (30%) and Tat-BH4 (48%) treated injured spinal cords compared to vehicle-treated injured spinal cords. Necrosis initiates inflammatory responses via activation of microglia and macrophages which release soluble factors including nitric oxide, free radicals, proteolytic enzymes, arachidonic acid metabolites, tumor necrosis factor, interleukin-1, cyclooxygenase -2 and prostaglandins (PG) (Schnell et al., 1999;Popovich et al., 2002;Beattie, 2004;Ahn et al., 2006). A large body of evidence suggests that these microglial molecules can induce neuronal cell death (Beattie, 2004;Skaper et al., 2006;Gibbons and Dragunow, 2006), and in turn, promote further microglial activation (Gomes-Leal et al., 2004). As shown in **Fig 21C**, enhanced labeling of OX-42 in rounded cells and hypertrophic cell with thin processes, indicative of activated macrophages and microglia, was found in perineuronal spaces enclosing neurons through gray matter in Tat-Bcl-x_L and Tat-BH4 treated SCI rats, compared to vehicle treated SCI rats. This supports our hypothesis that both anti-apoptotic agents trigger positive feedback loops between neuronal necrosis and microglial activation. Alternatively, it is also possible, that Tat-Bcl-x_L and Tat-BH4 treatments directly affected microglial/macrophage survival in injured spinal cords. It is known that SCI-induced microglial activation that peaks at 7 days after SCI in rats undergoes apoptotic cell death (Popovich et al., 1997). Thus, it is possible that Tat-Bcl-x_L and Tat-BH4 decreased microglial/macriphage apoptosis, which, may have increased the number of dying neurons in injured spinal cords. It would be interesting to determine in future studies whether all cell types in injured spinal cords (neurons and glia) are equally susceptible to the anti-apoptotic effect of Tat-Bcl-x_L and Tat-BH4 after SCI, and whether this susceptibility may be a helpful tool in designing more effective anti-apoptotic treatments.

Given that microglial activation and inflammation are main players in shaping pathological outcomes after SCI, in part by inducing cell death (Popovich et al., 2002;Gonzalez et al., 2003;Beattie, 2004) our result suggest that the therapeutic potential of Tat-Bcl-x_L or Tat-BH4 in injured spinal cords may be limited. Although a promising therapeutic tool in stroke and neurodegenerative diseases (Asoh et al., 2002;Dietz et al., 2002b;Yin et al., 2006), our results also indicate that chronic treatment of SCI with Tat-Bcl-x_L or other anti-apoptotic treatments targeting Bcl-x_L could be detrimental.

CHAPTER FIVE: SUMMARY AND FUTURE DIRECTIONS

SUMMARY

Long term deficits following moderate contusion to the spinal cord are due in part to significant secondary cell death of neurons and oligodendroglia at and around the site of injury. Apoptosis in the CNS is tightly regulated by members of the Bcl-2 family including anti-apoptotic Bcl-x_L. Bcl-x_L is the most robustly expressed pro-survival Bcl-2 molecule in adult spinal neurons and glia, and Bcl-x_L mRNA and protein levels decrease after SCI. However, the exact mechanism(s) of Bcl-x_L anti-apoptotic activity in the spinal cord and the extent to which Bcl-x_L anti-apoptotic activity is impaired after SCI are unknown. It has been suggested that the anti-apoptotic role of Bcl-x_L may be impaired by phosphorylation, cleavage (that yields pro-apoptotic fragments), or misrouting to subcellular organelles (endoplasmic reticulum- ER, nuclei). In this dissertation, I characterized the mechanisms that play a role in Bcl-x_L-inactivation and apoptosis after SCI by measuring Bcl-x_L protein levels and phosphorylation status at different subcellular compartments in sham-treated and injured- spinal cords, during the first 24h and up to seven days after trauma (Chapter 3).

Consistent with the hypothesis that Bcl-x_L regulates cell survival of neurons and glial cells before and after SCI, double staining with Bcl-x_L and NeuN (neurons) or CC-1 (oligodendrocytes) showed that Bcl-x_L is expressed throughout spinal cord in neurons and oligodendrocytes, but not in astrocytes or microglia. At 24h after injury, staining of Bcl-x_L decreased in those surviving neurons surrounding the lesion epicenter, supporting the hypothesis that Bcl-x_L decreases precede neuronal cell death after SCI. The time course of SCI-induced decreases in Bcl-x_L was different for cytosolic, mitochondrial, ER and nuclear extracts suggesting an independent regulation of Bcl-x_L shuttling among compartments after injury.

Interestingly, I found a phosphorylated form of Bcl-x_L (p-Ser^{62}-Bcl-x_L) in mitochondrial, nuclear and ER fractions of sham SC but not in the cytosolic fraction. Immunohistochemical analysis revealed that phosphorylated Bcl-x_L was present only in organelles in neurons, where it was preferentially expressed throughout neurites and axons in the uninjured spinal cord. After injury, P-ser^{62}Bcl-x_L appeared in the cytosolic fractions (as measured by western blot) and strongly stained some neuronal cell bodies (observed in the lesion-periphery), concomitant with SCI-induced decreases in cytosolic Bcl-x_L. Since the increases in cytosolic P-ser^{62}-Bcl-x_L occurred without evident changes in the levels of phosphorylated Bcl-x_L at organelles, it is likely that cytosolic Bcl-x_L undergoes phosphorylation early after SCI. To determine if phosphorylation of Bcl-x_L contributes to the impairment of Bcl-x_L anti-apoptotic function, I used an *in vitro* model of apoptotic cell death induced by vinblastine, a compound known to induce apoptosis in neuronal and non-neuronal cell lines, which also induces Bcl-x_L and Bcl-2 phosphorylation. Consistent with the observations in injured spinal-cord neurons, NGF-differentiated-PC12 cells undergo cell death after 24h vinblastine treatment, with significant increases in cytosolic P-ser^{62}Bcl-x_L levels and nuclear condensation. Interestingly, only a few cells were found that showed both DNA-fragmentation (measured by TUNEL assay) and p-ser^{62}Bcl-x_L staining, suggesting that phosphorylation of Bcl-x_L is an early event in the path to cell death.

The second goal of this dissertation was to evaluate the therapeutic potential of Bcl-x_L-administration after SCI (Chapter 4). To counteract SCI-induced decreases in Bcl-x_L and the resultant apoptosis, I used intrathecal delivery of the TAT protein transduction domain fused to Bcl-x_L (Tat-Bcl-x_L), or its anti-apoptotic domain BH4 (Tat-BH4). Considering that phosphorylation of Bcl-x_L could prevent exogenous Bcl-x_L from exerting its antiapoptotic role, I also used Tat-BH4 peptide, a construct that contains the anti-apoptotic domain of Bcl-x_L but lacks the phosphorylation sites. Even though I found evidence for the anti-apoptotic function of both Tat-Bcl-x_L and Tat-BH4 24h or 7 days after SCI, long-term

delivery (7 days) of these proteins impaired locomotor recovery and increased neuronal loss to a greater extent than SCI alone. Furthermore, the long-term administration of TAT-Bcl-x_L significantly increased microglia/macrophage levels in injured spinal cords compared to vehicle treated SCI rats, suggesting an enhanced inflammatory reaction induced by Tat-Bcl-x_L treatment. These results suggest that the anti-apoptotic treatment may shift neuronal apoptosis to necrosis, and initiate an inflammatory response (microglial activation) in SCI rats. As a result, Tat-Bcl-x_L/Tat-BH4-induced increases in proinflammatory reactions may amplify SCI-induced neuronal cell death and additionally impair functional recovery. Moreover, chronic treatment of SCI with Tat-Bcl-x_L or other anti-apoptotic treatments targeting Bcl-x_L could be detrimental.

Paradoxically, one of the advantages of using Tat-mediated delivery of Bcl-x_L could have increased its deleterious effects after SCI. Since Tat-Bcl-x_L can transduce a variety of cells, it is possible that the survival of macrophages/microglia benefited from the long-term delivery used here. In the first part of this dissertation (Chapter 3), I have shown that activated microglia/macrophages robustly express Bcl-x_L 7 days after SCI, and it has been shown that this cell population increases as early as 1 day after injury. Thus, it is possible that the long-term delivery of Tat-Bcl-x_L and Tat-BH4 had targeted not only neurons but also microglia, thus contributing to the exacerbated inflammatory response. Thus, to be effective in the spinal cord model, anti-apoptotic therapies should be designed to target neurons and later oligodendrocytes, limiting the therapeutic potential of Tat-Bcl-x_L or Tat-BH4 in injured spinal cords.

FUTURE DIRECTIONS

What is the role of Bcl-x_L phosphorylation in the normal CNS?

One of our unexpected findings was the presence of phosphorylated Bcl-x_L in the uninjured spinal cord. To the best of my knowledge, this is the first report of a

phosphorylated form of Bcl-x_L in the normal CNS, particularly in neurons. While it was not the goal of this dissertation, several observations suggest that phosphorylated Bcl-x_L could play an important role in neuronal differentiation and axonal function, probably roles that can represent functions different to apoptosis-prevention. First, the subcellular localization of this Bcl-x_L form was restricted to organelles throughout the developing neurites in NGF-differentiated PC12 and spinal cord axons. Second, our preliminary results showed levels of phosphorylated Bcl-x_L to increase over the time during the NGF-induced differentiation of PC12 cells and the RA-induced differentiation of neuroblastoma cells (SK-N-SH-SY5Y), and one of the hallmarks of differentiation to a neuronal phenotype is the formation and elongation of neurites.

Several reports support our interpretation: a) staurosporine-induced differentiation of neuroblastoma SH-SY5Y show elongated neurites, concomitant with increases in Bcl-x_L but not Bcl-2 mRNA levels (Pregi et al., 2006); b) adenovirus-mediated-Bcl-x_L overexpression in RGCs retinal explants increased both numbers and total length of emerging neurites and, in axotomized RGCs of adult rats *in vivo*, Bcl-x_L promoted intraretinal axon sprouting and fiber growth into the proximal optic nerve stump (Kretz et al., 2004) ; c). Malik et al, showed that the axons of AAV-Bcl-X_L-transduced RGCs remained morphologically intact after transection of the optic nerve (Malik et al., 2005); d) grafted mouse embryonic stem cells overexpressing Bcl-x_L differentiated into midbrain dopamine neurons, exhibited more extensive fiber outgrowth with long and numerous processes (Shim et al., 2004). However, none of these studies addressed the phosphorylation status of overexpressed Bcl-x_L; therefore, it is not possible to evaluate if the increase in neurite formation or axonal sprouting correlates with levels of Bcl-x_L phosphorylation. For instance, it would be interesting to evaluate if overexpression of a Bcl-x_L mutant lacking the phosphorylation site is able to promote neurite formation to a similar extent.

Interestingly, Tagami et al suggested a mechanism by which Bcl-x_L (not specifically phosphorylated Bcl-x_L) could regulate neurite outgrowth. They demonstrated that RTN/xL, a protein of the reticulon family (RT) interacts with Bcl-x_L at the ER. Since RTN/xL is the rat homologue of NogoA, a myelin associated protein that inhibits axonal regeneration, these authors suggest that neurite outgrowth could be inhibited by an intrinsic neuronal Nogo-A/RTN-xL, and that Bcl-x_L may promote neurite outgrowth by sequestering Nogo/ RTN-xL at the ER (Tagami et al., 2000). However, to probe this hypothesis, the putative NogoA/RTNxL protein must be first identified in neuronal ER, and then its Bcl-x_L binding properties further confirmed.

The presence of P-ser^{62}Bcl-x_L at the axonal mitochondria and the fact that microtubule disruption induces Bcl-x_L phosphorylation, suggests a role for Bcl-x_L in response to cytoskeletal disturbance, and might explain the high levels of phosphorylated Bcl-x_L present after SCI. Given that neuronal axons display a granular appearance with disarray of their neurofilaments and an unusual abundance of intracellular organelles (including mitochondria) and abortive growth cones, phosphorylation of Bcl-x_L after SCI could represent a failed attempt of the neurons to regenerate that leads to apoptosis by diminishing the pool of anti-apoptotic Bcl-x_L. In fact, it has been proposed that failed attempts to regenerate triggers apoptosis in neurons.

Finally, the mechanisms by which Tat-Bcl-x_L and Tat-BH4 increased microglial activation and neuronal death are still undefined. I previously mentioned the possibility of a direct effect on microglial survival by Tat-Bcl-x_L and Tat-BH4. However, it is also possible that the anti-apoptotic effect observed in this study shifted apoptosis to necrosis. Is it possible that Tat-Bcl-x_L and Tat-BH4 can become cell-death inducers? I cannot exclude the possibility that exogenous Tat-Bcl-x_L underwent cleavage by activated caspases, resulting in a cleavage fragment that augmented cell death.

However, the differences in the levels of neuronal death between Tat-Bcl-x_L and Tat-BH4 treated animals, suggest that this is not a likely scenario since Tat-BH4 (not susceptible to cleavage) induced a bigger neuronal loss. Given the technical difficulties associated with the study of the intracellular distribution of exogenous Tat-Bcl-x_L and Tat-BH4 after SCI, and its susceptibility to phosphorylation and caspase-mediated cleavage, in vitro studies might be more useful. They could be used to determine if Tat-Bcl-x_L treatment indeed induces cell death by shifting apoptosis to necrosis in injured spinal cord neurons. Also, if this signaling is due to modifications converting Bcl-x_L into an inducer of cell death.

BIBLIOGRAPHY

Abe,T., Takagi,N., Nakano,M., Furuya,M., and Takeo,S. (2004). Altered Bad localization and interaction between Bad and Bcl-xL in the hippocampus after transient global ischemia. Brain Res. *1009*, 159-168.

Ahn,Y.H., Bae Yeon,Y., Lee,G., Kang Mee,K., and Kang,S.K. (2006). Molecular insights of the injured lesions of rat spinal cords: Inflammation, apoptosis, and cell survival. Biochemical and Biophysical Research Communications *348*, 560-570.

Alonso,G., Guillemain,I., Dumoulin,A., Privat,A., and Patey,G. (1997). Immunolocalization of Bcl-xL/S in the central nervous system of neonatal and adult rats. Cell Tissue Res. *288*, 59-68.

Aritomi,M., Kunishima,N., Inohara,N., Ishibashi,Y., Ohta,S., and Morikawa,K. (1997). Crystal structure of rat Bcl-xL. Implications for the function of the Bcl-2 protein family. J. Biol. Chem. *272*, 27886-27892.

Asoh,S., Ohsawa,I., Mori,T., Katsura,K., Hiraide,T., Katayama,Y., Kimura,M., Ozaki,D., Yamagata,K., and Ohta,S. (2002). Protection against ischemic brain injury by protein therapeutics. Proc. Natl. Acad. Sci. U. S. A *99*, 17107-17112.

Asoh,S., Ohtsu,T., and Ohta,S. (2000). The super anti-apoptotic factor Bcl-xFNK constructed by disturbing intramolecular polar interactions in rat Bcl-xL. J. Biol. Chem. *275*, 37240-37245.

Bao,F., John,S.M., Chen,Y., Mathison,R.D., and Weaver,L.C. (2006). The tripeptide phenylalanine-(D) glutamate-(D) glycine modulates leukocyte infiltration and oxidative damage in rat injured spinal cord. Neuroscience *140*, 1011-1022.

Bao,F., and Liu,D. (2004). Hydroxyl radicals generated in the rat spinal cord at the level produced by impact injury induce cell death by necrosis and apoptosis: protection by a metalloporphyrin. Neuroscience *126*, 285-295.

Baptiste,D.C., and Fehlings,M.G. (2006). Pharmacological approaches to repair the injured spinal cord. J. Neurotrauma *23*, 318-334.

Barut,S., Unlu,Y.A., Karaoglan,A., Tuncdemir,M., Dagistanli,F.K., Ozturk,M., and Colak,A. (2005). The neuroprotective effects of z-DEVD.fmk, a caspase-3 inhibitor, on traumatic spinal cord injury in rats. Surg. Neurol. *64*, 213-220.

Bassik,M.C., Scorrano,L., Oakes,S.A., Pozzan,T., and Korsmeyer,S.J. (2004). Phosphorylation of BCL-2 regulates ER Ca2+ homeostasis and apoptosis. EMBO J. *23*, 1207-1216.

Basso,D.M., Beattie,M.S., and Bresnahan,J.C. (1995). A sensitive and reliable locomotor rating scale for open field testing in rats. J. Neurotrauma *12*, 1-21.

Basso,D.M., Beattie,M.S., and Bresnahan,J.C. (1996). Graded histological and locomotor outcomes after spinal cord contusion using the NYU weight-drop device versus transection. Exp. Neurol. *139*, 244-256.

Basu,A., and Haldar,S. (2003). Identification of a novel Bcl-xL phosphorylation site regulating the sensitivity of taxol- or 2-methoxyestradiol-induced apoptosis. FEBS Lett. *538*, 41-47.

Beattie,M.S., Farooqui,A.A., and Bresnahan,J.C. (2000a). Review of current evidence for apoptosis after spinal cord injury. J. Neurotrauma *17*, 915-925.

Beattie,M.S., Hermann,G.E., Rogers,R.C., and Bresnahan,J.C. (2002). Cell death in models of spinal cord injury. Prog. Brain Res. *137*, 37-47.

Beattie,M.S., Li,Q., and Bresnahan,J.C. (2000b). Cell death and plasticity after experimental spinal cord injury. Prog. Brain Res. *128*, 9-21.

Beattie,M.S. (2004). Inflammation and apoptosis: linked therapeutic targets in spinal cord injury. Trends in Molecular Medicine *10*, 580-583.

Boise,L.H., Gonzalez-Garcia,M., Postema,C.E., Ding,L., Lindsten,T., Turka,L.A., Mao,X., Nunez,G., and Thompson,C.B. (1993). bcl-x, a bcl-2-related gene that functions as a dominant regulator of apoptotic cell death. Cell *74*, 597-608.

Bredesen,D.E., Rao,R.V., and Mehlen,P. (2006). Cell death in the nervous system. Nature *443*, 796-802.

Brichese,L., Barboule,N., Heliez,C., and Valette,A. (2002). Bcl-2 phosphorylation and proteasome-dependent degradation induced by paclitaxel treatment: consequences on sensitivity of isolated mitochondria to Bid. Exp. Cell Res. *278*, 101-111.

Bunge,R.P., Puckett,W.R., Becerra,J.L., Marcillo,A., and Quencer,R.M. (1993). Observations on the pathology of human spinal cord injury. A review and classification of 22 new cases with details from a case of chronic cord compression with extensive focal demyelination. Adv. Neurol. *59*, 75-89.

Burnett,D.M., Cifu,D.X., Kolakowsky-Hayner,S., and Kreutzer,J.S. (2001). Predicting "charge outliers" after spinal cord injury: a multicenter analysis of demographics, injury characteristics, outcomes, and rehabilitation charges. Arch. Phys. Med. Rehabil. *82*, 114-119.

Cao,G., Pei,W., Ge,H., Liang,Q., Luo,Y., Sharp,F.R., Lu,A., Ran,R., Graham,S.H., and Chen,J. (2002a). In Vivo Delivery of a Bcl-xL Fusion Protein Containing the TAT Protein Transduction Domain Protects against Ischemic Brain Injury and Neuronal Apoptosis. J. Neurosci. *22*, 5423-5431.

Cao,G., Pei,W., Ge,H., Liang,Q., Luo,Y., Sharp,F.R., Lu,A., Ran,R., Graham,S.H., and Chen,J. (2002b). In Vivo Delivery of a Bcl-xL Fusion Protein Containing the TAT Protein Transduction Domain Protects against Ischemic Brain Injury and Neuronal Apoptosis. J. Neurosci *22*, 5423-5431.

Casha,S., Yu,W.R., and Fehlings,M.G. (2001). Oligodendroglial apoptosis occurs along degenerating axons and is associated with FAS and p75 expression following spinal cord injury in the rat. Neuroscience *103*, 203-218.

Chadebech,P., Brichese,L., Baldin,V., Vidal,S., and Valette,A. (1999). Phosphorylation and proteasome-dependent degradation of Bcl-2 in mitotic-arrested cells after microtubule damage. Biochem. Biophys. Res. Commun. *262*, 823-827.

Chen,M., and Wang,J. (2002). Initiator caspases in apoptosis signaling pathways. Apoptosis. *7*, 313-319.

Cheng,E.H., Kirsch,D.G., Clem,R.J., Ravi,R., Kastan,M.B., Bedi,A., Ueno,K., and Hardwick,J.M. (1997). Conversion of Bcl-2 to a Bax-like death effector by caspases. Science *278*, 1966-1968.

Cheng,E.H., Levine,B., Boise,L.H., Thompson,C.B., and Hardwick,J.M. (1996). Bax-independent inhibition of apoptosis by Bcl-XL. Nature *379*, 554-556.

Cherbonnel-Lasserre,C., and Dosanjh,M.K. (1997). Suppression of apoptosis by overexpression of Bcl-2 or Bcl-xL promotes survival and mutagenesis after oxidative damage. Biochimie *79*, 613-617.

Chipuk,J.E., Bouchier-Hayes,L., and Green,D.R. (2006). Mitochondrial outer membrane permeabilization during apoptosis: the innocent bystander scenario. Cell Death. Differ. *13*, 1396-1402.

Citron,B.A., Arnold,P.M., Sebastian,C., Qin,F., Malladi,S., Ameenuddin,S., Landis,M. E., and Festoff,B.W. (2000). Rapid upregulation of caspase-3 in rat spinal cord after injury: mRNA, protein, and cellular localization correlates with apoptotic cell death. Exp. Neurol. *166*, 213-226.

Cittelly,D., Nesic-Taylor,O., Hulsebosch,C.E., and Perez-Polo,J.R. Effect of Spinal Cord Injury on Bcl-x$_L$ Expression Levels and their Subcellular Distributions. J.Neurotrauma 22[10], 1164. 2005.
Ref Type: Abstract

Clem,R.J., Cheng,E.H., Karp,C.L., Kirsch,D.G., Ueno,K., Takahashi,A., Kastan,M.B., Griffin,D.E., Earnshaw,W.C., Veliuona,M.A., and Hardwick,J.M. (1998). Modulation of cell death by Bcl-XL through caspase interaction. Proc. Natl. Acad. Sci. U. S. A *95*, 554-559.

Colak,A., Karaoglan,A., Barut,S., Kokturk,S., Akyildiz,A.I., and Tasyurekli,M. (2005). Neuroprotection and functional recovery after application of the caspase-9 inhibitor z-LEHD-fmk in a rat model of traumatic spinal cord injury. J. Neurosurg. Spine *2*, 327-334.

Crowe,M.J., Bresnahan,J.C., Shuman,S.L., Masters,J.N., and Beattie,M.S. (1997). Apoptosis and delayed degeneration after spinal cord injury in rats and monkeys. Nat. Med. *3*, 73-76.

Crown,E.D., Ye,Z., Johnson,K.M., Xu,G.Y., McAdoo,D.J., and Hulsebosch,C.E. (2006). Increases in the activated forms of ERK 1/2, p38 MAPK, and CREB are correlated with

the expression of at-level mechanical allodynia following spinal cord injury. Exp. Neurol. *199*, 397-407.

Danial,N.N., and Korsmeyer,S.J. (2004). Cell Death: Critical Control Points. Cell *116*, 205-219.

Diem,R., Taheri,N., Dietz,G.P., Kuhnert,A., Maier,K., Sattler,M.B., Gadjanski,I., Merkler,D., and Bahr,M. (2005). HIV-Tat-mediated Bcl-XL delivery protects retinal ganglion cells during experimental autoimmune optic neuritis. Neurobiol. Dis. *20*, 218-226.

Dietz,G.P., Kilic,E., and Bahr,M. (2002a). Inhibition of neuronal apoptosis in vitro and in vivo using TAT-mediated protein transduction. Mol. Cell Neurosci. *21*, 29-37.

Dietz,G.P., Kilic,E., and Bahr,M. (2002b). Inhibition of neuronal apoptosis in vitro and in vivo using TAT-mediated protein transduction. Mol. Cell Neurosci *21*, 29-37.

Drache,B., Diehl,G.E., Beyreuther,K., Perlmutter,L.S., and Konig,G. (1997). Bcl-xl-specific antibody labels activated microglia associated with Alzheimer's disease and other pathological states. J. Neurosci. Res. *47*, 98-108.

Du,L., Lyle,C.S., and Chambers,T.C. (2005). Characterization of vinblastine-induced Bcl-xL and Bcl-2 phosphorylation: evidence for a novel protein kinase and a coordinated phosphorylation/dephosphorylation cycle associated with apoptosis induction. Oncogene *24*, 107-117.

Dumont,A.S., Dumont,R.J., and Oskouian,R.J. (2002). Will improved understanding of the pathophysiological mechanisms involved in acute spinal cord injury improve the potential for therapeutic intervention? Curr. Opin. Neurol. *15*, 713-720.

Earnshaw,W.C., Martins,L.M., and Kaufmann,S.H. (1999). Mammalian caspases: structure, activation, substrates, and functions during apoptosis. Annu. Rev Biochem. *68*, 383-424.

Faitova,J., Krekac,D., Hrstka,R., and Vojtesek,B. (2006). Endoplasmic reticulum stress and apoptosis. Cell Mol. Biol Lett. *11*, 488-505.

Fan,M., Du,L., Stone,A.A., Gilbert,K.M., and Chambers,T.C. (2000a). Modulation of mitogen-activated protein kinases and phosphorylation of Bcl-2 by vinblastine represent persistent forms of normal fluctuations at G2-M1. Cancer Res. *60*, 6403-6407.

Fan,M., Goodwin,M., Vu,T., Brantley-Finley,C., Gaarde,W.A., and Chambers,T.C. (2000b). Vinblastine-induced phosphorylation of Bcl-2 and Bcl-XL is mediated by JNK and occurs in parallel with inactivation of the Raf-1/MEK/ERK cascade. J. Biol. Chem. *275*, 29980-29985.

Ferguson,A.R., Hook,M.A., Garcia,G., Bresnahan,J.C., Beattie,M.S., and Grau,J.W. (2004). A simple post hoc transformation that improves the metric properties of the BBB scale for rats with moderate to severe spinal cord injury. J. Neurotrauma *21*, 1601-1613.

Figueroa,B., Jr., Sauerwald,T.M., Oyler,G.A., Hardwick,J.M., and Betenbaugh,M.J. (2003). A comparison of the properties of a Bcl-xL variant to the wild-type anti-apoptosis inhibitor in mammalian cell cultures. Metab Eng *5*, 230-245.

Fisher,C.G., Noonan,V.K., and Dvorak,M.F. (2006). Changing face of spine trauma care in North America. Spine *31*, S2-S8.

Fleming,J.C., Norenberg,M.D., Ramsay,D.A., Dekaban,G.A., Marcillo,A.E., Saenz,A.D., Pasquale-Styles,M., Dietrich,W.D., and Weaver,L.C. (2006). The cellular inflammatory response in human spinal cords after injury. Brain awl296.

Foyouzi-Youssefi,R., Arnaudeau,S., Borner,C., Kelley,W.L., Tschopp,J., Lew,D.P., Demaurex,N., and Krause,K.H. (2000). Bcl-2 decreases the free Ca2+ concentration within the endoplasmic reticulum. PNAS *97*, 5723-5728.

Friedlander,A.M. (1986). Macrophages are sensitive to anthrax lethal toxin through an acid-dependent process. J. Biol. Chem. *261*, 7123-7126.

Fujita,E., Urase,K., Egashira,J., Miho,Y., Isahara,K., Uchiyama,Y., Isoai,A., Kumagai,H., Kuida,K., Motoyama,N., and Momoi,T. (2000). Detection of caspase-9 activation in the cell death of the Bcl-x-deficient mouse embryo nervous system by cleavage sites-directed antisera. Brain Res. Dev. Brain Res. *122*, 135-147.

Fujita,N., Nagahashi,A., Nagashima,K., Rokudai,S., and Tsuruo,T. (1998). Acceleration of apoptotic cell death after the cleavage of Bcl-XL protein by caspase-3-like proteases. Oncogene *17*, 1295-1304.

Ganju,N., and Eastman,A. (2002). Bcl-X(L) and calyculin A prevent translocation of Bax to mitochondria during apoptosis. Biochem. Biophys. Res. Commun. *291*, 1258-1264.

Garcia-Saez,A.J., Mingarro,I., Perez-Paya,E., and Salgado,J. (2004). Membrane-insertion fragments of Bcl-xL, Bax, and Bid. Biochemistry *43*, 10930-10943.

Gibbons,H.M., and Dragunow,M. (2006). Microglia induce neural cell death via a proximity-dependent mechanism involving nitric oxide. Brain Res. *1084*, 1-15.

Gollapudi,L., and Oblinger,M.M. (1999). Estrogen and NGF synergistically protect terminally differentiated, ERalpha-transfected PC12 cells from apoptosis. J. Neurosci. Res. *56*, 471-481.

Gomes-Leal,W., Corkill,D.J., Freire,M.A., Picanco-Diniz,C.W., and Perry,V.H. (2004). Astrocytosis, microglia activation, oligodendrocyte degeneration, and pyknosis following acute spinal cord injury. Exp. Neurol. *190*, 456-467.

Gonzalez,R., Glaser,J., Liu,M.T., Lane,T.E., and Keirstead,H.S. (2003). Reducing inflammation decreases secondary degeneration and functional deficit after spinal cord injury. Exp. Neurol. *184*, 456-463.

Gonzalez-Garcia,M., Garcia,I., Ding,L., O'Shea,S., Boise,L.H., Thompson,C.B., and Nunez,G. (1995). bcl-x is expressed in embryonic and postnatal neural tissues and functions to prevent neuronal cell death. Proc. Natl. Acad. Sci. U. S. A *92*, 4304-4308.

Gonzalez-Garcia,M., Perez-Ballestero,R., Ding,L., Duan,L., Boise,L.H., Thompson,C. B., and Nunez,G. (1994). bcl-XL is the major bcl-x mRNA form expressed during murine development and its product localizes to mitochondria. Development *120*, 3033-3042.

Gottlieb,E., Vander Heiden,M.G., and Thompson,C.B. (2000). Bcl-x(L) prevents the initial decrease in mitochondrial membrane potential and subsequent reactive oxygen species production during tumor necrosis factor alpha-induced apoptosis. Mol. Cell Biol *20*, 5680-5689.

Grad,J.M., Zeng,X.R., and Boise,L.H. (2000). Regulation of Bcl-xL: a little bit of this and a little bit of STAT. Curr. Opin. Oncol. *12*, 543-549.

Green,D.R., and Kroemer,G. (2004). The pathophysiology of mitochondrial cell death. Science *305*, 626-629.

Grethe,S., Ares,M.P., Andersson,T., and Porn-Ares,M.I. (2004). p38 MAPK mediates TNF-induced apoptosis in endothelial cells via phosphorylation and downregulation of Bcl-x(L). Exp. Cell Res. *298*, 632-642.

Grill,R.J. (2005). User-defined variables that affect outcome in spinal cord contusion/ compression models. Experimental Neurology *196*, 1-5.

Gross,A., Pilcher,K., Blachly-Dyson,E., Basso,E., Jockel,J., Bassik,M.C., Korsmeyer,S.J., and Forte,M. (2000). Biochemical and genetic analysis of the mitochondrial response of yeast to BAX and BCL-X(L). Mol. Cell Biol. *20*, 3125-3136.

Grossman,S.D., Rosenberg,L.J., and Wrathall,J.R. (2001). Temporal-spatial pattern of acute neuronal and glial loss after spinal cord contusion. Exp. Neurol. *168*, 273-282.

Hall,E.D., and Braughler,J.M. (1993). Free radicals in CNS injury. Res. Publ. Assoc. Res. Nerv. Ment. Dis. *71*, 81-105.

Hallin,U., Kondo,E., Ozaki,Y., Hagberg,H., Shibasaki,F., and Blomgren,K. (2006). Bcl-2 phosphorylation in the BH4 domain precedes caspase-3 activation and cell death after neonatal cerebral hypoxic-ischemic injury. Neurobiol. Dis. *21*, 478-486.

Hammond,P.W., Alpin,J., Rise,C.E., Wright,M., and Kreider,B.L. (2001). In vitro selection and characterization of Bcl-X(L)-binding proteins from a mix of tissue-specific mRNA display libraries. J. Biol. Chem. *276*, 20898-20906.

Hamner,S., Skoglosa,Y., and Lindholm,D. (1999). Differential expression of bcl-w and bcl-x messenger RNA in the developing and adult rat nervous system. Neuroscience *91*, 673-684.

Hengartner,M.O. (2000). The biochemistry of apoptosis. Nature *407*, 770-776.

Hoetelmans,R., van Slooten,H.J., Keijzer,R., Erkeland,S., van,d., V, and Dierendonck,J. H. (2000). Bcl-2 and Bax proteins are present in interphase nuclei of mammalian cells. Cell Death. Differ. *7*, 384-392.

Hoetelmans,R.W. (2004). Nuclear partners of Bcl-2: Bax and PML. DNA Cell Biol. *23*, 351-354.

Hoetelmans,R.W., van,d., V, and Van Dierendonck,J.H. (2003). The presence of 19-kDa Bcl-2 in dividing cells. Cell Prolif. *36*, 293-306.

Hotchkiss,R.S., McConnell,K.W., Bullok,K., Davis,C.G., Chang,K.C., Schwulst,S. J., Dunne,J.C., Dietz,G.P., Bahr,M., McDunn,J.E., Karl,I.E., Wagner,T.H., Cobb,J.P., Coopersmith,C.M., and Piwnica-Worms,D. (2006). TAT-BH4 and TAT-Bcl-xL peptides protect against sepsis-induced lymphocyte apoptosis in vivo. J. Immunol. *176*, 5471-5477.

Hou,Q., Cymbalyuk,E., Hsu,S.C., Xu,M., and Hsu,Y.T. (2003). Apoptosis modulatory activities of transiently expressed Bcl-2: roles in cytochrome C release and Bax regulation. Apoptosis. *8*, 617-629.

Hulsebosch,C.E. (2002). Recent advances in pathophysiology and treatment of spinal cord injury. Adv. Physiol Educ. *26*, 238-255.

Ishikawa,Y., Kusaka,E., Enokido,Y., Ikeuchi,T., and Hatanaka,H. (2003). Regulation of Bax translocation through phosphorylation at Ser-70 of Bcl-2 by MAP kinase in NO-induced neuronal apoptosis. Mol. Cell Neurosci. *24*, 451-459.

Itoh,T., Itoh,A., and Pleasure,D. (2003). Bcl-2-related protein family gene expression during oligodendroglial differentiation. J. Neurochem. *85*, 1500-1512.

Jeong,S.Y., Gaume,B., Lee,Y.J., Hsu,Y.T., Ryu,S.W., Yoon,S.H., and Youle,R.J. (2004). Bcl-x(L) sequesters its C-terminal membrane anchor in soluble, cytosolic homodimers. EMBO J. *23*, 2146-2155.

Jonas,E.A., Hickman,J.A., Chachar,M., Polster,B.M., Brandt,T.A., Fannjiang,Y., Ivanovska,I., Basanez,G., Kinnally,K.W., Zimmerberg,J., Hardwick,J.M., and Kaczmarek,L.K. (2004). Proapoptotic N-truncated BCL-xL protein activates endogenous mitochondrial channels in living synaptic terminals. Proc. Natl. Acad. Sci. U. S. A *101*, 13590-13595.

Jonas,E.A., Hoit,D., Hickman,J.A., Brandt,T.A., Polster,B.M., Fannjiang,Y., McCarthy,E., Montanez,M.K., Hardwick,J.M., and Kaczmarek,L.K. (2003). Modulation of synaptic transmission by the BCL-2 family protein BCL-xL. J. Neurosci. *23*, 8423-8431.

Jones,T.B., McDaniel,E.E., and Popovich,P.G. (2005). Inflammatory-mediated injury and repair in the traumatically injured spinal cord. Curr. Pharm. Des *11*, 1223-1236.

Jordan,J., Galindo,M.F., Tornero,D., Gonzalez-Garcia,C., and Cena,V. (2004). Bcl-x L blocks mitochondrial multiple conductance channel activation and inhibits 6-OHDA-induced death in SH-SY5Y cells. J. Neurochem. *89*, 124-133.

Kaplan,I.M., Wadia,J.S., and Dowdy,S.F. (2005). Cationic TAT peptide transduction domain enters cells by macropinocytosis. J. Control Release *102*, 247-253.

Kaufmann,T., Schlipf,S., Sanz,J., Neubert,K., Stein,R., and Borner,C. (2003). Characterization of the signal that directs Bcl-x(L), but not Bcl-2, to the mitochondrial outer membrane. J. Cell Biol. *160*, 53-64.

Kerschensteiner,M., Schwab,M.E., Lichtman,J.W., and Misgeld,T. (2005). In vivo imaging of axonal degeneration and regeneration in the injured spinal cord. Nat Med. *11*, 572-577.

Kharbanda,S., Saxena,S., Yoshida,K., Pandey,P., Kaneki,M., Wang,Q., Cheng,K., Chen,Y. N., Campbell,A., Sudha,T., Yuan,Z.M., Narula,J., Weichselbaum,R., Nalin,C., and Kufe,D. (2000). Translocation of SAPK/JNK to mitochondria and interaction with Bcl-x(L) in response to DNA damage. J. Biol. Chem. *275*, 322-327.

Kigerl,K.A., McGaughy,V.M., and Popovich,P.G. (2006). Comparative analysis of lesion development and intraspinal inflammation in four strains of mice following spinal contusion injury. J. Comp Neurol. *494*, 578-594.

Kilic,E., Dietz,G.P., Hermann,D.M., and Bahr,M. (2002). Intravenous TAT-Bcl-Xl is protective after middle cerebral artery occlusion in mice. Ann. Neurol. *52*, 617-622.

Kim,J.A., Mitsukawa,K., Yamada,M.K., Nishiyama,N., Matsuki,N., and Ikegaya,Y. (2002). Cytoskeleton disruption causes apoptotic degeneration of dentate granule cells in hippocampal slice cultures. Neuropharmacology *42*, 1109-1118.

Kirsch,D.G., Doseff,A., Chau,B.N., Lim,D.S., Souza-Pinto,N.C., Hansford,R., Kastan,M. B., Lazebnik,Y.A., and Hardwick,J.M. (1999). Caspase-3-dependent cleavage of Bcl-2 promotes release of cytochrome c. J. Biol. Chem. *274*, 21155-21161.

Klein,D., Ribeiro,M.M., Mendoza,V., Jayaraman,S., Kenyon,N.S., Pileggi,A., Molano,R. D., Inverardi,L., Ricordi,C., and Pastori,R.L. (2004). Delivery of Bcl-XL or its BH4 domain by protein transduction inhibits apoptosis in human islets. Biochem. Biophys. Res. Commun. *323*, 473-478.

Knoblach,S.M., Huang,X., VanGelderen,J., Calva-Cerqueira,D., and Faden,A.I. (2005). Selective caspase activation may contribute to neurological dysfunction after experimental spinal cord trauma. J. Neurosci Res. *80*, 369-380.

Krause,J.S. (2003). Years to employment after spinal cord injury. Arch. Phys. Med. Rehabil. *84*, 1282-1289.

Krause,J.S., and Terza,J.V. (2006). Injury and demographic factors predictive of disparities in earnings after spinal cord injury. Arch. Phys. Med. Rehabil. *87*, 1318-1326.

Kretz,A., Kugler,S., Happold,C., Bahr,M., and Isenmann,S. (2004). Excess Bcl-XL increases the intrinsic growth potential of adult CNS neurons in vitro. Mol. Cell Neurosci. *26*, 63-74.

Kuwana,T., Bouchier-Hayes,L., Chipuk,J.E., Bonzon,C., Sullivan,B.A., Green,D.R., and Newmeyer,D.D. (2005). BH3 domains of BH3-only proteins differentially regulate Bax-mediated mitochondrial membrane permeabilization both directly and indirectly. Mol. Cell *17*, 525-535.

Liang,Y., Yan,C., Nylander,K.D., and Schor,N.F. (2003). Early events in Bcl-2-enhanced apoptosis. Apoptosis. *8*, 609-616.

Liu,X.H., Collier,R.J., and Youle,R.J. (2001). Inhibition of axotomy-induced neuronal apoptosis by extracellular delivery of a Bcl-XL fusion protein. J. Biol. Chem. *276*, 46326-46332.

Liu,X.Z., Xu,X.M., Hu,R., Du,C., Zhang,S.X., McDonald,J.W., Dong,H.X., Wu,Y.J., Fan,G.S., Jacquin,M.F., Hsu,C.Y., and Choi,D.W. (1997). Neuronal and glial apoptosis after traumatic spinal cord injury. J. Neurosci. *17*, 5395-5406.

Lu,J., Ashwell,K.W., and Waite,P. (2000). Advances in secondary spinal cord injury: role of apoptosis. Spine *25*, 1859-1866.

Lu,Q.L., Hanby,A.M., Nasser Hajibagheri,M.A., Gschmeissner,S.E., Lu,P.J., Taylor-Papadimitriou,J., Krajewski,S., Reed,J.C., and Wright,N.A. (1994). Bcl-2 protein localizes to the chromosomes of mitotic nuclei and is correlated with the cell cycle in cultured epithelial cell lines. J. Cell Sci. *107 (Pt 2)*, 363-371.

Malik,J.M., Shevtsova,Z., Bahr,M., and Kugler,S. (2005). Long-term in vivo inhibition of CNS neurodegeneration by Bcl-XL gene transfer. Mol. Ther. *11*, 373-381.

Matsuoka,N., Ishii,K., Akimoto,M., Hamada,H., Hashimoto,N., and Miyatake,S. (2002). Overexpression of basic fibroblast growth factor and Bcl-xL with adenoviral vectors protects primarily cultured neurons against glutamate insult. Neurosurgery *50*, 857-862.

McEwen,M.L., and Springer,J.E. (2005). A mapping study of caspase-3 activation following acute spinal cord contusion in rats. J. Histochem. Cytochem. *53*, 809-819.

Minn,A.J., Kettlun,C.S., Liang,H., Kelekar,A., Vander Heiden,M.G., Chang,B. S., Fesik,S.W., Fill,M., and Thompson,C.B. (1999). Bcl-xL regulates apoptosis by heterodimerization-dependent and -independent mechanisms. EMBO J. *18*, 632-643.

Mizuguchi,M., Sohma,O., Takashima,S., Ikeda,K., Yamada,M., Shiraiwa,N., and Ohta,S. (1996). Immunochemical and immunohistochemical localization of Bcl-x protein in the rat central nervous system. Brain Res. *712*, 281-286.

Morishima,N., Nakanishi,K., Tsuchiya,K., Shibata,T., and Seiwa,E. (2004). Translocation of Bim to the endoplasmic reticulum (ER) mediates ER stress signaling for activation of caspase-12 during ER stress-induced apoptosis. J. Biol. Chem. *279*, 50375-50381.

Muhlethaler-Mottet,A., Bourloud,K.B., Auderset,K., Joseph,J.M., and Gross,N. (2004). Drug-mediated sensitization to TRAIL-induced apoptosis in caspase-8-complemented neuroblastoma cells proceeds via activation of intrinsic and extrinsic pathways and caspase-dependent cleavage of XIAP, Bcl-xL and RIP. Oncogene *23*, 5415-5425.

Murriel,C.L., and Dowdy,S.F. (2006). Influence of protein transduction domains on intracellular delivery of macromolecules. Expert. Opin. Drug Deliv. *3*, 739-746.

Nagahara,H., Vocero-Akbani,A.M., Snyder,E.L., Ho,A., Latham,D.G., Lissy,N.A., Becker-Hapak,M., Ezhevsky,S.A., and Dowdy,S.F. (1998). Transduction of full-length

TAT fusion proteins into mammalian cells: TAT-p27Kip1 induces cell migration. Nat Med. *4*, 1449-1452.

Nesic,O., Svrakic,N.M., Xu,G.Y., McAdoo,D., Westlund,K.N., Hulsebosch,C.E., Ye,Z., Galante,A., Soteropoulos,P., Tolias,P., Young,W., Hart,R.P., and Perez-Polo,J.R. (2002). DNA microarray analysis of the contused spinal cord: effect of NMDA receptor inhibition. J. Neurosci. Res. *68*, 406-423.

Nesic,O., Xu,G.Y., McAdoo,D., High,K.W., Hulsebosch,C., and Perez-Pol,R. (2001). IL-1 receptor antagonist prevents apoptosis and caspase-3 activation after spinal cord injury. J. Neurotrauma *18*, 947-956.

Nesic-Taylor,O., Cittelly,D., Ye,Z., Xu,G.Y., Unabia,G., Lee,J.C., Svrakic,N.M., Liu,X. H., Youle,R.J., Wood,T.G., McAdoo,D., Westlund,K.N., Hulsebosch,C.E., and Perez-Polo,J.R. (2005). Exogenous Bcl-xL fusion protein spares neurons after spinal cord injury. J. Neurosci. Res. *79*, 628-637.

Ng,F.W., and Shore,G.C. (1998). Bcl-XL cooperatively associates with the Bap31 complex in the endoplasmic reticulum, dependent on procaspase-8 and Ced-4 adaptor. J. Biol. Chem. *273*, 3140-3143.

Nomura,M., Shimizu,S., Sugiyama,T., Narita,M., Ito,T., Matsuda,H., and Tsujimoto,Y. (2003). 14-3-3 Interacts directly with and negatively regulates pro-apoptotic Bax. J. Biol. Chem. *278*, 2058-2065.

Norenberg,M.D., Smith,J., and Marcillo,A. (2004). The pathology of human spinal cord injury: defining the problems. J. Neurotrauma *21*, 429-440.

Nuydens,R., Dispersyn,G., Van Den,K.G., de,J.M., Connors,R., Ramaekers,F., Borgers,M., and Geerts,H. (2000). Bcl-2 protects against apoptosis-related microtubule alterations in neuronal cells. Apoptosis. *5*, 43-51.

Oakes,S.A., Lin,S.S., and Bassik,M.C. (2006). The control of endoplasmic reticulum-initiated apoptosis by the BCL-2 family of proteins. Curr. Mol. Med. *6*, 99-109.

Oakes,S.A., Scorrano,L., Opferman,J.T., Bassik,M.C., Nishino,M., Pozzan,T., and Korsmeyer,S.J. (2005). Proapoptotic BAX and BAK regulate the type 1 inositol trisphosphate receptor and calcium leak from the endoplasmic reticulum. Proc. Natl. Acad. Sci. U. S. A *102*, 105-110.

Ojala,P.M., Yamamoto,K., Castanos-Velez,E., Biberfeld,P., Korsmeyer,S.J., and Makela,T.P. (2000). The apoptotic v-cyclin-CDK6 complex phosphorylates and inactivates Bcl-2. Nat. Cell Biol. *2*, 819-825.

Panickar,K.S., Nonner,D., and Barrett,J.N. (2005). Overexpression of Bcl-xl protects septal neurons from prolonged hypoglycemia and from acute ischemia-like stress. Neuroscience *135*, 73-80.

Park,E., Velumian,A.A., and Fehlings,M.G. (2004). The role of excitotoxicity in secondary mechanisms of spinal cord injury: a review with an emphasis on the implications for white matter degeneration. J. Neurotrauma *21*, 754-774.

Parsadanian,A.S., Cheng,Y., Keller-Peck,C.R., Holtzman,D.M., and Snider,W.D. (1998). Bcl-xL is an antiapoptotic regulator for postnatal CNS neurons. J. Neurosci. *18*, 1009-1019.

Pearse,D.D., Pereira,F.C., Marcillo,A.E., Bates,M.L., Berrocal,Y.A., Filbin,M.T., and Bunge,M.B. (2004). cAMP and Schwann cells promote axonal growth and functional recovery after spinal cord injury. Nat. Med. *10*, 610-616.

Petros,A.M., Olejniczak,E.T., and Fesik,S.W. (2004). Structural biology of the Bcl-2 family of proteins. Biochim. Biophys. Acta *1644*, 83-94.

Pinton,P., and Rizzuto,R. (2006). Bcl-2 and Ca2+ homeostasis in the endoplasmic reticulum. Cell Death. Differ. *13*, 1409-1418.

Pinton,P., Ferrari,D., Magalhaes,P., Schulze-Osthoff,K., Di Virgilio,F., Pozzan,T., and Rizzuto,R. (2000). Reduced Loading of Intracellular Ca2+ Stores and Downregulation of Capacitative Ca2+ Influx In Bcl-2-Overexpressing Cells. J. Cell Biol. *148*, 857-862.

Popovich,P.G., Guan,Z., McGaughy,V., Fisher,L., Hickey,W.F., and Basso,D.M. (2002). The neuropathological and behavioral consequences of intraspinal microglial/macrophage activation. J. Neuropathol. Exp. Neurol. *61*, 623-633.

Popovich,P.G., Guan,Z., Wei,P., Huitinga,I., van,R.N., and Stokes,B.T. (1999). Depletion of hematogenous macrophages promotes partial hindlimb recovery and neuroanatomical repair after experimental spinal cord injury. Exp. Neurol. *158*, 351-365.

Popovich,P.G., van,R.N., Hickey,W.F., Preidis,G., and McGaughy,V. (2003). Hematogenous macrophages express CD8 and distribute to regions of lesion cavitation after spinal cord injury. Exp. Neurol. *182*, 275-287.

Popovich,P.G., Wei,P., and Stokes,B.T. (1997). Cellular inflammatory response after spinal cord injury in Sprague-Dawley and Lewis rats. J. Comp Neurol. *377*, 443-464.

Poruchynsky,M.S., Wang,E.E., Rudin,C.M., Blagosklonny,M.V., and Fojo,T. (1998). Bcl-xL is phosphorylated in malignant cells following microtubule disruption. Cancer Res. *58*, 3331-3338.

Potocky,T.B., Menon,A.K., and Gellman,S.H. (2003). Cytoplasmic and Nuclear Delivery of a TAT-derived Peptide and a {beta}-Peptide after Endocytic Uptake into HeLa Cells. J. Biol. Chem. *278*, 50188-50194.

Pregi,N., Vittori,D., Perez,G., Leiros,C.P., and Nesse,A. (2006). Effect of erythropoietin on staurosporine-induced apoptosis and differentiation of SH-SY5Y neuroblastoma cells. Biochim. Biophys. Acta *1763*, 238-246.

Putcha,G.V., Harris,C.A., Moulder,K.L., Easton,R.M., Thompson,C.B., and Johnson,E. M., Jr. (2002). Intrinsic and extrinsic pathway signaling during neuronal apoptosis: lessons from the analysis of mutant mice. J. Cell Biol *157*, 441-453.

Qiu,J., Nesic,O., Ye,Z., Rea,H., Westlund,K.N., Xu,G.Y., McAdoo,D., Hulsebosch,C.E., and Perez-Polo,J.R. (2001). Bcl-xL expression after contusion to the rat spinal cord. J. Neurotrauma *18*, 1267-1278.

Reed,J.C. (2006). Proapoptotic multidomain Bcl-2/Bax-family proteins: mechanisms, physiological roles, and therapeutic opportunities. Cell Death. Differ. *13*, 1378-1386.

Reimertz,C., Kogel,D., Rami,A., Chittenden,T., and Prehn,J.H. (2003). Gene expression during ER stress-induced apoptosis in neurons: induction of the BH3-only protein Bbc3/PUMA and activation of the mitochondrial apoptosis pathway. J. Cell Biol. *162*, 587-597.

Riederer,B.M., Pellier,V., Antonsson,B., Di,P.G., Stimpson,S.A., Lutjens,R., Catsicas,S., and Grenningloh,G. (1997). Regulation of microtubule dynamics by the neuronal growth-associated protein SCG10. Proc. Natl. Acad. Sci. U. S. A *94*, 741-745.

Rosenberg,L.J., Zai,L.J., and Wrathall,J.R. (2005). Chronic alterations in the cellular composition of spinal cord white matter following contusion injury. Glia *49*, 107-120.

Sastry,P.S., and Rao,K.S. (2000). Apoptosis and the nervous system. J. Neurochem. *74*, 1-20.

Savitt,J.M., Jang,S.S., Mu,W., Dawson,V.L., and Dawson,T.M. (2005). Bcl-x is required for proper development of the mouse substantia nigra. J. Neurosci. *25*, 6721-6728.

Scheff,S.W., Rabchevsky,A.G., Fugaccia,I., Main,J.A., and Lumpp,J.E., Jr. (2003). Experimental modeling of spinal cord injury: characterization of a force-defined injury device. J. Neurotrauma *20*, 179-193.

Schnell,L., Fearn,S., Schwab,M.E., Perry,V.H., and Anthony,D.C. (1999). Cytokine-induced acute inflammation in the brain and spinal cord. J. Neuropathol. Exp. Neurol. *58*, 245-254.

Schroeter,H., Boyd,C.S., Ahmed,R., Spencer,J.P., Duncan,R.F., Rice-Evans,C., and Cadenas,E. (2003). c-Jun N-terminal kinase (JNK)-mediated modulation of brain mitochondria function: new target proteins for JNK signalling in mitochondrion-dependent apoptosis. Biochem. J. *372*, 359-369.

Schwab,J.M., Brechtel,K., Mueller,C.A., Failli,V., Kaps,H.P., Tuli,S.K., and Schluesener,H.J. (2006). Experimental strategies to promote spinal cord regeneration--an integrative perspective. Prog. Neurobiol. *78*, 91-116.

Schwarze,S.R., Ho,A., Vocero-Akbani,A., and Dowdy,S.F. (1999). In vivo protein transduction: delivery of a biologically active protein into the mouse. Science *285*, 1569-1572.

Sharpe,J.C., Arnoult,D., and Youle,R.J. (2004). Control of mitochondrial permeability by Bcl-2 family members. Biochim. Biophys. Acta *1644*, 107-113.

Shim,J.W., Koh,H.C., Chang,M.Y., Roh,E., Choi,C.Y., Oh,Y.J., Son,H., Lee,Y. S., Studer,L., and Lee,S.H. (2004). Enhanced in vitro midbrain dopamine neuron differentiation, dopaminergic function, neurite outgrowth, and 1-methyl-4-

phenylpyridium resistance in mouse embryonic stem cells overexpressing Bcl-XL. J. Neurosci. *24*, 843-852.

Shimizu,S., Shinohara,Y., and Tsujimoto,Y. (2000a). Bax and Bcl-xL independently regulate apoptotic changes of yeast mitochondria that require VDAC but not adenine nucleotide translocator. Oncogene *19*, 4309-4318.

Shimizu,S., Konishi,A., Kodama,T., and Tsujimoto,Y. (2000b). BH4 domain of antiapoptotic Bcl-2 family members closes voltage-dependent anion channel and inhibits apoptotic mitochondrial changes and cell death. PNAS *97*, 3100-3105.

Shinoura,N., Satou,R., Yoshida,Y., Asai,A., Kirino,T., and Hamada,H. (2000). Adenovirus-mediated transfer of Bcl-X(L) protects neuronal cells from Bax-induced apoptosis. Exp. Cell Res. *254*, 221-231.

Shuman,S.L., Bresnahan,J.C., and Beattie,M.S. (1997). Apoptosis of microglia and oligodendrocytes after spinal cord contusion in rats. J. Neurosci. Res. *50*, 798-808.

Silver,J., and Miller,J.H. (2004). Regeneration beyond the glial scar. Nat Rev Neurosci *5*, 146-156.

Simizu,S., Tamura,Y., and Osada,H. (2004). Dephosphorylation of Bcl-2 by protein phosphatase 2A results in apoptosis resistance. Cancer Sci. *95*, 266-270.

Skaper,S.D., Facci,L., Culbert,A.A., Evans,N.A., Chessell,I., Davis,J.B., and Richardson,J.C. (2006). P2X(7) receptors on microglial cells mediate injury to cortical neurons in vitro. Glia *54*, 234-242.

Soane,L., and Fiskum,G. (2005a). Inhibition of mitochondrial neural cell death pathways by protein transduction of Bcl-2 family proteins. J. Bioenerg. Biomembr. *37*, 179-190.

Soane,L., and Fiskum,G. (2005b). TAT-mediated endocytotic delivery of the loop deletion Bcl-2 protein protects neurons against cell death. J. Neurochem. *95*, 230-243.

Spierings,D., McStay,G., Saleh,M., Bender,C., Chipuk,J., Maurer,U., and Green,D.R. (2005). Connected to death: the (unexpurgated) mitochondrial pathway of apoptosis. Science *310*, 66-67.

Springer,J.E., Azbill,R.D., and Knapp,P.E. (1999). Activation of the caspase-3 apoptotic cascade in traumatic spinal cord injury. Nat. Med. *5*, 943-946.

Springer,J.E., Azbill,R.D., Nottingham,S.A., and Kennedy,S.E. (2000). Calcineurin-mediated BAD dephosphorylation activates the caspase-3 apoptotic cascade in traumatic spinal cord injury. J. Neurosci. *20*, 7246-7251.

Stokes,B.T., and Jakeman,L.B. (2002). Experimental modelling of human spinal cord injury: a model that crosses the species barrier and mimics the spectrum of human cytopathology. Spinal Cord. *40*, 101-109.

Sugioka,R., Shimizu,S., Funatsu,T., Tamagawa,H., Sawa,Y., Kawakami,T., and Tsujimoto,Y. (2003). BH4-domain peptide from Bcl-xL exerts anti-apoptotic activity in vivo. Oncogene *22*, 8432-8440.

Tagami,S., Eguchi,Y., Kinoshita,M., Takeda,M., and Tsujimoto,Y. (2000). A novel protein, RTN-XS, interacts with both Bcl-XL and Bcl-2 on endoplasmic reticulum and reduces their anti-apoptotic activity. Oncogene *19*, 5736-5746.

Tamura,Y., Simizu,S., and Osada,H. (2004). The phosphorylation status and anti-apoptotic activity of Bcl-2 are regulated by ERK and protein phosphatase 2A on the mitochondria. FEBS Letters *569*, 249-255.

Thomenius,M.J., Wang,N.S., Reineks,E.Z., Wang,Z., and Distelhorst,C.W. (2003). Bcl-2 on the endoplasmic reticulum regulates Bax activity by binding to BH3-only proteins. J. Biol. Chem. *278*, 6243-6250.

Thuret,S., Moon,L.D.F., and Gage,F.H. (2006). Therapeutic interventions after spinal cord injury. Nat Rev Neurosci *7*, 628-643.

Tsujimoto,Y. (2003). Cell death regulation by the Bcl-2 protein family in the mitochondria. J. Cell Physiol *195*, 158-167.

Tsuruta,F., Sunayama,J., Mori,Y., Hattori,S., Shimizu,S., Tsujimoto,Y., Yoshioka,K., Masuyama,N., and Gotoh,Y. (2004). JNK promotes Bax translocation to mitochondria through phosphorylation of 14-3-3 proteins. EMBO J. *23*, 1889-1899.

Uo,T., Kinoshita,Y., and Morrison,R.S. (2005). Neurons exclusively express N-Bak, a BH3 domain-only Bak isoform that promotes neuronal apoptosis. J. Biol. Chem. *280*, 9065-9073.

Upreti,M., Lyle,C.S., Skaug,B., Du,L., and Chambers,T.C. (2006). Vinblastine-induced apoptosis is mediated by discrete alterations in subcellular location, oligomeric structure, and activation status of specific Bcl-2 family members. J. Biol. Chem. *281*, 15941-15950.

Vander Heiden,M.G., Chandel,N.S., Schumacker,P.T., and Thompson,C.B. (1999). Bcl-xL prevents cell death following growth factor withdrawal by facilitating mitochondrial ATP/ADP exchange. Mol. Cell *3*, 159-167.

Vander Heiden,M.G., Chandel,N.S., Williamson,E.K., Schumacker,P.T., and Thompson,C.B. (1997). Bcl-xL regulates the membrane potential and volume homeostasis of mitochondria. Cell *91*, 627-637.

Vander Heiden,M.G., Li,X.X., Gottleib,E., Hill,R.B., Thompson,C.B., and Colombini,M. (2001). Bcl-xL promotes the open configuration of the voltage-dependent anion channel and metabolite passage through the outer mitochondrial membrane. J. Biol Chem. *276*, 19414-19419.

Vyas,S., Juin,P., Hancock,D., Suzuki,Y., Takahashi,R., Triller,A., and Evan,G. (2004). Differentiation-dependent sensitivity to apoptogenic factors in PC12 cells. J. Biol. Chem. *279*, 30983-30993.

Wadia,J.S., and Dowdy,S.F. (2005). Transmembrane delivery of protein and peptide drugs by TAT-mediated transduction in the treatment of cancer. Adv. Drug Deliv. Rev *57*, 579-596.

Wadia,J.S., Stan,R.V., and Dowdy,S.F. (2004). Transducible TAT-HA fusogenic peptide enhances escape of TAT-fusion proteins after lipid raft macropinocytosis. Nat Med. *10*, 310-315.

Wang,X.J., Kong,K.M., Qi,W.L., Ye,W.L., and Song,P.S. (2005). Interleukin-1 beta induction of neuron apoptosis depends on p38 mitogen-activated protein kinase activity after spinal cord injury. Acta Pharmacol. Sin. *26*, 934-942.

WANG,X.U.E., ZHANG,J.I.N.G., KIM,H.P., WANG,Y.O.N.G., CHOI,A.M.K., and RYTER,S.W. (2004). Bcl-XL disrupts death-inducing signal complex formation in plasma membrane induced by hypoxia/reoxygenation. FASEB J. *18*, 1826-1833.

Warden,P., Bamber,N.I., Li,H., Esposito,A., Ahmad,K.A., Hsu,C.Y., and Xu,X.M. (2001). Delayed glial cell death following wallerian degeneration in white matter tracts after spinal cord dorsal column cordotomy in adult rats. Exp. Neurol. *168*, 213-224.

Wen,T.C., Sadamoto,Y., Tanaka,J., Zhu,P.X., Nakata,K., Ma,Y.J., Hata,R., and Sakanaka,M. (2002). Erythropoietin protects neurons against chemical hypoxia and cerebral ischemic injury by up-regulating Bcl-xL expression. J. Neurosci. Res. *67*, 795-803.

White,C., Li,C., Yang,J., Petrenko,N.B., Madesh,M., Thompson,C.B., and Foskett,J.K. (2005). The endoplasmic reticulum gateway to apoptosis by Bcl-XL modulation of the InsP3R. Nat Cell Biol *7*, 1021-1028.

Xu,L., Koumenis,I.L., Tilly,J.L., and Giffard,R.G. (1999). Overexpression of bcl-xL protects astrocytes from glucose deprivation and is associated with higher glutathione, ferritin, and iron levels. Anesthesiology *91*, 1036-1046.

Xue,L.Y., Chiu,S.M., Fiebig,A., Andrews,D.W., and Oleinick,N.L. (2003). Photodamage to multiple Bcl-xL isoforms by photodynamic therapy with the phthalocyanine photosensitizer Pc 4. Oncogene *22*, 9197-9204.

Yajima,H., and Suzuki,F. (2003). Identification of a Bcl-XL binding region within the ATPase domain of Apaf-1. Biochem. Biophys. Res. Commun. *309*, 520-527.

Yakovlev,A.G., and Faden,A.I. (2004). Mechanisms of neural cell death: implications for development of neuroprotective treatment strategies. NeuroRx. *1*, 5-16.

Yates,J.R., Heyes,M.P., and Blight,A.R. (2006). 4-chloro-3-hydroxyanthranilate reduces local quinolinic acid synthesis, improves functional recovery, and preserves white matter after spinal cord injury. J. Neurotrauma *23*, 866-881.

Yin,W., Cao,G., Johnnides,M.J., Signore,A.P., Luo,Y., Hickey,R.W., and Chen,J. (2006). TAT-mediated delivery of Bcl-xL protein is neuroprotective against neonatal hypoxic-ischemic brain injury via inhibition of caspases and AIF. Neurobiol. Dis. *21*, 358-371.

Young,W. (2002). Spinal cord contusion models. Prog. Brain Res. *137*, 231-255.

Yu,F., Sugawara,T., Nishi,T., Liu,J., and Chan,P.H. (2006). Overexpression of SOD1 in transgenic rats attenuates nuclear translocation of endonuclease G and apoptosis after spinal cord injury. J. Neurotrauma *23*, 595-603.

Yuan,J., Lipinski,M., and Degterev,A. (2003). Diversity in the Mechanisms of Neuronal Cell Death. Neuron *40*, 401-413.

Zai,L.J., and Wrathall,J.R. (2005). Cell proliferation and replacement following contusive spinal cord injury. Glia *50*, 247-257.

Zaidi,A.U., Sa-Eipper,C., Brenner,J., Kuida,K., Zheng,T.S., Flavell,R.A., Rakic,P., and Roth,K.A. (2001). Bcl-X(L)-caspase-9 interactions in the developing nervous system: evidence for multiple death pathways. J. Neurosci. *21*, 169-175.

Zamzami,N., Brenner,C., Marzo,I., Susin,S.A., and Kroemer,G. (1998). Subcellular and submitochondrial mode of action of Bcl-2-like oncoproteins. Oncogene *16*, 2265-2282.

Zhang,X., Chen,J., Graham,S.H., Du,L., Kochanek,P.M., Draviam,R., Guo,F., Nathaniel,P.D., Szabo,C., Watkins,S.C., and Clark,R.S. (2002). Intranuclear localization of apoptosis-inducing factor (AIF) and large scale DNA fragmentation after traumatic brain injury in rats and in neuronal cultures exposed to peroxynitrite. J. Neurochem. *82*, 181-191.

Zhang,Z., and Guth,L. (1997). Experimental spinal cord injury: Wallerian degeneration in the dorsal column is followed by revascularization, glial proliferation, and nerve regeneration. Exp. Neurol. *147*, 159-171.

Zhang,Z., Krebs,C.J., and Guth,L. (1997). Experimental analysis of progressive necrosis after spinal cord trauma in the rat: etiological role of the inflammatory response. Exp. Neurol. *143*, 141-152.

Zhu,Y., Swanson,B.J., Wang,M., Hildeman,D.A., Schaefer,B.C., Liu,X., Suzuki,H., Mihara,K., Kappler,J., and Marrack,P. (2004). Constitutive association of the proapoptotic protein Bim with Bcl-2-related proteins on mitochondria in T cells. Proc. Natl. Acad. Sci. U. S. A *101*, 7681-7686.

Zimmermann,A.K., Loucks,F.A., Le,S.S., Butts,B.D., Florez-McClure,M.L., Bouchard,R. J., Heidenreich,K.A., and Linseman,D.A. (2005). Distinct mechanisms of neuronal apoptosis are triggered by antagonism of Bcl-2/Bcl-x(L) versus induction of the BH3-only protein Bim. J. Neurochem. *94*, 22-36.

Vita

Diana M. Cittelly was born to Enrique and Marina Cittelly in Bogotá, Colombia, on June 6th, 1976. She attended The National University of Colombia, graduating with Bachelor of Science in Biology in 1998. Between 1999 and 2001, Diana completed post-graduated studies and graduated with Master of Science in Biochemistry at The National University of Colombia, Bogotá, Colombia. She moved to The University of Texas Medical Branch at Galveston in 2002. After completing the first year of the Graduate School curriculum, she joined the laboratory of Dr. Regino Perez-Polo to explore apoptotic mechanisms triggered by CNS trauma. Diana is a PhD Candidate in the Cell Biology Graduate Program and continued her studies with Dr. Perez-Polo in the Department of Neuroscience and Cell Biology. While at graduate school, Diana received several honors. In 2005, Diana was awarded the University Federal Credit Union scholarship and the Society of Neurotrama student award. In 2006, she was awarded the George Sealy research Award in Neurology; the Society of Neurotrama student award and the Who's who among students in American Universities and Colleges award. Diana can be contacted through the Graduate School of Biomedical sciences at UTMB.

Education

1999-2001	**M.S. in Biochemistry.** Universidad Nacional de Colombia, Bogotá, Colombia Facultad de Medicina. Departamento de Bioquimica.
1993-1998	**B.S. in Biology** Universidad Nacional de Colombia, Bogotá, Colombia Facultad de Ciencias. Departamento de Biologia.

Publications

- **Cittelly D**, Nesic-Taylor O, Perez-Polo JR. Phosphorylation of Bcl-x_L after spinal cord Injury. In review process at *J. Neurosc. Res.*

- **Cittelly D.** Nesic-Taylor O, Perez-Polo JR. Detrimental effect of anti-apoptotic therapies in the injured spinal cord. Submitted *to Experimental Neurology*.

- Nesic-Taylor O, **Cittelly D**, Ye Z, Xu GY, Unabia G, Lee JC, Svrakic NM, Liu XH, Youle RJ, Wood TG, McAdoo D, Westlund KN, Hulsebosch CE, Perez-Polo JR. Exogenous Bcl-x_L fusion protein spares neurons after spinal cord injury. *J Neurosci Res*. 2005;79(5):628-37.

- HSU PI, Hwang IR, **Cittelly D**, Lai KH, El-Zimaity HM, Gutierrez O et al. Clinical presentation in relation to diversity within the Helicobacter pylori cag pathogenicity island. *Am J Gastroenterol* 2002; 97: 2231-8.

- **Cittelly DM**, Huertas MG, Martinez JD. Oliveros R, Posso H, Bravo MM, Orozco. 2002. [Helicobacter pylori genotypes in non atrophic gastritis are different of the found in peptic ulcer, premalignant lesions and gastric cancer in Colombia]. *Rev Med Chil.* 2002 Feb;130(2):143-51.

- **Cittelly DM**, Henao SC, Martinez JD. Oliveros R, Orozco O. 2001 Helicobacter pylori in Gastric Cancer and Peptic Ulcer Disease in a Colombian Population. Strain Heterogeneity and Antibody Profiles. *Helicobacter* 6(3):199-206

Abstracts

2006 **Cittelly,D**, Nesic-Taylor, O., Perez-Polo, J. R. Tat-Bcl-x_L and Tat-BH4 decreases spinal cord injury induced apoptosis, but does not improve locomotor function. Poster presentation National Society of Neurotrauma symposium. St. Louis. MI

2005 **Cittelly,D**, Nesic-Taylor, O., Perez-Polo, J. R. Phosphorylated Bcl-x_L in spinal cord: are apoptosis regulation and neuronal differentiation related? Poster presentation.11th International Symposium on Neural Regeneration, Dec.14-18 Asilomar, Pacific Grove,CA.

2005 **Cittelly,D***, Rafati D*, Nesic-Taylor, O., Perez-Polo, J. R. Interventions in NF-kappaB mediated pathways improve functional outcome after spinal cord injury. Christopher Reeve Paralysis Foundation Spinal Cord Symposium. Sept. 16-18.Boston, MA.

2005 **Cittelly, D.,** Nesic, O., Hulsebosch, C.E., Perez-Polo, J.R. Effect of Spinal Cord Injury on Bcl-x_L Expression Levels and their Subcellular Distributions. Poster presentation. 23th National Society of Neurotrauma symposium. Washington, DC, November 9-11

2005 **Cittelly, D.,** Nesic, O., Hulsebosch, C.E., Perez-Polo, J.R. Subcellular distribution of Bcl-xL in Injured Spinal Cord. Poster presentation. Society of Neuroscience Meeting. Washington DC. November 13-16

2004 **Cittelly, D.,** Nesic, O., McAdoo, D., Hulsebosch, C.E., Perez-Polo, J.R. Effect of Spinal Cord Injury on Bax and Bcl-x_L Expression Levels and their Subcellular Distributions. Oral presentation. American Society of Neurochemistry (ASN) 36th Annual meeting. New York City. August 14-16

Permanent address: 210 Market St. Galveston, TX, 77550

This dissertation was typed by Diana M. Cittelly.